EVALUATING THE USE OF SATELLITE-BASED PRECIPITATION ESTIMATES FOR DISCHARGE ESTIMATION IN UNGAUGED BASINS

A THESIS SUBMITTED TO
THE GRADUATE SCHOOL OF NATURAL AND APPLIED SCIENCES
OF
MIDDLE EAST TECHNICAL UNIVERSITY

BY

ARZU SOYTEKİN

IN PARTIAL FULFILLMENT OF THE REQUIREMENTS
FOR
THE DEGREE OF MASTER OF SCIENCE
IN
CIVIL ENGINEERING

SEPTEMBER 2010

Approval of the thesis:

EVALUATING THE USE OF SATELLITE-BASED PRECIPITATION ESTIMATES FOR DISCHARGE ESTIMATION IN UNGAUGED BASINS

submitted by **ARZU SOYTEKİN** in partial fulfillment of the requirements for the degree of **Master of Science in Civil Engineering Department, Middle East Technical University** by,

Prof. Dr. Canan Özgen _____________________
Dean, Graduate School of **Natural and Applied Sciences**

Prof. Dr. Güney Özcebe _____________________
Head of Department, **Civil Engineering**

Assoc. Prof. Dr. Zuhal Akyürek _____________________
Supervisor, **Civil Engineering Dept., METU**

Examining Committee Members:

Prof. Dr. Melih Yanmaz _____________________
Civil Engineering Dept., METU

Assoc. Prof. Dr. Zuhal Akyürek _____________________
Civil Engineering Dept., METU

Assoc. Prof. Dr. Nurünnisa Usul _____________________
Civil Engineering Dept., METU

Inst. Dr. Koray Yılmaz _____________________
Geological Engineering Dept., METU

Dr. Ali Ümran Kömüşçü _____________________
Turkish State Meteorological Service

Date: 17.09.2010

I hereby declare that all information in this document has been obtained and presented in accordance with academic rules and ethical conduct. I also declare that, as required by these rules and conduct, I have fully cited and referenced all material and results that are not original to this work.

Name, Last Name : Arzu SOYTEKİN

Signature :

ABSTRACT

EVALUATING THE USE OF SATELLITE-BASED PRECIPITATION ESTIMATES FOR DISCHARGE ESTIMATION IN UNGAUGED BASINS

Soytekin, Arzu

M.Sc., Department of Civil Engineering

Supervisor: Assoc. Prof. Dr. Zuhal Akyürek

September 2010, 106 pages

For the process of social and economic development, hydropower energy has an important role such as being renewable, clean, and having less impact on the environment. In decision of the hydropower potential of a study area, the preliminary condition is the availability of the gages in the area. However, in Turkey, the gages in working order are limited and getting decreased in recent years. Therefore, the satellite based precipitation estimates has been gaining importance to predict runoff for ungauged basins. In this study, Çoruh basin, which is located in the north-eastern part of Turkey, is selected to perform hydrologic modeling. The input precipitation data for the model are provided from the observations at meteorological stations and the Tropical Rainfall Measuring Mission (TRMM) satellite products (3B42 and 3B43). TRMM satellite is used to monitor and study the rainfall distribution. The precipitation radar on the TRMM is the first radar to make precipitation estimation from the space. Using both precipitation data, HEC-HMS, being well known hydrological model, is applied to the Çoruh Basin for 2005 and 2003 water years. To distinguish the differences in the runoff simulations and water budget, comparisons are done with respect to flow monitoring stations. Statistical criteria show that model simulation results obtained from TRMM 3B42 products are promising in estimating the water potential in ungauged basins.

Keywords: TRMM, satellite based rainfall, HEC-HMS, ungauged basin, hydrologic modeling

ÖZ

ÖLÇÜM ARAÇLARININ OLMADIĞI HAVZALARDA AKIM TAHMİNİNİN UYDU BAZLI YAĞIŞ TAHMİNLERİ KULLANILARAK DEĞERLENDİRİLMESİ

Soytekin, Arzu

Yüksek Lisans, İnşaat Mühendisliği Bölümü

Tez Yöneticisi: Doç. Dr. Zuhal Akyürek

Eylül 2010, 106 sayfa

Hidroelektrik enerji, yenilenebilir, temiz ve doğaya etkisinin az olması sebebiyle; sosyal ve ekonomik gelişim sürecinde önemli bir role sahiptir. Üzerinde çalışılan bir alanın hidroelektrik potansiyeline karar vermede ön koşul, o alandaki ölçüm araçlarının mevcudiyetidir. Ancak, Türkiye'de kullanılabilir ölçüm araçları oldukça sınırlıdır ve sayıları son yıllarda azalmıştır. Bu sebeple, uydu tabanlı yağış tahminleri, ölçüm araçları olmayan havzalarda önem kazanmaktadır. Bu çalışmada, Türkiye'nin kuzeydoğusunda yer alan Çoruh Havzası, hidrolojik modelleme uygulaması için seçilmiştir. Model için gereken yağış girdi verisi meteoroloji istasyonlarındaki gözlemlerden ve Tropical Rainfall Measuring Mission (TRMM) uydusundan temin edilmiştir (3B42 ve 3B43). TRMM uydusu, yağış dağılımını gözlemlemekte ve araştırılmasında kullanılmaktadır. TRMM üzerindeki yağış radarı, uzaydan yağış ölçüm tahmini yapan ilk radardır. Bilinen bir hidrolojik model olan HEC-HMS, her iki yağış verisini de kullanarak, 2005 ve 2003 su yılları için Çoruh Havzasına uygulanmıştır. Akım simülasyonu ve su miktarı dengesinde elde edilen farklı sonuçların ayrımı, akım gözlem istasyonundan elde edilen sonuçlarla kıyaslanarak yapılmıştır. İstatistiksel kriterler, TRMM 3B42 ürünü ile elde edilen model simülasyonu sonuçlarının, ölçüm istasyonu olmayan havzalarda su potansiyeli belirlemede umut verici sonuçlar verdiğini göstermiştir.

Anahtar Kelimeler: TRMM, uydu tabanlı yağış verileri, HEC-HMS, ölçümsüz havza, hidrolojik modelleme

To My Grandmother and Grandfather...

ACKNOWLEDGEMENTS

The author wishes to express her deepest gratitude to her supervisor Assoc. Prof. Dr. Zuhal Akyürek for her invaluable encouragement, support and understanding throughout the research.

The author also wishes to express her gratitude to Reşat Köymen and Nadi Bakır from ERE group for their financial support.

Moreover, sincere thanks are extended to State Meteorological Service (DMI) for meteorological station data. The author is grateful to Serdar Sürer in helping to download the data during this study.

Furthermore, the author would like to thank faculty members and administrative staff of METU Water Resources Laboratory for creating good study environment.

Finally, the author would like to thank to her colleagues: M. Emrah Özkaya, Meriç Apaydın, Ayça Öztürk, Boran Ekin Aydın, Reyhan Mutlu, and Onur Arı for not leaving her alone during this study.

TABLE OF CONTENTS

LIST OF TABLES

TABLES

LIST OF FIGURES

FIGURES

CHAPTER 1

INTRODUCTION

1.1 Definition of the Problem

Estimation of the water movement in a basin has been gaining importance not only for water use but also for water control. Moreover, it is vital for sustaining life. Having knowledge about the water movement in a basin is also necessary for discharge estimation which is the key element in describing water potential.

Water resources engineering deals with the basin management to procure information about the water movement. For the few decades, rainfall-runoff modeling studies have become widespread to figure out the processes in the water movement. With the increase of water demand and difficulty of accessing fresh water, studies which denote relationship between rainfall and runoff have achieved great significance.

In order to obtain accurate relationship between rainfall and runoff in modeling, suitable data are required. However, scarcity of the data is a common problem in most of the basins in the world especially in undeveloped and developing countries. For solving this problem, new approaches are used to get hydrological prediction in data-sparse regions. With the technological progress, getting real time data using satellite products become easier and this represents a potential solution for ungauged basins.

Data is the key element in a modeling effort. When viewed from spatial continuity, data can be two types; point-based (lumped), like observations at meteorological stations or distributed, like satellite products. In hydrology, type of the data is important because representation of the basin depends on it. All cycles in the nature are continuous in time or space. Thus, spatially distributed data are more convenient than the point-based data in modeling.

Precipitation is a major driving force in the water cycle and accurate data with sufficient spatial detail are of key importance in assessing basin-scale hydrology. According to Nijssen and Lettenmaier (2004), in land surface hydrological system, the most important atmospheric input is the precipitation data. To establish model in regions where surface observation networks are sparse, other estimation techniques like weather radars, which are sensitive to precipitation elements and satellites, which have advantage to provide spatial homogeneous observation can be used (Csiszár et al., 1997).

In addition to sparse network distribution issue, gathering available information from the existent surface observation network and performing ground surveys are common problems in complex terrains like mountainous regions. Thus, modeling studies are performed with uncertainty. To reduce uncertainty of the predictions performed in ungauged or poorly gauged basins, International Association of Hydrological Sciences (IAHS) made a new initiative, the IAHS Decade on Predictions in Ungauged Basins (PUB) (Sivapalan et al., 2003). By implementing appropriate programs to scientific community, PUB aims to improve predictions in ungauged basins. Some of the objectives of this initiative are demonstrating the value of data, advancing the understanding of climatic controls, improving the ability of the hydrologist and developing new hydrological models.

“Satellite images are a source of information for several water cycle components. Even before the launch of the first meteorological satellite (The Television and Infrared Observation Satellite – TIROS 1) in April 1960, it was hypothesized that the occurrence, and even the intensity of rain might be inferred from the appearance of the parent cloud systems” (Pretty, 1995 in Collischonn et al., 2008).

Rainfall estimation from satellite products is a good remedy for areas where raingauge density is low and rainfall amount is variable. By using satellite images, various efforts have been carried out to estimate rainfall. Several methods have been proposed for estimating rain rates from satellite images using several bands of electromagnetic spectrum (Dingman, 2002). According to Kummerow et al. (2005), Geostationary Operational Environmental System (GOES, METEOSAT) and the Tropical Rainfall Measuring Mission (TRMM) are the most popular satellites to measure precipitation over the oceans and tropics.

This study evaluates the rainfall estimates of Tropical Rainfall Measuring Mission (TRMM) Multisatellite Precipitation Analysis (TMPA; 3B42 V.6 and 3B43 V.6) over Çoruh basin. TMPA rainfall estimates are compared with the ground observations on monthly basis. Three hour TMPA rainfall estimates are aggregated to daily values and then used as input to a hydrological model. Simulated hydrographs are then compared with observations at the outlet of the basin to make a decision about the discharge potential. The main motivation for evaluating remote sensing rainfall estimates by running hydrological model is to obtain an integration of rainfall effects over the basin in terms of river discharge. Results of the hydrological modeling with the satellite based rainfall data indicate the use of simulated runoff hydrographs.

1.2 Purpose of the Study

The main purpose of this study is to examine if satellite based rainfall estimates are useful as input for rainfall-runoff models applied to a mountainous basin in Turkey during non-snowy season. To achieve this purpose, stages completed in the study can be listed as follows:

- Obtaining daily and monthly satellite based precipitation data at the Çoruh basin,
- Comparing satellite based precipitation data (distributed) and ground based precipitation data (point based),
- Obtaining land use and land cover data and generating curve number distribution for the basin,
- Using DEM data, to construct terrain processing,
- Using HEC-GeoHMS to create input data from terrain process output and curve number map,
- Applying rainfall-runoff model using satellite based and ground based precipitation data separately,
- Calibrating model parameters by using flow monitoring stations,

Schematic representation of the methodology can be seen in Figure1.1.

This thesis consists of six chapters.

- In chapter 1, the purpose of the study and the proposed methodology are provided.
- In chapter 2, a brief literature survey about hydrological modeling software, HEC-HMS and satellite precipitation data (TMPA) are summarized. Examples from hydrological modeling with the satellite based rainfall data are given.
- Chapter 3 describes the study area and information about data used in the study. The processes used in the data preparation and basin preprocessing are presented.

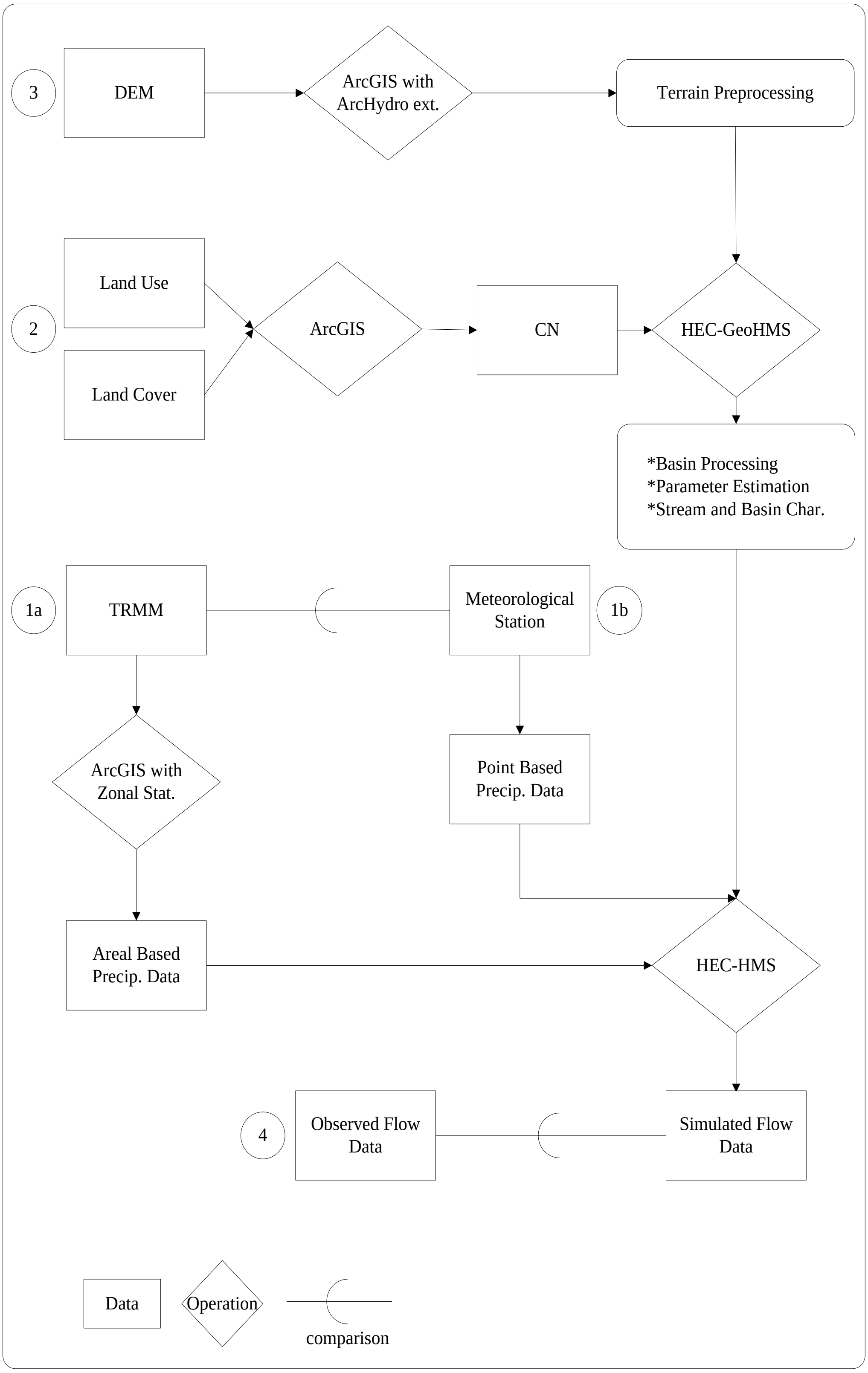

Figure 1.1 Schematic representation of the methodology

- Chapter 4 describes the comparison of TMPA data with the raingauge data considering two different products, TMPA 3B43 (monthly scale) and TMPA 3B42 (daily scale) data.

- Chapter 5 mainly deals with rainfall-runoff modeling, model simulations and performance evaluation.

- Chapter 6 is the last chapter of the thesis, final discussions and conclusions about the study are presented here.

CHAPTER 2

LITERATURE SURVEY

The literature survey is performed in two subsections. In the first section, modeling studies, where Hydrologic Modeling System (HEC-HMS) is used, are summarized. In the second one, studies, in which satellite based precipitation data are used, are emphasized with main points.

2.1 Modeling Studies

In hydrological systems, the main difficulty is the limitations of the measurement techniques in time and space. Thus, all variables in the hydrologic cycle cannot be measured satisfactorily. This situation led to the development of hydrologic models. With the progress of computer technology, hydrologic simulation studies began in the 1950s and 1960s (Donigian and Imhoff, 2006). Stanford Watershed Model (SWM) is the first computer based hydrologic model created by Stanford University for this purpose (Crawford and Linsley, 1966). Since then many hydrologic models were designed, improved and used. These models like, Watershed Modeling System (WMS), Snowmelt Runoff Model (SRM), Hydrologiska Byråns Vattenbalansavdelningare Model (HBV), MIKE and HEC-HMS are the most popular hydrologic modeling software packages in the last two decades (Yener, 2006). Among these hydrologic models, specific requirements and needs designate the selection of the proper model (Cunderlik and Simonovic, 2007).

According to Cunderling and Simonovic (2007), there are four fundamental criteria that help to select the conformable model from a number of alternatives, these are; required model outputs, required hydrologic process to find outputs, input data availability and price. In light of all these, in this study, the Hydrologic Modeling System (HEC-HMS) designed by US Army Corps of Engineers is selected in rainfall-runoff modeling.

By using HEC-HMS, possible range of water management problems like water availability, flow forecasting, and future urbanization impact can be solved by designing precipitation runoff processes in watershed systems. Furthermore, program has a capability to divide hydrologic cycle components into small chunks (USACE, 2009c). The first version of the program was developed in 1967 by Leo R. Bread, namely, Flood Hydrograph Package (HEC-1) and published in 1968 (USACE, 1998). With the improvement of the software technology, some innovations have been included to the software like utilization of gridded data. The newest version of the program, HEC-HMS 3.4 is released to market in August 2009.

Due to easy access and usability, considerable studies are performed by using HEC-HMS. Some of the studies are listed as follows.

Hoblit and Curtis (2001) created a hydrologic model by using radar rainfall estimates to predict storm events. Heppner, located in east of Portland, was chosen as a study area which was faced with the most severe weather event in the 20th century among Oregon state (National Weather Service Oregon, 2001 in Hoblit and Curtis, 2001). The required physical data like digital elevation model (DEM), land use, land cover were obtained from USGS and governmental agencies via web freely. Flow path and the basin characteristics were formed to render preliminary input for modeling by processing DEM data in HEC-GeoHMS. In modeling, radar rainfall data were used together with curve number method for infiltration computations. Muskingum-Cunge method was used for routing process, and recession baseflow method was used for baseflow computation. After superimposing the observed and simulated flows, it was concluded that the model presented acceptable adequacy, however still needed calibration and validation to improve the results.

Pistocchi and Mazzoli (2002) made a study about risk assessment in Romagna River basin, which is located in North Central Italy. Using HEC-HMS and HEC-RAS models, event based simulation was performed. The aim was to find estimation about the water budget and rainfall flood response by using rating curve parameters, water depth and discharge. At the end of this study, it was pointed out that the progress of the work depends on the reduction of the uncertainty related with flow measurements.

Al-Abed et al. (2005) studied hydrologic models in Zaqra River basin in Jordan, where water has a great importance due to the exploitation of groundwater sources. In this study, hydrologic model simulation was handled in HEC-HMS and Spatial Water Budget Management Model (SWBM) to implement test scenario on climate change. The output of models led to good result in prediction of the water potential. Moreover, it was denoted that HEC-HMS gave more permissible result than the SWBM.

Knebl et al. (2005), made a flood modeling study with HEC-HMS/RAS using radar based rainfall estimation in San Antonio river basin in Central Texas, USA with 2002 summer storm event data. The studied basin has a 10000 km^2 area and the region is subject to severe flash flooding frequently. In the study, topography was obtained from USGS National elevation Dataset (NED), for infiltration calculation curve number technique was selected. For translation calculation ModClark algorithm and for baseflow computation exponential decrease function were used. In the study, evapotranspiration losses were considered to be negligible. After the simulation of the model, it is concluded that the model has a reasonable fit with the observations, so study can be incorporated with regional flood alert system.

Another flood risk assessment was made by Cunderlik et al. (2007) in Upper Thames River Basin, south-western Ontario using present and future climatic conditions. According to the study, there is a positive effect on hydrologic extreme distribution in the basin with climate change, maximum and low flows may become less extreme and less variable in terms of magnitude and occurrence respectively.

Furthermore, some efficient studies were accomplished in Turkey. Using HEC-1 function, Şensoy et al. (2003) made a study in Upper Karasu basin located in the eastern part of Turkey. Yener (2006) performed a study in Yuvacık basin to get a decision about the operation and the management of Yuvacık Dam by making event based simulation using HEC-HMS (3.0.1).

2.2 Studies with Satellite Based Precipitation Data

Precipitation is the leading component of hydrologic cycle. In order to measure precipitation amount, rain gage instruments have been used over many years. These instruments are placed within the basin so information about distribution of rainfall amount can be gathered from these points. However, rainfall characteristics may change rapidly from one place to another even in small basins. Moreover, in developing countries, networks of ground based observations are generally sparse due to the lack of resources available. Even in technologically developed countries, where rain gauge samplings are extensive, areal precipitation estimates are considered to be unreliable due to local convective events (Wilheit, 1986 in Collischonn et al., 2008).

Hence, working with spatial rainfall data can be a better source than the data obtained from point measurements (Wang et al., 2009). However, according to Nicholson et al. (2003), neither raingauges nor satellite based estimates are perfect indicators of rainfall.

Recently, due to the afford of replacing the available stations with automatic weather observation stations, there is limited number of ground based stations and radar instruments in Turkey. There are four radar sites; which are located in Ankara, Istanbul, Zonguldak and Balıkesir. These instruments do not cover the eastern part of the Turkey. According to Kadıoğlu (2010), the number of meteorological stations is reduced from 1200 to 500 in recent years. And 450 meteorological stations are in operation. It is known that to represent the distribution of the meteorological parameters properly, this number for Turkey should be around 3000 (Kutoğlu, 2010).

In hydrological literature there are a number of satellite precipitation products which are used in the studies, like TAMSAT (Tropical Applications of Meteorological Satellites), TOVS (TIROS Operational Vertical Sounder), GPCP (Global Precipitation Climatology Project) and PERSIANN (Precipitation Estimation from Remotely Sensed Information using Artificial Neural Networks) (Hughes D. A., 2006).

In this study, another satellite-based precipitation estimates, widely seen in the literature, namely, TMPA (Tropical Rainfall Measuring Mission (TRMM) Multisatellite Precipitation Analysis) is used. TMPA combines the precipitation data from multiple satellites and raingauges where feasible, but TMPA calibration is based on TRMM product (Huffman et al., 2007). In this study, the selected datasets of TMPA are referred as TRMM 3B43 (V6), which is monthly based and TRMM 3B42 (V6), which is daily based product. The terminology, V6 is the indicator of TMPA algorithm **(**Chokngamwong and Chiu, 2008). TRMM satellite, which is a collective production of NASA (National Aeronautics and Space Administration) and JAXA (Japan Aerospace Exploration Agency) was launched in November 1997 with the aim of providing rainfall data for tropical regions. Since then in order to enhance the accuracy of the code, algorithms have been reprocessed and now Version 6 (V6) algorithm is used (Huffman et al., 2007). TRMM Satellite is 402 km above the Earth, and has spatial and temporal resolutions of 0.25° and 92.5

minute, respectively. Precipitation Radar (PR), TRMM Microwave Imager (TMI), and Visible and Infrared Radiometer (VIRS) are the main rainfall sensors on TRMM. Some of the TRMM products with their coverage, resolution and sensor information derived from NASA webpage (http://mirador.gsfc.nasa.gov) are summarized in Table 2.1

Table 2.1 Some of the TRMM Products and their characteristics

Standard Product	Coverage	Spatial Resolution (degree)	Temporal Resolution	Sensor
3A25	Global tropics (40N-40S, 0-360E)	5 x 5 and 0.5 x 0.5	monthly	PR
3A12	Global tropics (40N-40S, 0-360E)	0.5 x 0.5	monthly	TMI
3A11	Tropical Oceans (40N-40S, 0-360E)	5 x 5	monthly	TMI
3B31	Global tropics (40N-40S, 0-360E)	5 x 5	monthly	Combined PR/TMI
3B42	Global tropics (50N-50S, 0-360E)	0.25 x 0.25	3 hourly	Combined PR/TMI/IR
3B43	Global tropics (50N-50S, 0-360E)	0.25 x 0.25	monthly	Combined PR/TMI/IR

After starting to produce satellite products for a long time, it was challenging to get proper data for most of the users. Therefore, to get easy access to satellite products, Hydrology Data Support Team (HDST) at NASA made a project, the TRMM Online Visualization and Analysis System (TOVAS) (Liu et al., 2007). Using this internet based system; user can select the suitable product, time range and output type for the study. Using TOVAS system, and considering geographical location of Turkey, TRMM 3B42 (V6) and TRMM 3B43 (V6) satellite products are downloaded for the study.

2.2.1 Comparison of TRMM Data with Other Satellite Data and Ground Based Observations

In interdisciplinary research and applications, the use of the TRMM data is frequently observed. For instance; to monitor heavy rains (Minghu et al., 2008), to study historical events like El Nino (Adler et al., 2000), to study tropical infection disease (Liu et al., 2002), to determine land surface wetness (Gu et al., 2002) and to estimate crop yield (Chiu et al., 2004), TRMM data products are used.

Successful outcome of these researches and applications relies on the accurate representation of the precipitation data. In order to determine the accuracy of the satellite based precipitation data, comparison studies are conducted using the ground based observations.

Feidas and Chrysoulakis (2008) performed a study on validation and comparison of three TRMM rainfall products; 3A12, 3B42 and 3B43 with 76 ground based stations over Greece for a period of 1998 to 2006. Interpolation was done using inverse distance weighted method on rain gauge data and comparisons of gauge and three satellite products were done for monthly and seasonal precipitation totals using statistical scores. The results of the study demonstrate that on 0.5 space scale 3B42 and 3B43 products had a good agreement with the gauge data for summer and autumn seasons. However, 3B43 products had a better result than 3B42 product due to less random errors of 3B43. In addition to that, 3A12 products denoted poor performance over the Greece costal region because of algorithm inconsistencies.

Wang et al., (2009) made rainfall estimation studies by using TRMM 3B43 (V6) and 52 raingauge stations on Laohaohe basin, located in northeast of China. The results show that calculation period and location of site were the important factors for estimating rainfall from 3B43 product. Moreover, it is emphasized that comparisons showed strong dependency with the latitude but elevation factor seemed to be negligible.

Since launching of the TRMM satellite, several precipitation retrieval algorithms have been released. In November 1995, TRMM Version 5, V (5) was released and in April 2005, the newest version, Version 6, V (6) was released (Yuter, et al., 2006). Chokngamwong and Chiu (2008) made an alternate study about TRMM versions; 3B43 (V5) and (V6), 3B42 (V5) and (V6) and gauge data in Thailand. In the study, comparisons were done on monthly and daily scale. In terms of the bias, V6 TRMM products showed advancement over the V5 products. And also it was seen that satellite products had a deficiency about the detection of heavy rain rates in excess of 1000 mm/month.

Benchmarking studies can be performed in other rainfall satellite algorithms like CMORPH (CPC MORPHing technique). Dinku et al. (2010) evaluated two satellite products, CMORPH and TRMM over mountainous region of Africa and South America. Under the complex topography, it is observed that products had low correlation between each other and rainfall amount was underestimated. Furthermore, accomplishment of CMORPH product was more noticeable than TRMM product.

2.2.2 Modeling Studies Using TRMM Products

Despite the fact that satellite rainfall products' spatial scales are ranging from 0.25° to 5° and assumed to be coarse for hydrologic modeling, they are used in wide range of applications due to being cost effective and easy availability (Harris et al., 2007).

Flood early warning system is the most effective way to reduce life loss and damages (Negri et al., 2005). For flood modeling Harris et al. (2007) performed a study in upper Cumberland River basin, which is sharing a border with Virginia and Tennessee. In this study, real time product, 3B41 (RT) was used for March 2002 storm event. Using TOPMODEL and HEC–HMS with a number of different methods, model configurations were prepared. When comparisons were done between the observed hydrograph and simulated ones, it is pointed out that results from all methods had a systematic underestimation. After making a satellite data adjustment by a certain scalar factor, the simulated results were similar to the observed one. However, according to Hossain and Anagnostou, (2004) this kind of adjustments are not behaving well in terms of residual error in false detected rains. Thus, adjustments should be generalized considering regime, season and location.

Another flood forecasting study was made by the Kafle et al. (2007) in time period of 2004 rainy season in Bagmati River, Kathmandu, which is the capital of Nepal. Simulations were done using gauge data, TRMM data and together with TRMM and gauge data. Comparison of simulated hydrographs and the observed ones show that peak discharge obtained from simulation of the gauge rainfall data was quite accurate with the observed ones, namely 98%. Other simulation results (TRMM only and TRMM with gauge) required further clarifications but the trend of the hydrographs aligns with each other.

Casimiro et al. (2009) conducted a study about monthly water balance model over Peruvian Amazon Andes basin using TRMM 3B43 rainfall product by using GR2M water balance model. Three sets of data (gauge, TRMM and gauge and improved TRMM data based on gauge data) were used in this model. At the end of the study, it is concluded that TRMM and its improved data had a good tendency to characterize the hydrological regime over the data sparse regions and also it is stated that gauge data were inevitable for validation of the study.

More comprehensive study for flood modeling system was performed by Hong et al., (2010) over the time span from 1998 to 2006. Global Flood Monitoring (GFM) framework that used near real time rainfall flux, TRMM (3-h time scale) dataset, was developed to build flood alert system for data sparse regions of the world. In the study TRMM precipitation dataset, global land surface database and curve number-based distributed hydrological model were used. Comparison of simulated runoff results with the Global Runoff Data Center (GRDC) runoff fields shows that the framework represents consistent runoff estimation and accurate flood detection.

Another evaluation study was performed by Su et al. (2008). In this study, precipitation estimates from 9 yr. of 3B42 (V6) dataset were evaluated with gauge data and the Variable Infiltration Capacity (VIC) hydrology model applied to La Plata basin. It is seen that in monthly time scale, sensible results were obtained, but in daily time scale, agreement between datasets were reduced due to the particularly for high rain rates. Moreover, the model results show that simulations with satellite data were able to capture daily flooding events. End of the study, it is emphasized that in data sparse regions TMPA data had a potential for hydrologic forecasting.

CHAPTER 3

STUDY AREA AND DATA

3.1 Description of the Study Area

Çoruh basin is located in the north-eastern part of Turkey, an area from 39°55’ to 41°32’ north latitude and 39°40’ to 42°39’ east longitude (Figure 3.1). Basin is surrounded by mountains of Tatos and Soğanlı to the north and Kop, Mescit and Kargapazarı to the south. Elevations of the mountains are generally more than 3000 m. River originates from Mescit mountain and flows north-eastern part of Anatolia and reaches Black sea after extending over Georgia. Median elevation of the basin is 1920 m. Total length of main river is 410 km and the length in Turkish territory is 390 km. The basin has a drainage area of approximately 20000 km^2 and is bounded by mainly the provinces: Bayburt, Erzurum and Artvin.

In Çoruh basin, continental climate is dominant. The annual precipitation amount is about 475 mm and about half of this rainfall amount comes in between March and June. Melting snow has a great effect on flow (Temelsu, 1982).

3.2 Data

Input data which are used in this study include satellite based precipitation data and ground based precipitation data for precipitation input, soil data and land use data for generating curve number, digital elevation model (DEM) for obtaining base of the model, and discharge data.

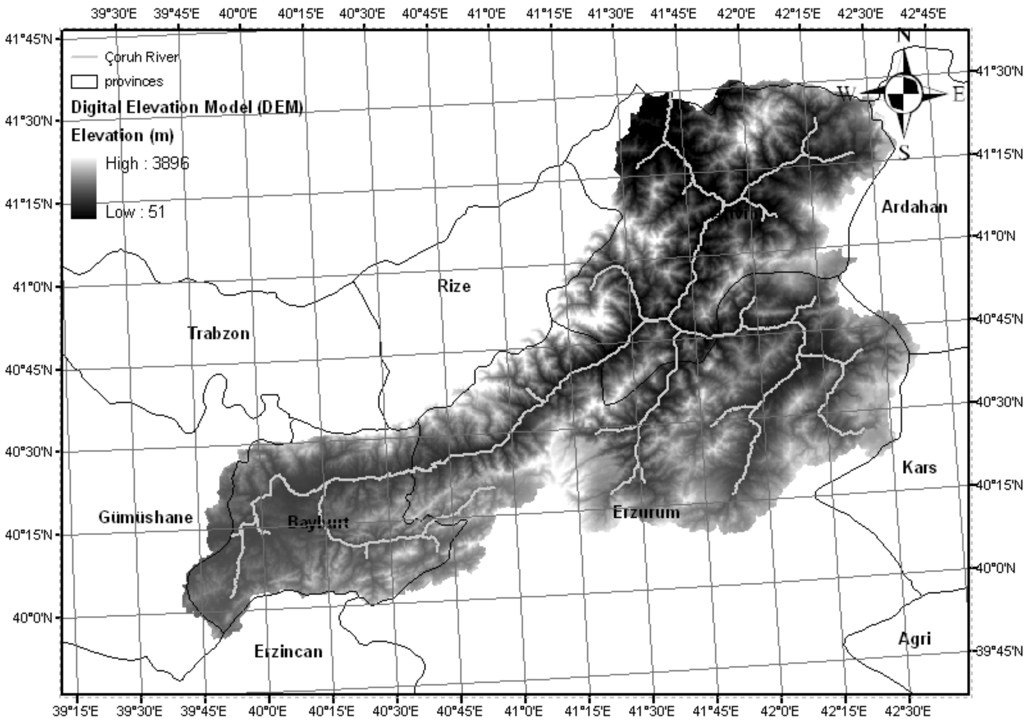

Figure 3.1 Digital Elevation Model (DEM) of Çoruh Basin

3.2.1 Precipitation Data

3.2.1.1 Ground Based Precipitation Data

For the study, meteorological station observations are used for ground based observations. Data from 250 meteorological stations were gathered from Turkish State Meteorological Service (Figure 3.2). The information on geographical location, id number, height, and cumulative rainfall amount for the period 1998-2008 of the selected stations, which are located in the study area are summarized in Table 3.1. In this table, cumulative rainfall amount of some stations are left as empty due to absence of long term data in the study.

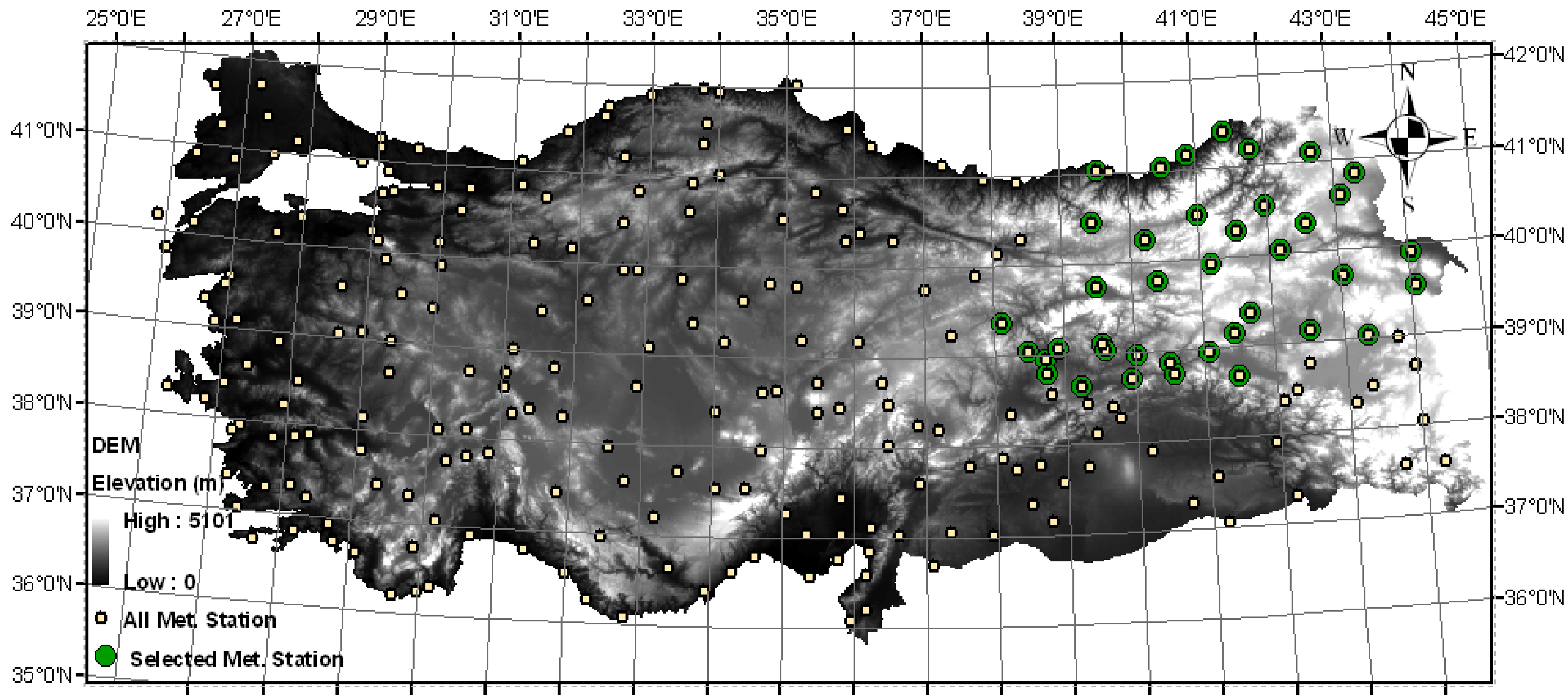

Figure 3.2 Distribution of meteorological stations in Turkey

Table 3.1 General Information about Meteorological Stations

Station Name	Station ID	Latitude (N)	Longitude (E)	Altitude (m)	Cumulated Rainfall Amount/year (mm) (derived from monthly values of 1998-2008 years)
Rize	17040	41°02'	40°30'	9	2337.8
Hopa	17042	41°24'	41°26'	33	2304.0
Pazar Rize	17628	41°10'	40°54'	79	2252.9
Artvin	17045	41°11'	41°49'	628	749.2
Akçaabat	17626	41°02'	39°33'	3	741.8
Mazgirt	17736	39°02'	39°36'	1400	710.7
Sarıkamış	17692	40°20'	42°34'	2102	656.5
Solhan	17776	38°58'	41°04'	1366	655.4
Ardahan	17630	41°07'	42°43'	1829	637.2
Karakocan	17774	38°58'	40°02'	1090	609.4
Hinis	17740	39°22'	41°42'	1715	563.5
Arpaçay	17656	40°51'	43°20'	1687	529.8
Tortum	17688	40°18'	41°33'	1572	498.4
Varto	17778	39°10'	41°27'	1650	485.6
Bayburt	17686	40°15'	40°14'	1584	483.7
İspir	17666	40°29'	41°00'	1222	479.4
Gümüşhane	17088	40°28'	39°28'	1219	473.4
Malazgirt	17780	39°09'	42°32'	1565	463.2
Ağrı	17099	39°43'	43°03'	1632	446.7
Tercan	17718	39°47'	40°23'	1425	439.2
Oltu	17668	40°33'	41°59'	1322	414.8
Horasan	17690	40°03'	42°10'	1540	412.2
Erzurum	17096	39°57'	41°10'	1758	404.8
Ercis	17784	39°02'	43°21'	1678	402.6
Doğubeyazıt	17720	39°33'	44°05'	1584	326.3
Iğdır	17100	39°55'	44°03'	858	275.5
Erzincan	17094	39° 44'	39° 29'	1218	-
Kars	17097	40° 36'	43° 05'	1775	-
Tunceli	17165	39° 06'	39° 32'	978	-
Elazığ	17201	38° 38'	39° 14'	990	-
Bingöl	17203	38° 51'	40° 29'	1177	-
Muş	17204	38° 40'	41° 28'	1320	-

Table 3.1 General Information about Meteorological Stations (cont.)

Divriği	17734	39° 21'	38° 06'	1225	-
Arapkır	17764	39° 02'	38° 29'	1200	-
Ağın	17766	38° 57'	38° 43'	900	-
Cemişgezek	17768	39° 03'	38° 54'	953	-
Keban	17804	38° 47'	38° 44'	808	-
Palu	17806	38° 42'	39° 57'	1000	-
Genç	17808	38° 44'	40° 33'	1250	-

*Underlined station names are used in only daily based comparisons, other stations are used in both monthly and daily based comparisons

3.2.1.2 Satellite Based Precipitation Data

In this study two TRMM products are used, 3B43 (monthly temporal resolution) and 3B42 (daily temporal resolution). In modeling due to the time restriction (maximum time interval can be one day) only 3B42 is used but the comparison studies are done for both products. Data were gathered through TOVAS system (http://gdata1.sci.gsfc.nasa.gov/daacbin/G3/gui.cgi?instance _id=TRMM_Monthly (NASA, 2010)).

For modeling study, 730 precipitation layers of 3B42 (daily), for comparison study, 132 precipitation layers of 3B43 (monthly) were downloaded. To download data from TOVAS, first, area of interest is defined (Figure 3.3), and then with the selection of time interval, data are visualized. There are four format types to download data, HDF, NetCDF, ASCII, and Google Earth KMZ. In this study, results are downloaded using NetCDF format to operate in ArcGIS.

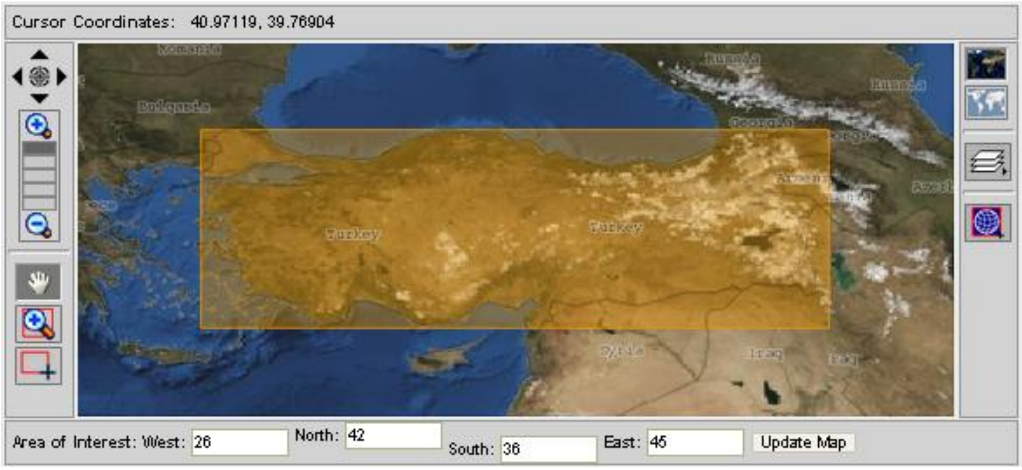

Figure 3.3 Data downloading from TOVAS

3.2.2 Soil Data

To predict direct runoff or infiltration from rainfall, curve number is a parameter to use in hydrology (United States Department of Agriculture, 1986). Curve number represents the soil characteristics; large number indicates high surface runoff potential while low numbers are for decreasing surface runoff potential.

In this study using the land cover layer information obtained from the Ministry of Agriculture and Rural Affairs about the Çoruh basin, hydrologic soil group determination is implemented. All layers are cut in ArcGIS with respect to location and then letters are defined with the help of average runoff conditions for land use which was defined by Kızılkaya (1983; see Appendix C). The result of the soil groups can be seen Figure 3.4

- Great soil groups (basaltic, alluvial, colluvial, organic soil…)
- Land use capability classes (arable land and its classes, land unsuitable for agriculture)
- Degree of erosion (water erosion and its classes)

- Depth (dense soil and its classes)

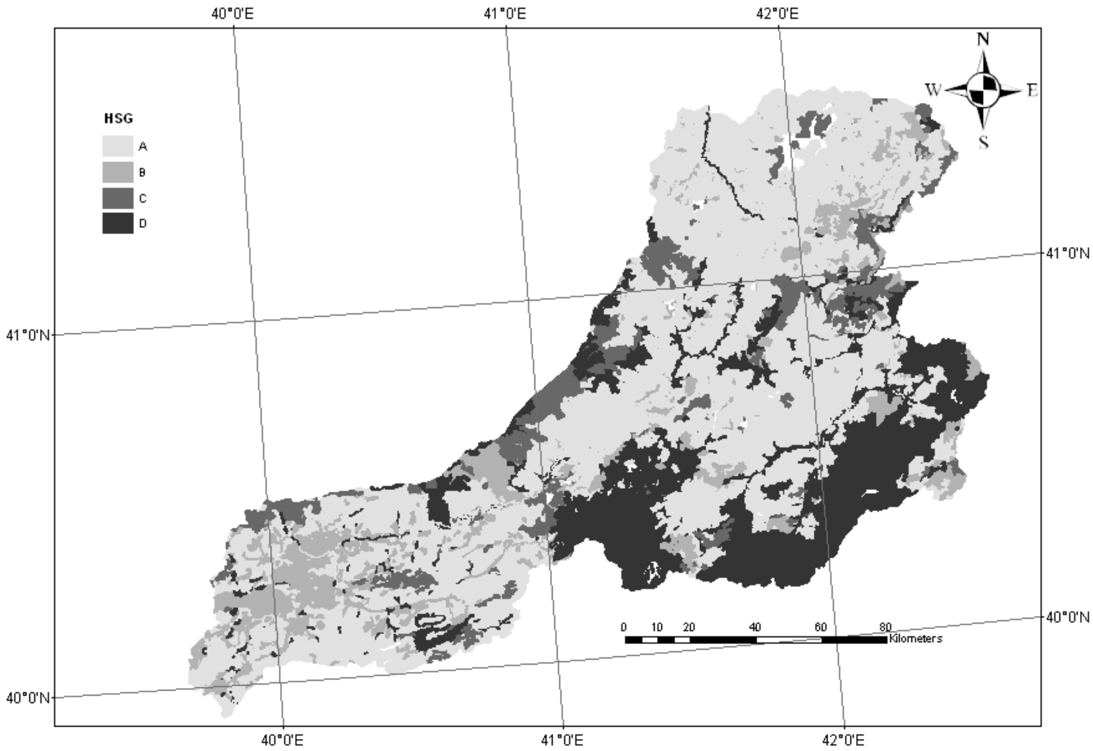

Figure 3.4 Hydrologic soil group representation

To represent soil characteristics as a curve number, land use information which is obtained from CORINE (Coordination of Information on the Environment) is used (Figure 3.5). CORINE is founded by European Union Global Monitoring for the Environment and Security (GMES) to reach to an environmetally sensitive land use decision and to detect land use changes in a more timely manner (Ministry of Environment and Forestry, 2010). Using this land use data and hydrologic soil group curve number determination is accomplished (Figure 3.6).

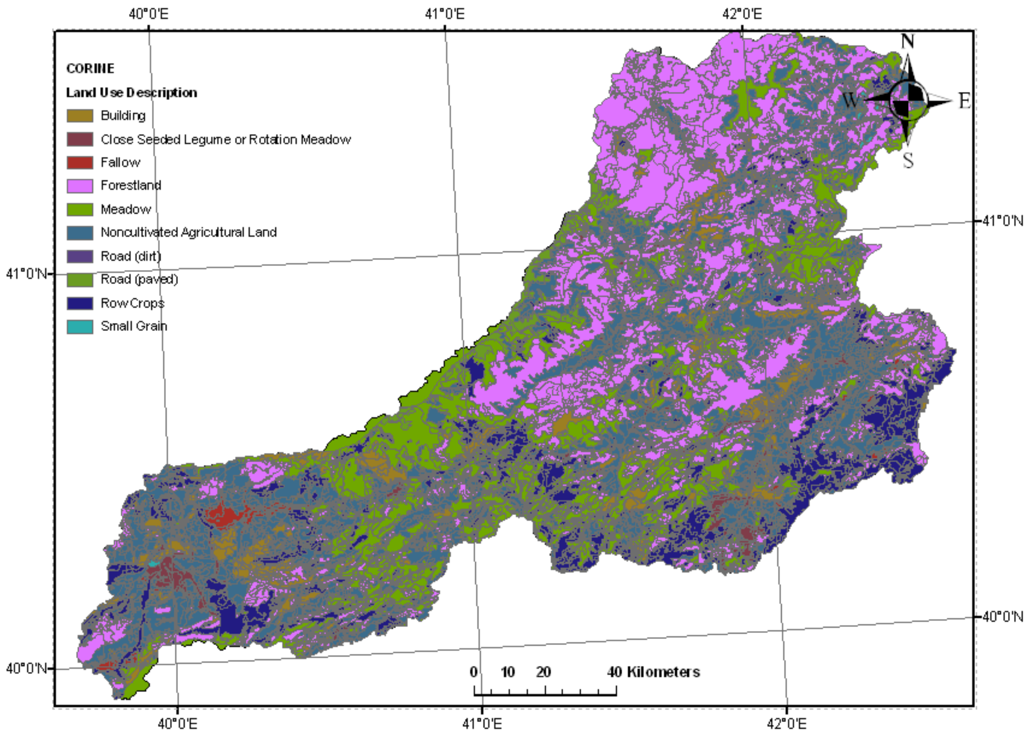

Figure 3.5 CORINE land use description

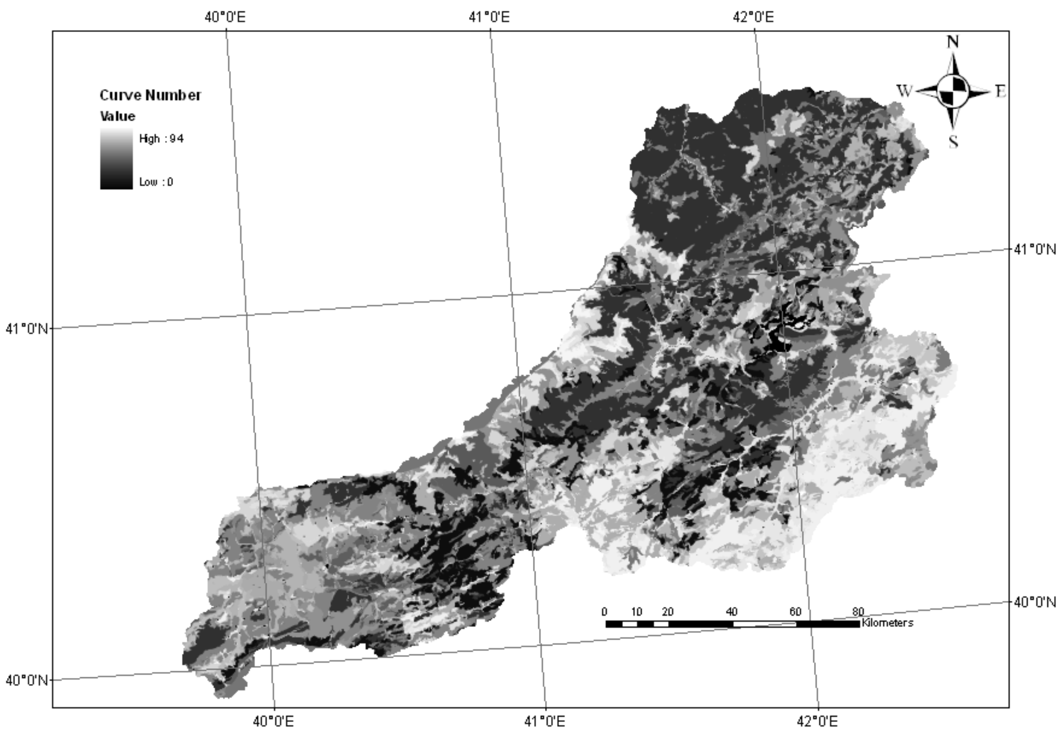

Figure 3.6 Curve number representation

3.2.3 Basin Preprocessing

To derive stream delineation, series of steps are performed in ArcGIS with the extension of ArcHydro. With the availability of digital elevation model (DEM) (Figure 3.1) and GIS tools, steps which are indicated below are executed.

- Fill sinks: This function modifies the depression cells which cause the water trap due to the higher elevation surround those cells. In order to determine flow direction, depressions are increased (Figure 3.7).

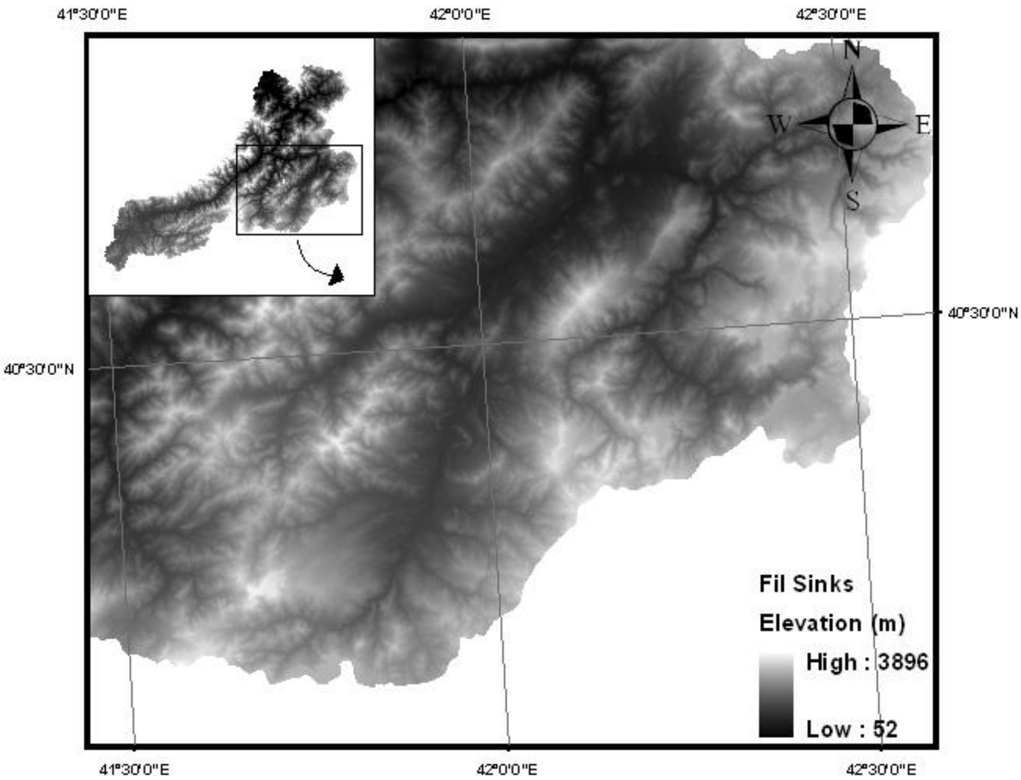

Figure 3.7 Fill sinks

- Flow direction: For a given grid, this function determines the flow direction. The values in the cell indicate the eight possible flow direction, 1 (east), 2 (southeast), 4 (south), 8 (southwest), 16 (west), 32 (northwest), 64 (north), 128 (northeast) (Figure 3.8).

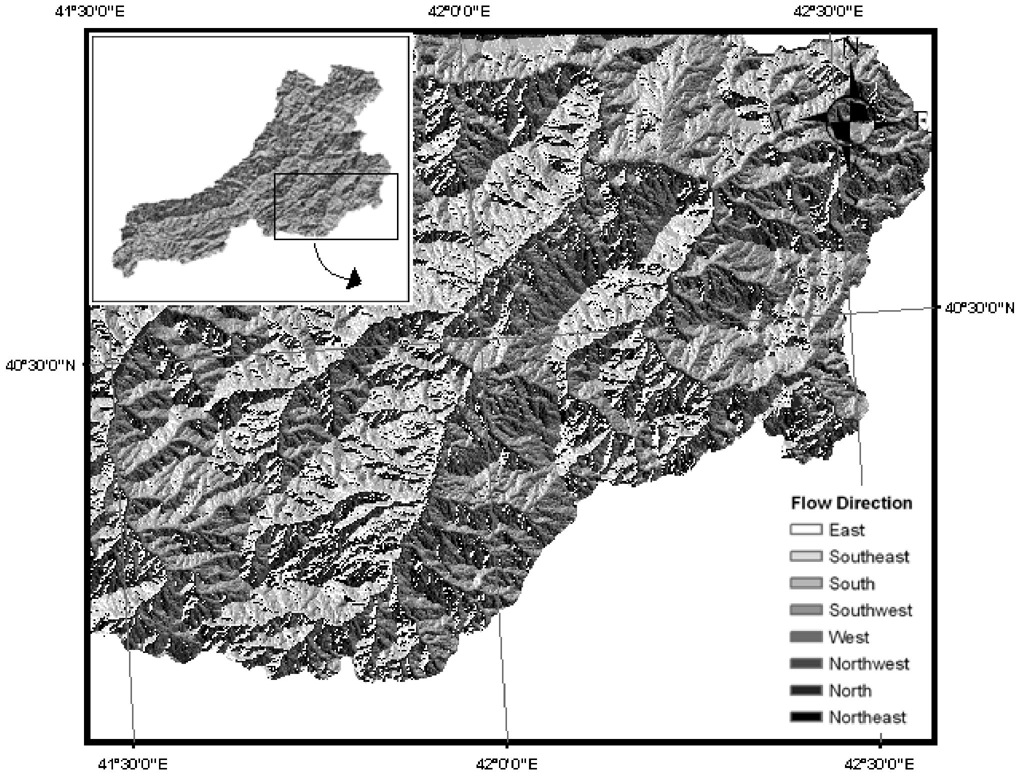

Figure 3.8 Flow direction

- Flow accumulation: This function calculates the accumulated number of cells in upstream which drain to the given cell (Figure 3.9).
- Stream definition: This function determines the stream network. For this purpose river threshold value is given. Smaller threshold represents the denser network and greater number of catchments. To define stream initiation, cell must exceed the user defined value. In this study, one percent (1%) of the maximum flow accumulation is selected (Figure 3.10).
- Stream segmentation: This function creates stream segments by dividing the stream developed in the previous step

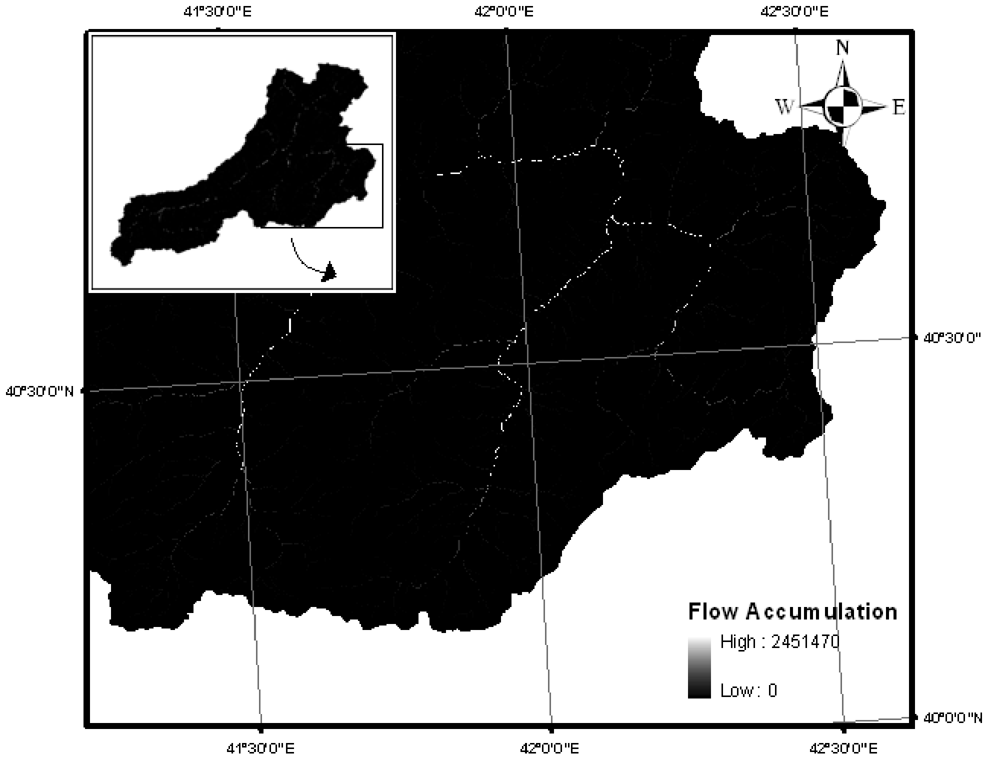

Figure 3.9 Flow accumulation

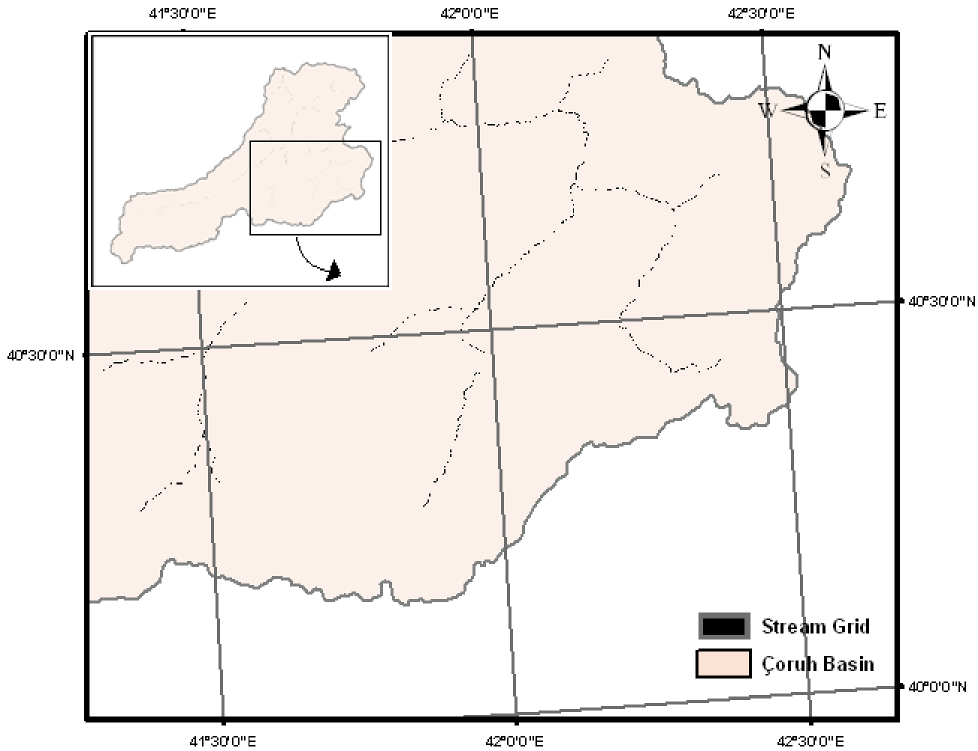

Figure 3.10 Stream definition

- Watershed delineation: This function delineates subbasin for each stream segment (Figure 3.11).

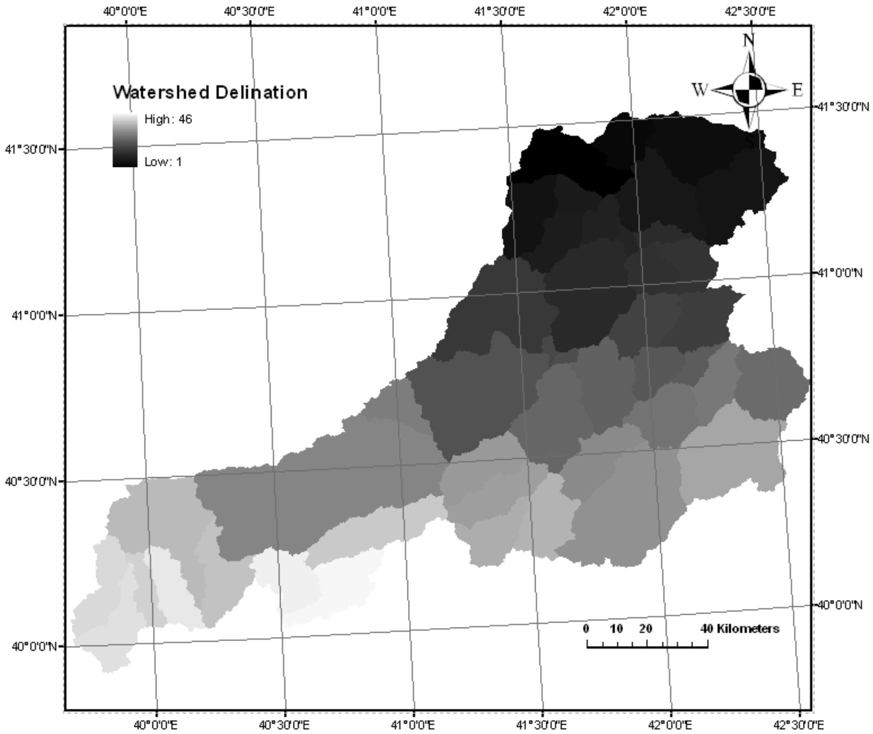

Figure 3.11 Watershed delineation

- Watershed polygon processing, watershed aggregation and stream segment processing: These three functions convert raster data to vector format (Figure 3.12 and 3.13).

3.2.4 Discharge Data

At the end of modeling studies, to compare the simulated runoff result, actual discharge data are required. For this purpose, from General Directorate of Electrical Power Resources survey and Development Administration, daily discharge data of station EIE 2323 are obtained from BAP-03-03-2009-05.

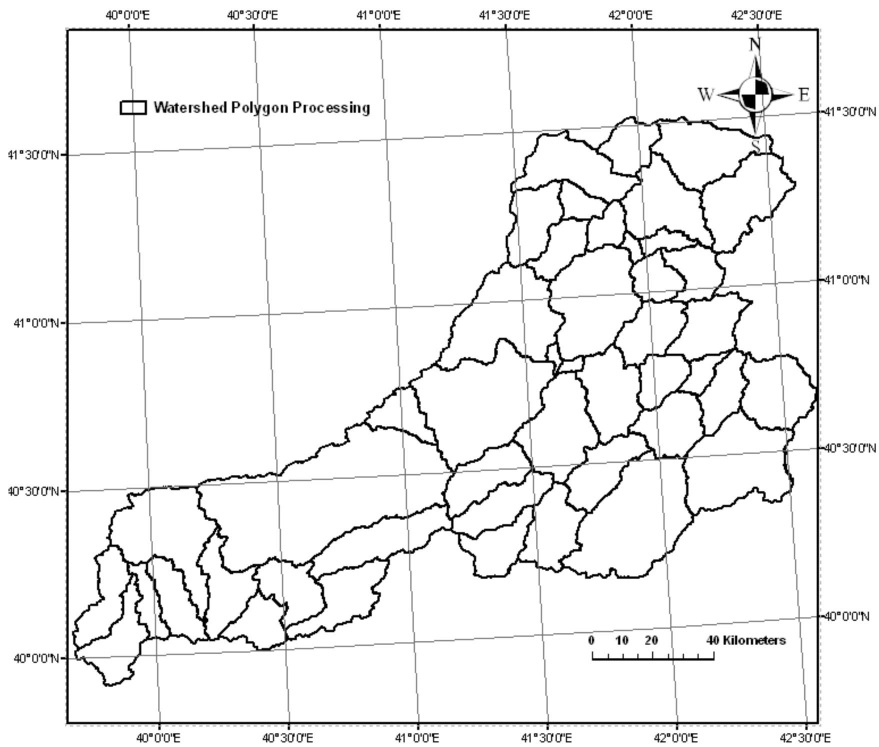

Figure 3.12 Watershed polygon processing

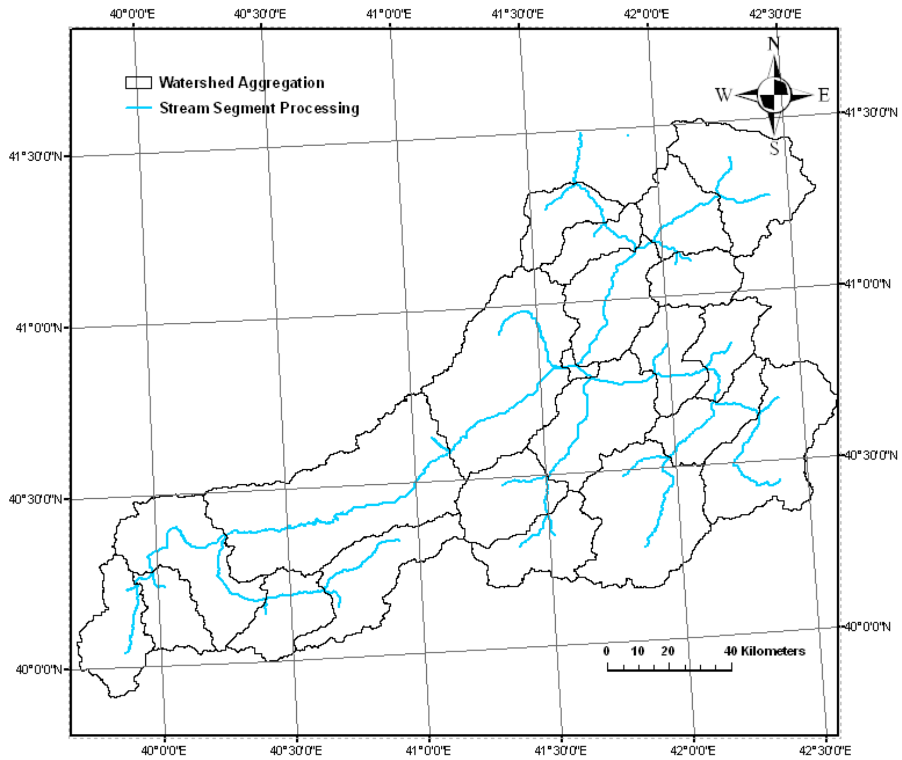

Figure 3.13 Watershed aggregation and stream segment processing

CHAPTER 4

COMPARISON OF TRMM (V6) WITH RAINGAUGE DATA

Comparisons are performed in two sections. In the first section, monthly based rainfall comparisons are done with the data obtained from TRMM 3B43 (V6) and 26 meteorological stations. In the second one, daily based rainfall comparisons are performed with the data obtained from TRMM 3B42 (V6) and 39 meteorological stations.

4.1 Comparison of TRMM 3B43 (V6) with Raingauge Data

In this part of the study, for the period from January 1998 to December 2008, TRMM 3B43 (V6) distributed precipitation data and observations from meteorological station network are compared for Çoruh basin and near sites. As shown in Figure 4.1, on the Digital Elevation Model (DEM), 26 meteorological stations are selected for the analysis. The selected stations' information is tabulated in Table 3.1 (first 26 stations).

TRMM 3B43 (V6) pixel values corresponding to the meteorological stations are processed in ArcGIS. An example of the satellite product and meteorological observations is given in Figure 4.2. It is taken into consideration that ground based data represents point, satellite based data represents distributed data.

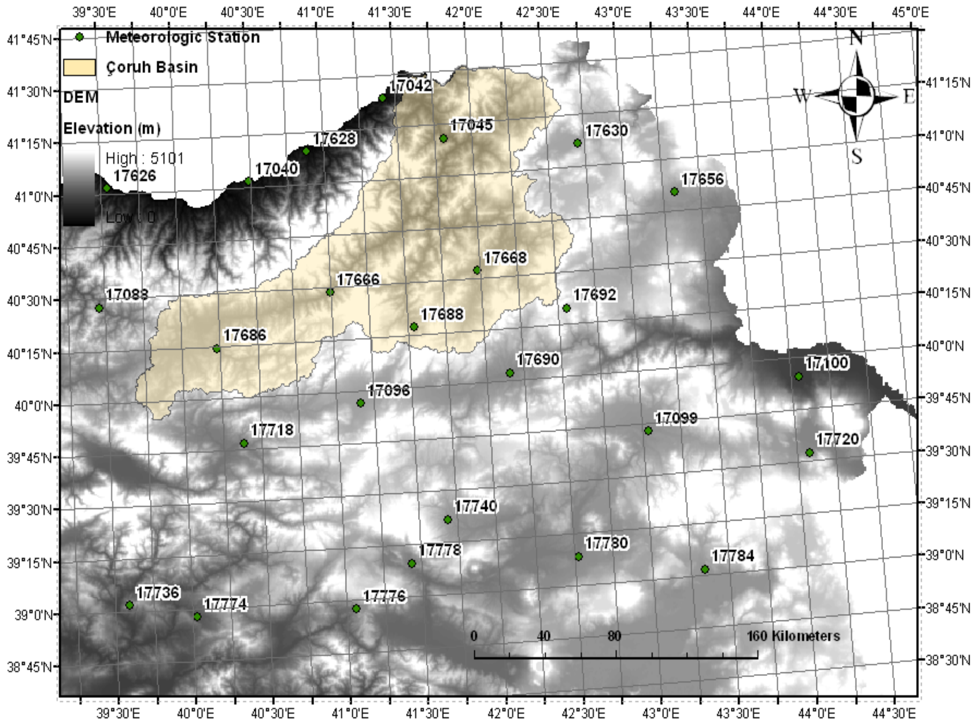

Figure 4.1 Distribution of the meteorological stations over the DEM

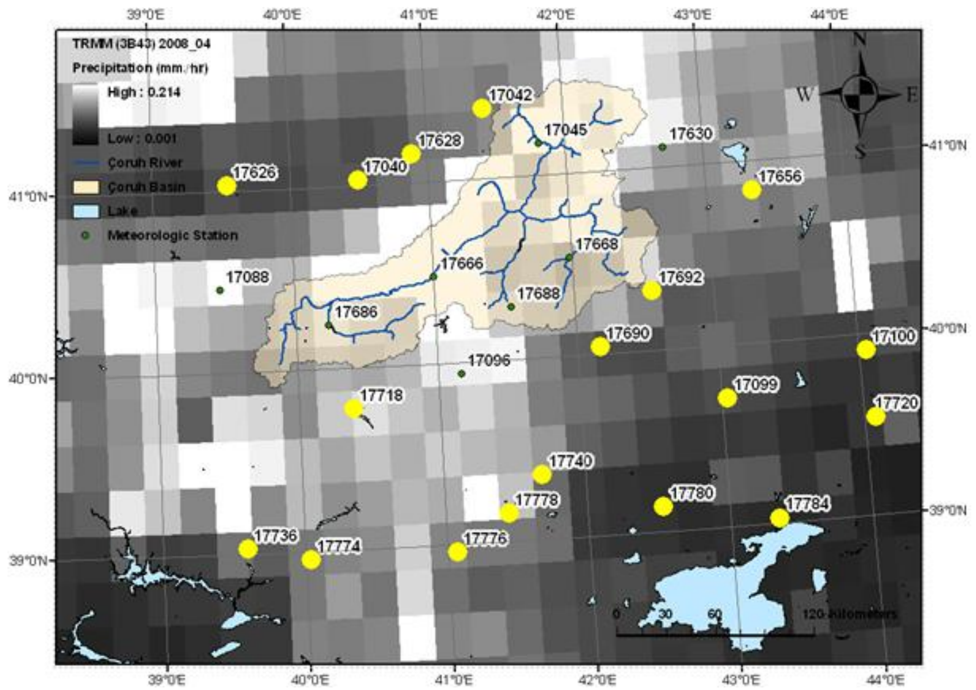

Figure 4.2 Meteorological stations over the TRMM 3B43 (V6) precipitation data (2008 April precipitation data (mm/hr))

4.1.1 Comparison of Cumulative Rainfall Distribution

In order to see accumulated mean monthly rainfall differences between ground and TRMM 3B43 (V6) data Figure 4.3 is constructed by averaging the precipitation values of 26 meteorological stations and corresponding TRMM 3B43 (V6) pixels.

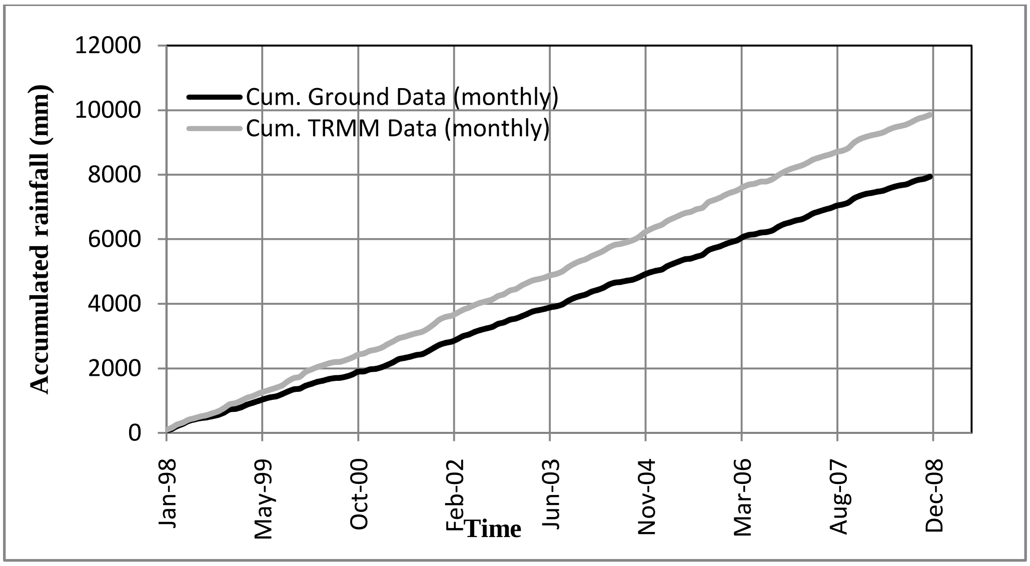

Figure 4.3 Accumulated mean monthly rainfall

From Figure 4.3, it is seen that, there is a 20% overestimation of rainfall obtained from accumulation of TRMM 3B43 (V6) products with respect to ground data. Moreover, the slopes of the lines do not change in the studied time period, so it can be said that the regime of the rainfall does not change in that period.

Another comparison is done by summing all precipitation values for each pixel and meteorological stations in time period from January 1998 to December 2008. The precipitation distribution can be seen in Figures 4.4 and 4.5.

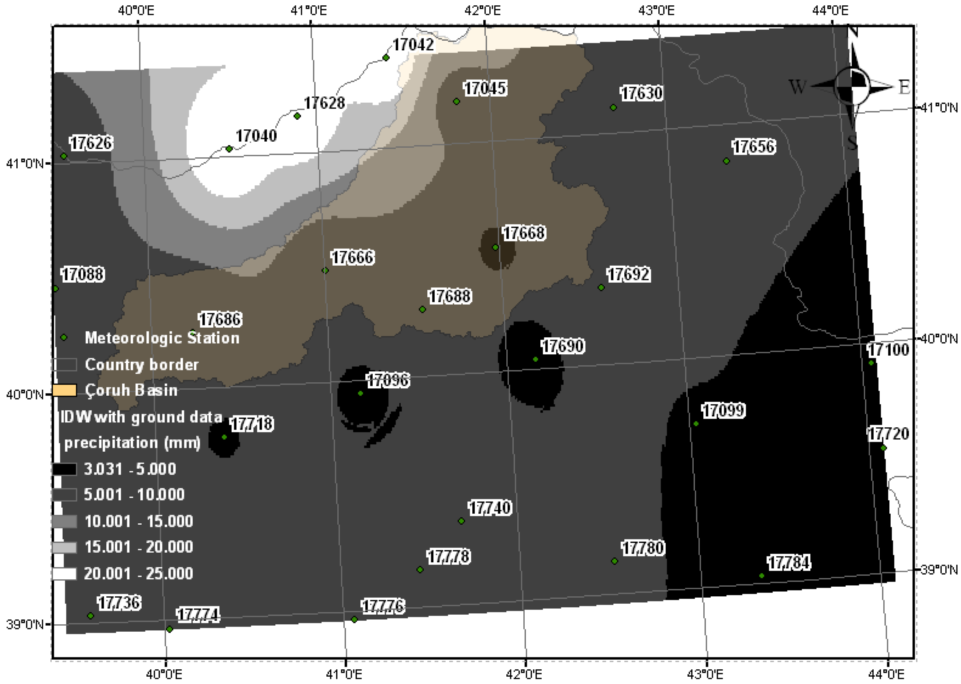

Figure 4.4 Distribution of accumulated precipitation values using ground data with IDW method

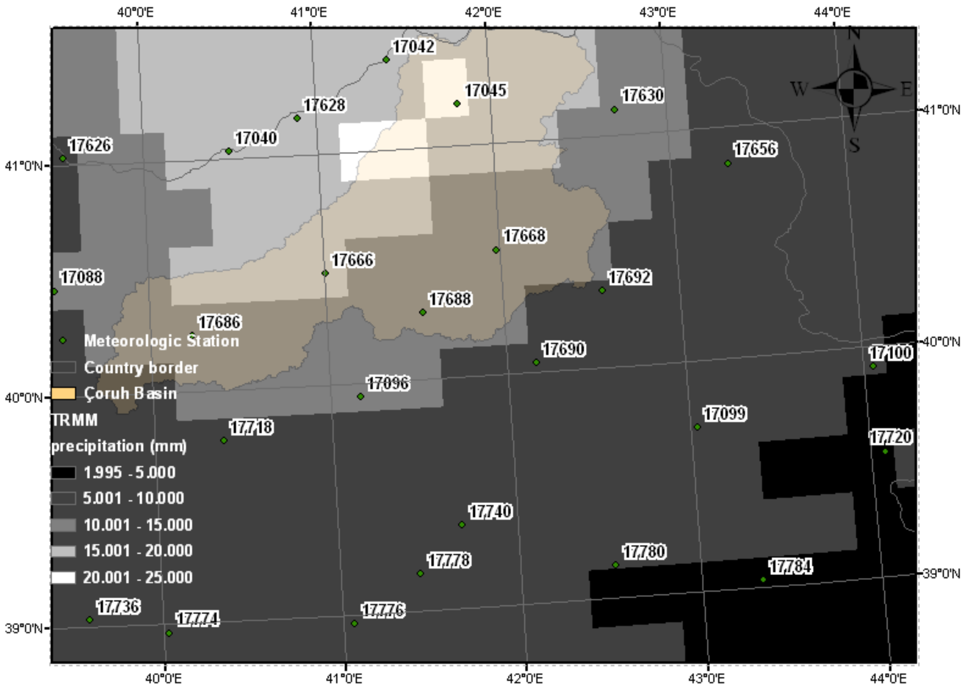

Figure 4.5 Distribution of accumulated precipitation values using TRMM 3B43 (V6) data

Figure 4.4 and 4.5 show the spatial distribution of the accumulated values. In these figures, there is a north-south gradient in the rainfall. In Figure 4.4, inverse distance weighted (IDW) method seems to capture orographic precipitation, but the TRMM 3B43 (V6) (Figure 4.5) does not. This is due to low resolution of the TRMM 3B43 (V6) data. In order to see longitude, latitude and elevation effect on the accumulated ground based rainfall values of meteorological stations, the correlation coefficients are obtained (Table 4.1). To obtain this table, for each station, all precipitation values are accumulated with respect to different time span (annual, winter, spring, summer and autumn) and then correlation coefficients (R^2) are formed with respect to longitude, latitude and elevation.

Table 4.1 Correlations between ground based accumulated rainfall from Jan 1998 to Dec 2008 and respective longitude, latitude and elevation at 26 meteorological stations in Çoruh basin and near sites

Correlation coefficient (R^2)	Annual	Winter	Spring	Summer	Autumn
Longitude (°)	0.075	0.142	0.124	0.002	0.074
Latitude (°)	0.287	0.145	0.023	**0.551**	0.307
Elevation (m)	**0.572**	**0.625**	0.195	0.390	**0.630**

From Table 4.1, it is pointed out that, rainfall derived from meteorological stations correlated with latitude in summer season (greater that 0.5). The rainfall based on meteorological stations is significantly correlated with elevation (greater than 0.5) in the autumn, winter and annual scale. Thus, it can be concluded that spatial distribution of ground rainfall values in Çoruh basin is mainly influenced by elevation and the latitude is the secondary factor.

4.1.2 Comparison of TRMM 3B43 (V6) Pixel Values with Raingauge Data

In extracting TRMM 3B43 (V6) pixel values corresponding to the meteorological station values two approaches are applied. In the first approach, the pixel value of the satellite data corresponding to the meteorological station location is extracted. In the second one the same approach is applied for the neighbourhood pixels which are the nearest pixels of corresponding meteorological station.

Comparisons are based on visual interpretation and linear regression method. Linear regression method is used because it is a measure of how satellite observation fit the ground observations. P_{sat} and P_{met} represent the satellite and meteorological station data respectively (Eq. 4.1).

$$P_{sat}=m*P_{met}+b \qquad \text{(Eq. 4.1)}$$

where, m: slope, b: intersection point.

4.1.2.1 Direct Point Pixel Comparison

Using linear regression method, 11 year precipitation data are evaluated for 26 meteorological stations. In order to see averaged monthly comparison of TRMM 3B43 (V6) and meteorological stations, Figures 4.6 and 4.7 are composed. The computed slope (m) and square root of correlation coefficient (r) values of the linear regression model are given in Table 4.2 for different time scales. Root mean square error (RMSE) variation for the stations is depicted in Figure 4.8.

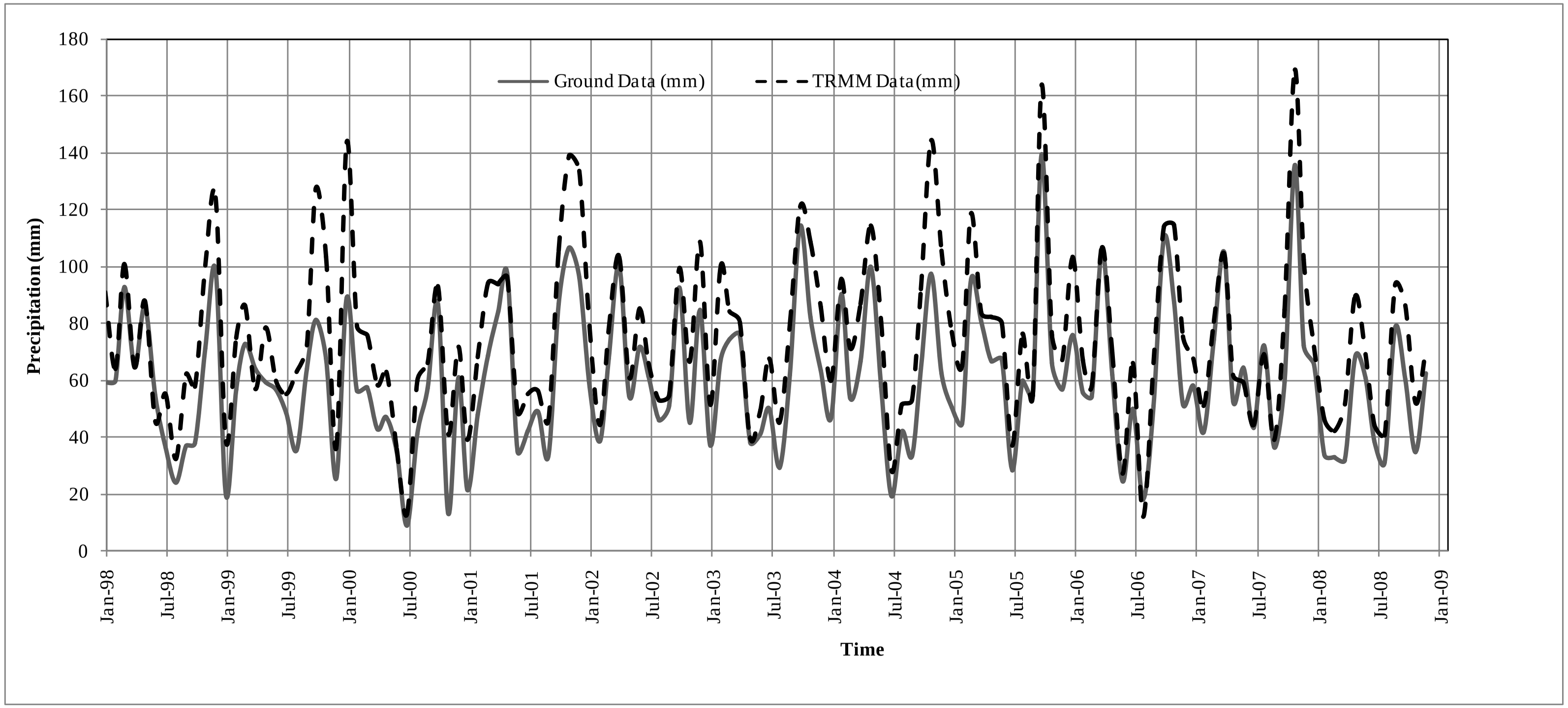

Figure 4.6 Average monthly rainfall diagrams (average of monthly precipitation values of 26 stations and corresponding TRMM 3B43 (V6) values)

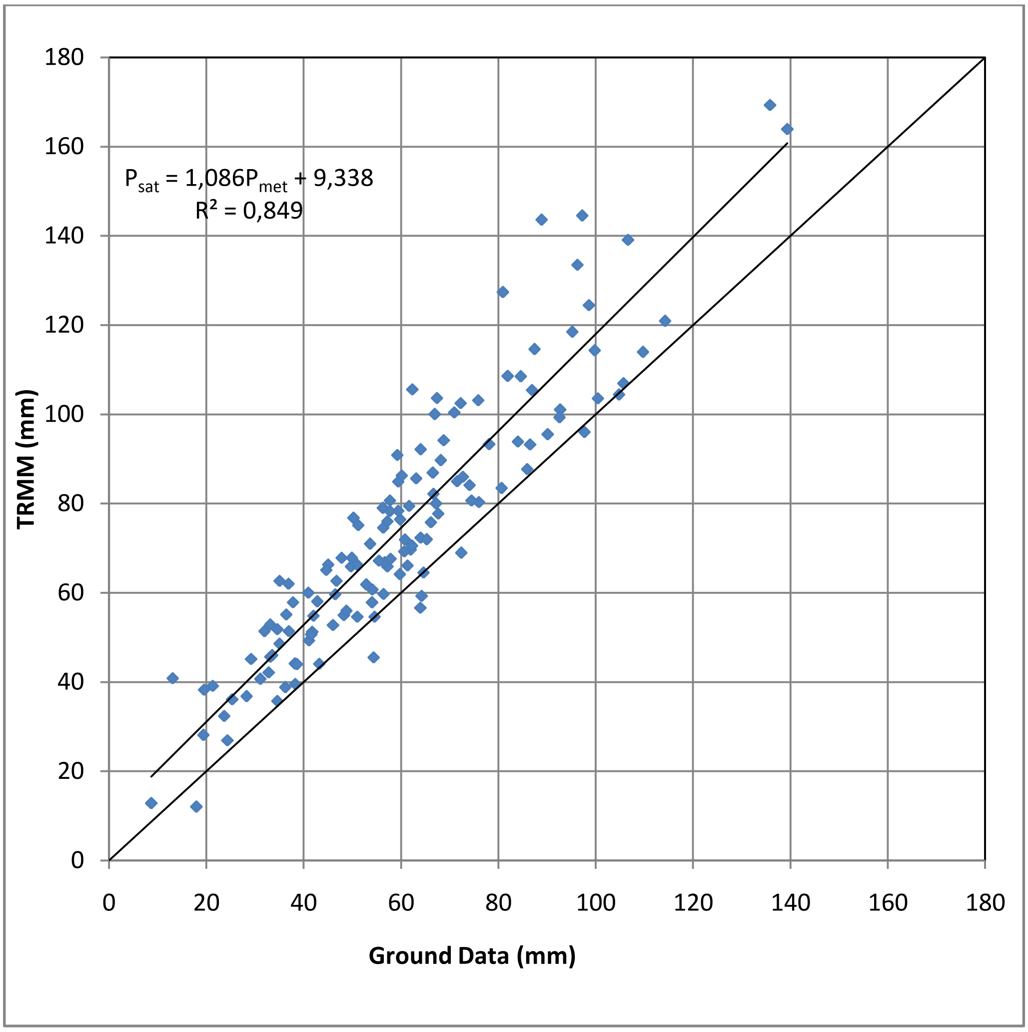

Figure 4.7 Average monthly values TRMM 3B43 (V6) vs. Ground Observations

The averaged monthly precipitation values of 26 meteorological stations and corresponding TRMM 3B43 (V6) values show that, there is an overestimation of TRMM 3B43 (V6) data but both dataset are significantly correlated with each other (r = 0.921).

Table 4.2 TRMM 3B43 (V6) and meteorological stations comparison results

Station No.	Station Name	Monthly Base										Seasonal Base								Annual Base	
		RMSE	GD min	TD min	GD max	TD max	GD mean	TD mean	r	m	Winter		Spring		Summer		Autumn				
											r	m	r	m	r	m	r	m	r	m	
17040	**Rize**	93.3	23.0	22.1	507.8	385.1	194.8	127.2	**0.81**	0.58	0.38	0.51	**0.78**	0.65	0.13	0.08	0.49	0.36	0.07	0.12	
17042	**Hopa**	80.9	9.3	16.0	607.5	428.9	192.0	139.3	**0.86**	0.59	**0.84**	1.23	**0.84**	0.64	**0.78**	0.47	0.65	0.54	0.68	0.54	
17045	Artvin	113.0	4.4	28.3	217.5	426.3	62.4	157.6	0.58	1.03	0.14	0.23	0.44	0.72	0.49	1.26	0.57	0.95	0.47	1.13	
17088	Gümüşhane	67.0	0.0	3.1	133.4	277.6	39.4	90.9	0.58	1.14	0.16	0.22	0.48	0.41	**0.71**	1.63	0	0.03	0.2	0.32	
17096	Erzurum	56.4	0.1	11.6	121.7	204.2	33.7	82.0	0.6	0.85	0.58	1.33	**0.76**	0.89	**0.89**	0.85	0.3	0.54	0.59	0.93	
17099	**Ağrı**	23.7	0.0	2.1	128.5	111.0	37.2	46.3	**0.7**	0.55	0.04	0.04	0.56	0.41	0.67	0.92	0.62	0.43	0.21	0.25	
17100	**Iğdır**	18.6	0.0	1.2	96.9	101.7	23.0	37.1	**0.85**	0.95	**0.72**	1.39	**0.72**	0.87	**0.88**	1.39	**0.84**	1.14	**0.78**	1.31	
17626	**Akçaabat**	26.9	2.6	7.4	195.9	217.5	61.8	66.7	**0.8**	0.78	0.07	0.06	0.21	0.3	**0.85**	1.1	0.43	0.29	0.6	0.79	
17628	**Pazar Rize**	86.6	21.1	15.8	703.2	494.8	187.7	137.8	**0.8**	0.56	0.53	0.53	**0.71**	0.63	0.44	0.23	0.45	0.45	0.36	0.3	
17630	Ardahan	51.3	2.9	20.3	174.8	171.8	53.1	87.4	0.44	0.38	0.61	1.1	0.49	0.54	**0.78**	0.86	0.66	0.7	**0.82**	1	
17656	**Arpaçay**	27.5	0.0	4.5	147.5	137.0	44.1	60.9	**0.79**	0.68	0.56	1.48	0.5	0.4	**0.94**	1.04	**0.91**	0.83	**0.78**	1.08	
17666	İspir	89.1	0.0	17.8	142.7	289.9	39.9	117.2	0.53	1.01	0.35	0.59	**0.8**	0.95	0.38	0.58	0.06	-0.09	0.1	0.1	
17668	Oltu	51.4	0.1	19.4	112.5	146.5	34.6	79.7	0.58	0.67	0.38	1.13	0.52	0.76	**0.82**	0.85	0.67	0.92	0.67	0.67	
17686	Bayburt	72.9	0.0	7.3	145.3	257.9	40.5	95.3	0.39	0.69	0.29	0.82	**0.79**	0.8	0.41	0.55	0.6	-1.21	0.08	0.24	
17688	Tortum	56.9	0.1	16.7	130.2	221.9	41.5	88.1	0.46	0.57	0.51	1.15	**0.84**	0.77	**0.91**	0.64	0.27	0.44	0.55	0.48	
17690	**Horasan**	28.2	0.3	7.5	116.1	128.5	34.3	57.1	**0.78**	0.74	0.62	1.49	**0.85**	0.6	0.65	0.61	**0.86**	0.8	**0.73**	0.65	
17692	**Sarıkamış**	24.3	0.0	6.8	150.0	133.4	54.7	63.9	**0.77**	0.61	0.63	0.57	**0.85**	0.58	0.67	0.5	0.69	0.58	**0.9**	0.77	

Table 4.2 TRMM 3B43 (V6)and meteorological stations comparison results (cont.)

Station No.	Station Name	Monthly Base									Seasonal Base								Annual Base	
		RMSE	GD min	TD min	GD max	TD max	GD mean	TD mean	r	m	Winter		Spring		Summer		Autumn			
											r	m	r	m	r	m	r	m	r	m
17718	**Tercan**	39.4	0.0	1.7	127.4	166.7	36.6	67.5	**0.74**	0.91	**0.7**	1.16	0.68	0.62	**0.93**	0.93	0.55	0.43	0.47	0.42
17720	**Doğubeyaz**	16.4	0.0	1.2	87.0	104.3	27.2	33.6	**0.76**	0.81	0.55	0.56	**0.87**	1.04	0.55	0.66	**0.81**	0.83	**0.74**	0.88
17736	**Mazgirt**	33.7	0.0	0.4	211.3	123.7	59.2	47.7	**0.82**	0.52	**0.86**	0.65	0.68	0.4	0.46	0.37	**0.82**	0.45	**0.88**	0.61
17740	**Hinis**	21.7	0.0	0.0	171.6	110.5	47.0	42.9	**0.83**	0.58	**0.77**	0.58	**0.8**	0.49	**0.81**	0.77	**0.87**	0.65	**0.87**	0.52
17774	**Karakocan**	22.5	0.0	0.6	175.1	157.4	50.8	54.4	**0.87**	0.72	**0.92**	0.89	**0.92**	0.48	0.47	0.75	0.64	0.37	**0.87**	0.6
17776	**Solhan**	24.2	0.0	0.4	181.2	142.0	54.6	50.9	**0.86**	0.64	**0.74**	0.5	**0.7**	0.44	**0.86**	1.11	**0.89**	0.89	**0.75**	0.69
17778	**Varto**	25.6	0.0	0.0	185.2	123.6	40.3	39.1	**0.81**	0.59	0.69	0.27	**0.72**	0.39	0.66	0.69	**0.82**	0.63	**0.94**	0.81
17780	**Malazgirt**	20.0	0.0	2.5	165.8	97.3	38.6	38.1	**0.81**	0.56	0.55	0.6	**0.72**	0.39	0.65	0.88	**0.75**	0.49	**0.77**	0.33
17784	**Ercis**	15.9	0.0	0.7	148.7	100.9	33.5	31.9	**0.86**	0.6	**0.87**	0.6	**0.77**	0.43	0.47	0.44	**0.89**	0.56	**0.86**	0.61

GD: Ground Data, TD: TRMM Data

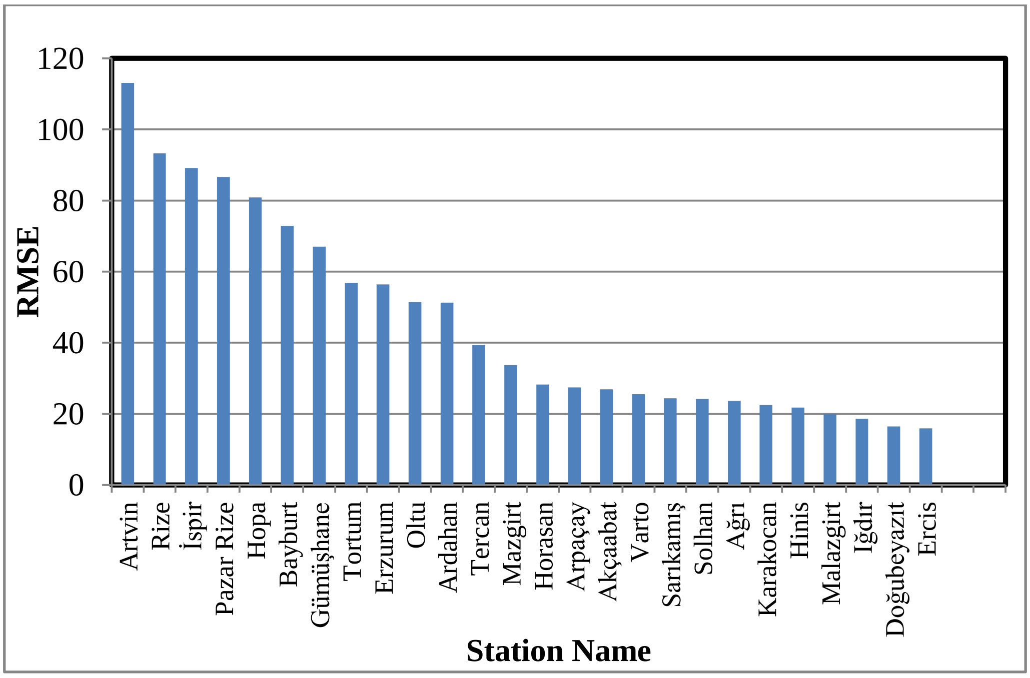

Figure 4.8 RMSE values vs. data of meteorological stations

The overestimations of TRMM 3B43 (V6) are seen for the autumn rainfalls. For 18 stations among 26 stations, the correlation coefficient is obtained greater than 0.7 where those stations are represented as bold in Table 4.2. And distribution of these stations on the TRMM 3B43 (V6) layer can be seen (yellow color) in Figure 4.2. The obtained correlation coefficient indicates the scattering of satellite observations with respect to ground observations. In addition to correlation coefficient, slope of the fitted line ‘m’ is also presented in Table 4.2. The stations having m value close to 1.0 and r value larger than 0.7, are Iğdır, Akçaabat, Horasan, Tercan, Doğubeyazıt, and Karakoçan. It is obvious to observe from Figure 4.8 lower RMSE (lower than 40) values for these stations indicating the satellite based rainfall observations are fitted properly with the ground based stations.

For the two stations, Karakocan and Bayburt which have the best and worst correlation coefficients, scatter plot diagrams and precipitation vs. time graphics are presented in Figures 4.9 - 4.12, respectively.

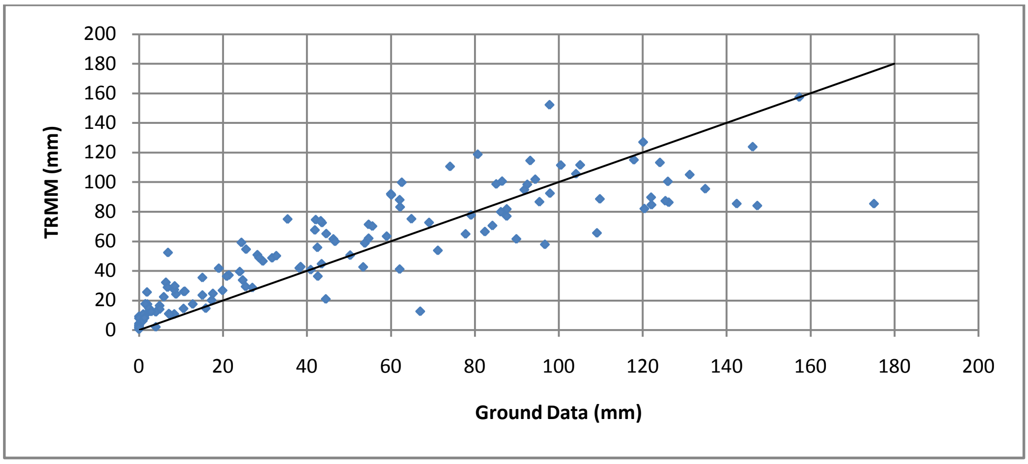

Figure 4.9 TRMM 3B43 (V6) vs. Ground Obser. (monthly) 17774 Karakoçan

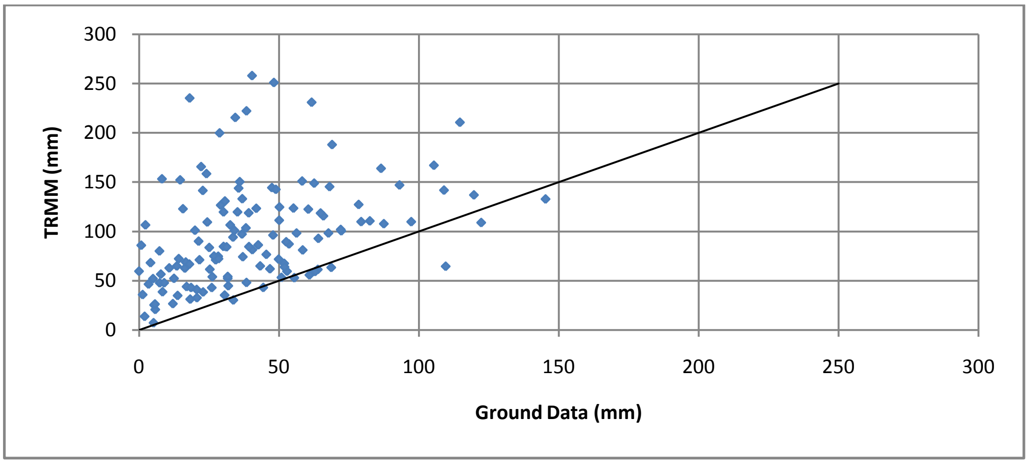

Figure 4.10 TRMM 3B43 (V6) vs. Ground Obser. (monthly) 17686 Bayburt

Other selected comparisons which have best, worst and average correlation coefficient results can be seen in Appendix A. In order to see the altitude of meteorological station effect on the comparison, slope of the fixed line and the correlation coefficient vs. altitude graph is formed (Figure 4.13).

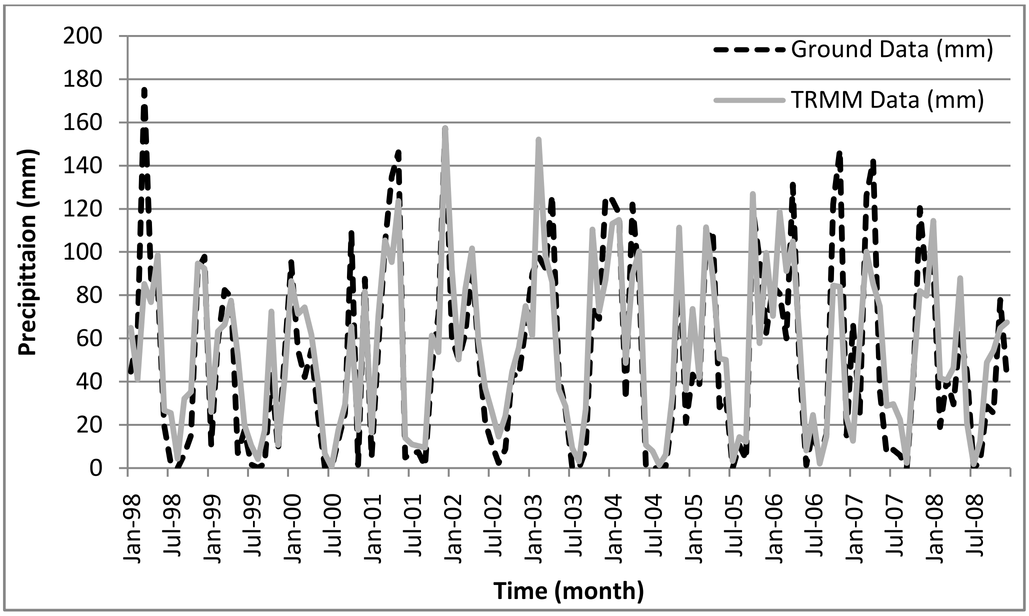

Figure 4.11 Monthly Rainfall Diagrams for 17774 Karakoçan

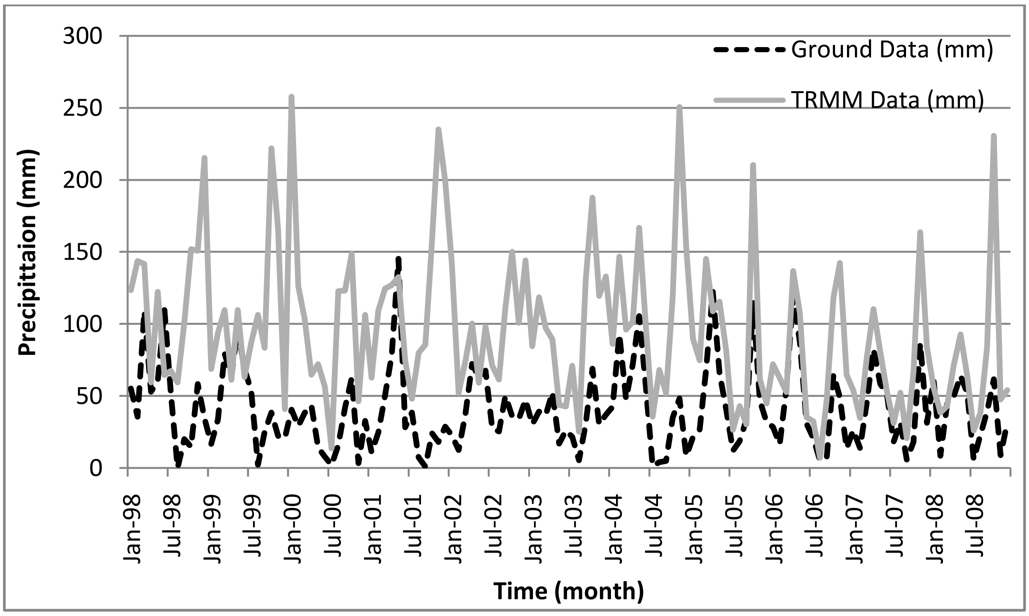

Figure 4.12 Monthly Rainfall Diagrams for 17686 Bayburt

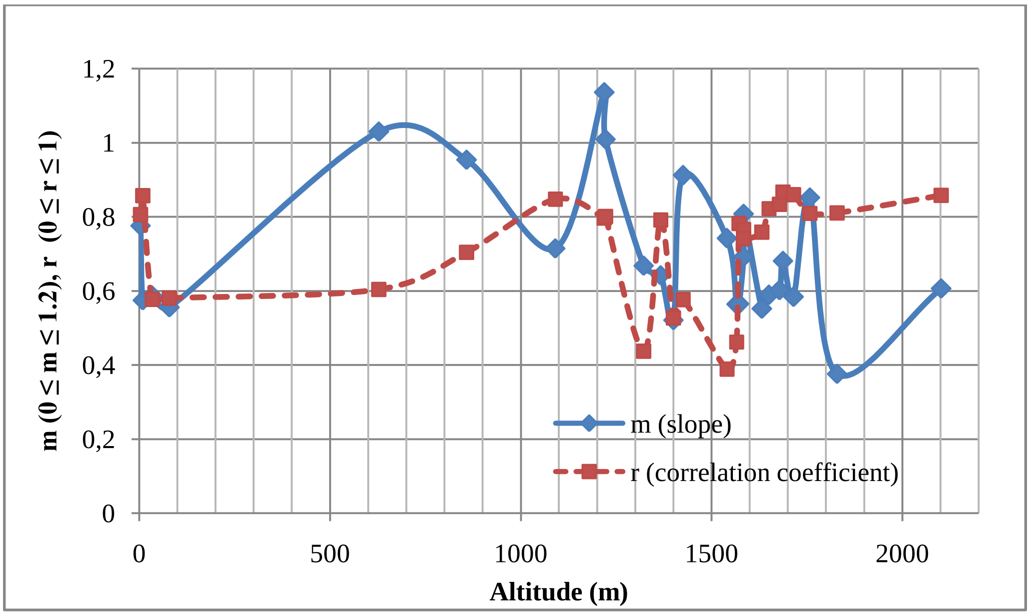

Figure 4.13 Comparison of m (slope) and r (correlation coefficient) vs. altitude

4.1.2.2 Point Neighbourhood Pixel Comparison

Meteorological station may not be located in the middle of the pixel. Thus, another comparison study is performed with the neighbourhood pixels which are the nearest pixels of corresponding meteorological station. To make the study easier, station id numbers are reordered by attaching number at the end of station id as shown Figure 4.14. Comparison result is summarized in Table 4.3.

	XX**1**	
XX**7**	XX (station id)	XX**3**
	XX**5**	

Figure 4.14 Reordering meteorological station id numbers

Table 4.3 Comparison of TRMM neighbour pixel and met. station

ID	Name	Monthly r	Monthly m	Annual r	Annual m	Seasonal r	Seasonal m	Aspect Ratio
17042	Hopa	0.86	0.59	0.88	0.61	0.68	0.54	SW
170425	Hopa	0.83	0.56	0.84	0.54	0.68	0.51	-
170427	Hopa	0.85	0.63	0.85	0.66	0.63	0.60	-
17628	Pazar Rize	0.80	0.56	0.81	0.61	0.36	0.30	N
176285	Pazar Rize	0.80	0.48	0.77	0.46	0.44	0.29	-
176287	Pazar Rize	0.81	0.54	0.79	0.53	0.22	0.19	-
17045	Artvin	0.58	1.03	0.51	1.17	0.47	1.13	SW
170453	Artvin	0.56	0.87	0.55	1.02	0.32	0.69	-
170455	Artvin	0.63	0.84	0.61	0.97	0.67	1.23	-
17100	Iğdır	0.85	0.95	0.87	0.97	0.78	1.31	W
171003	Iğdır	0.84	0.95	0.84	0.91	0.79	1.35	-
171005	Iğdır	0.81	0.88	0.86	0.85	0.81	1.03	-
17776	Solhan	0.86	0.64	0.91	0.66	0.75	0.69	S
177763	Solhan	0.87	0.61	0.92	0.67	0.75	0.68	-
17736	Mazgirt	0.82	0.52	0.88	0.58	0.88	0.61	N
177363	Mazgirt	0.84	0.56	0.90	0.63	0.91	0.65	-
17718	Tercan	0.74	0.91	0.71	0.83	0.47	0.42	NW
177187	Tercan	0.75	0.97	0.71	0.86	0.48	0.42	-
17690	Horasan	0.78	0.74	0.82	0.65	0.73	0.65	SE
176901	Horasan	0.70	0.70	0.73	0.59	0.65	0.60	-
17780	Malazgirt	0.81	0.56	0.84	0.57	0.77	0.33	N
177805	Malazgirt	0.83	0.60	0.87	0.63	0.73	0.38	-
17688	Tortum	0.46	0.57	0.25	0.26	0.55	0.48	S
176883	Tortum	0.55	0.61	0.42	0.39	0.59	0.54	-
17720	Doğubeyazıt	0.76	0.81	0.86	0.97	0.74	0.88	N
177203	Doğubeyazıt	0.57	0.90	0.59	1.03	0.29	0.57	-
17099	Ağrı	0.70	0.55	0.76	0.56	0.21	0.25	W
170993	Ağrı	0.68	0.62	0.74	0.62	0.14	0.21	-
17778	Varto	0.81	0.59	0.85	0.55	0.94	0.81	N
177785	Varto	0.84	0.59	0.87	0.56	0.95	0.75	-
177787	Varto	0.46	0.42	0.74	0.62	0.07	-0.05	-
17784	Ercıs	0.86	0.60	0.91	0.63	0.86	0.61	NW
177843	Ercıs	0.80	0.60	0.90	0.64	0.84	0.67	-

Table 4.3 Comparison of TRMM neighbour pixel and met. station (cont.)

17656	Arpaçay	0.79	0.68	0.85	0.75	0.78	1.08	E
176561	Arpaçay	0.71	0.62	0.77	0.62	0.83	1.08	-
176563	Arpaçay	0.79	0.65	0.83	0.69	0.74	0.99	-
17740	Hınıs	0.83	0.58	0.92	0.68	0.86	0.52	N
177401	Hınıs	0.77	0.55	0.83	0.63	0.71	0.45	-
177407	Hınıs	0.80	0.63	0.88	0.75	0.70	0.49	-
17096	Erzurum	0.60	0.85	0.57	0.72	0.59	0.93	E
170965	Erzurum	0.73	0.85	0.71	0.72	0.75	0.95	-
170967	Erzurum	0.59	0.87	0.53	0.67	0.52	0.86	-
17692	Sarıkamış	0.77	0.61	0.79	0.55	0.90	0.77	SW
176921	Sarıkamış	0.65	0.65	0.70	0.57	0.81	0.83	-
176923	Sarıkamış	0.78	0.58	0.82	0.55	0.87	0.79	-

Table 4.3 shows that some neighbour pixel results are better than the actual pixel comparison results due to the low spatial resolution of the satellite data and the effect of the complexity in the terrain.

4.1.3 Comparing the Spatial Variation of Regression Line Coefficients

Another comparison study is performed by considering spatial variation of the regression line coefficients. In the ideal case, spatial variation of the regression line coefficients for each meteorological station should be negligible (Kamarianakis et al., 2008). For this reason, to analyze the spatial non-stationarity in the relationship between meteorological station data and satellite data, a statistical tool, Geographically Weighted Regression (GWR) is used.

Geographically Weighted Regression (GWR) is used to evaluate data in considering space. The relationship between analyzed paired data is considered to be the same throughout the studied area. However, there may be relation differences in space. The GWR is basically formulated as,

$$y(u,v) = b_0 (u,v) + x_1 b_1 (u,v) + e (u,v) \quad \text{(Eq. 4.2)}$$

where, y: dependent variable, b_1: independent variable, b_0: intersection point, x_1: weighted value e: random error term and (u,v): coordinates of the data points.

GWR constructs an equation for each feature (meteorological station) according to the selected Kernel type and bandwidth method. In this study, GWR tool of ArcGIS is used. In the program, using spatial statistic tools, dependent and independent variables are defined. Then, appropriate Kernel type and bandwidth method are selected. In Kernel type which controls the geographic weighting, there are two options, adaptive or fixed. Fixed method is suitable for observations which are positioned regularly whereas; adaptive method is suitable for observations which vary around the study area. In bandwidth selection three are there methods: AICc, CV and bandwidth parameter. First two options select the bandwidth value automatically. Cases in which number of observation is less, AICc method is preferred. For the last option (bandwidth parameter), user defines the necessary value (Charlton and Fotheringham, 2009).

In this study, by using annual precipitation data of TRMM 3B43 (V6) and meteorological stations for the period from 1998 to 2008, analyses are performed by selecting Kernel type (adaptive) and bandwidth method (AICc) because of limited and irregular positioning of meteorological stations. The result of GWR can be seen in Figures 4.15 - 4.17.

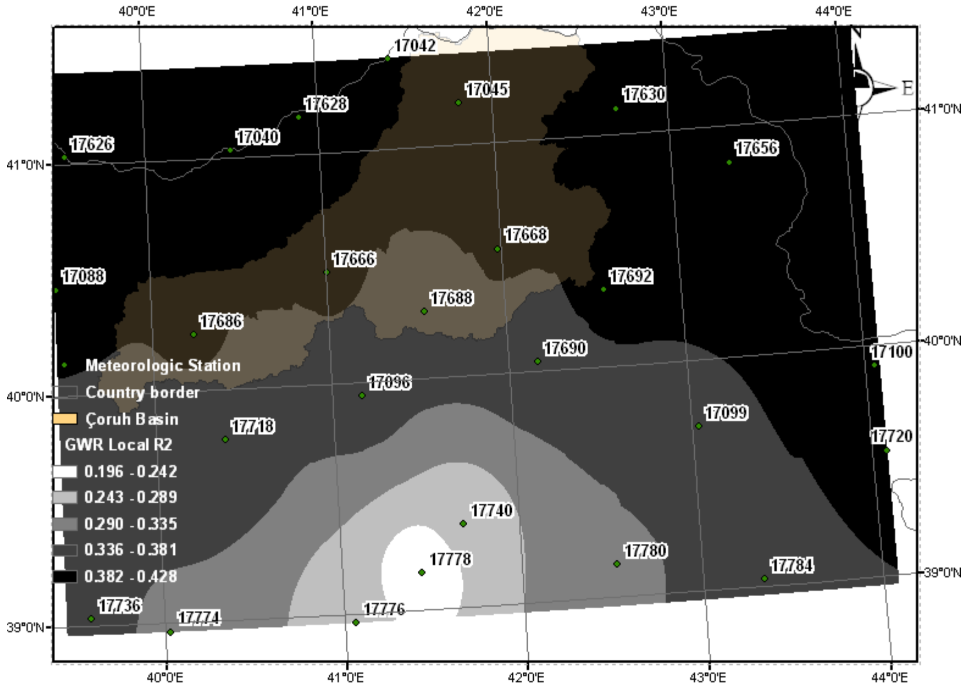

Figure 4.15 Representation of local R^2 distribution

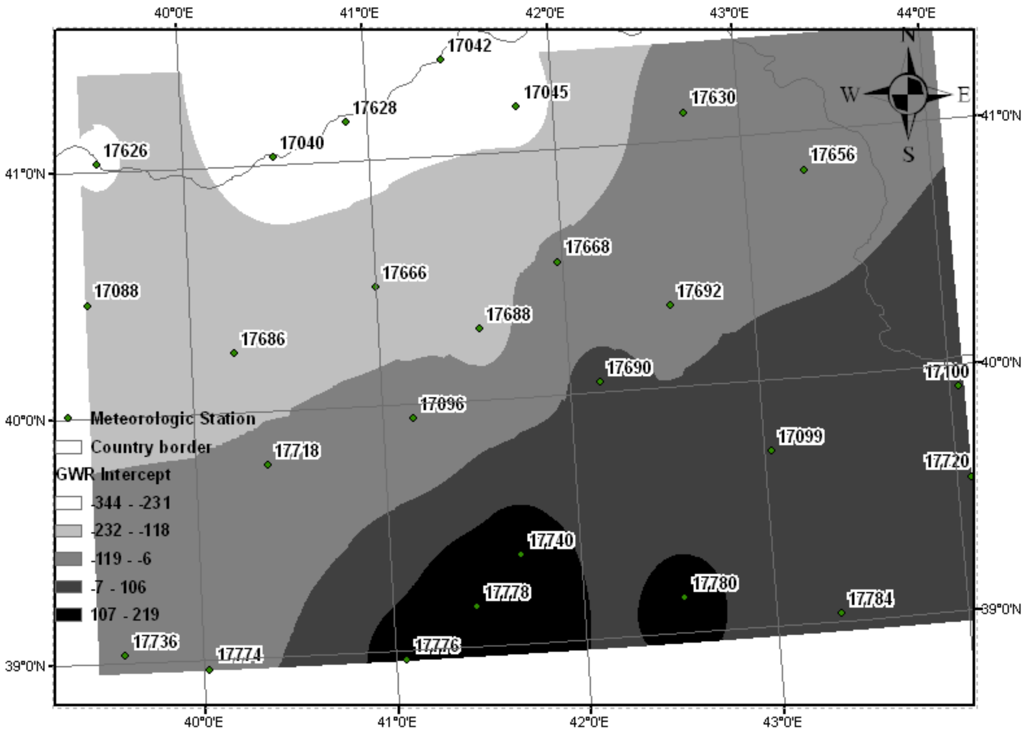

Figure 4.16 Representation of intercept distribution

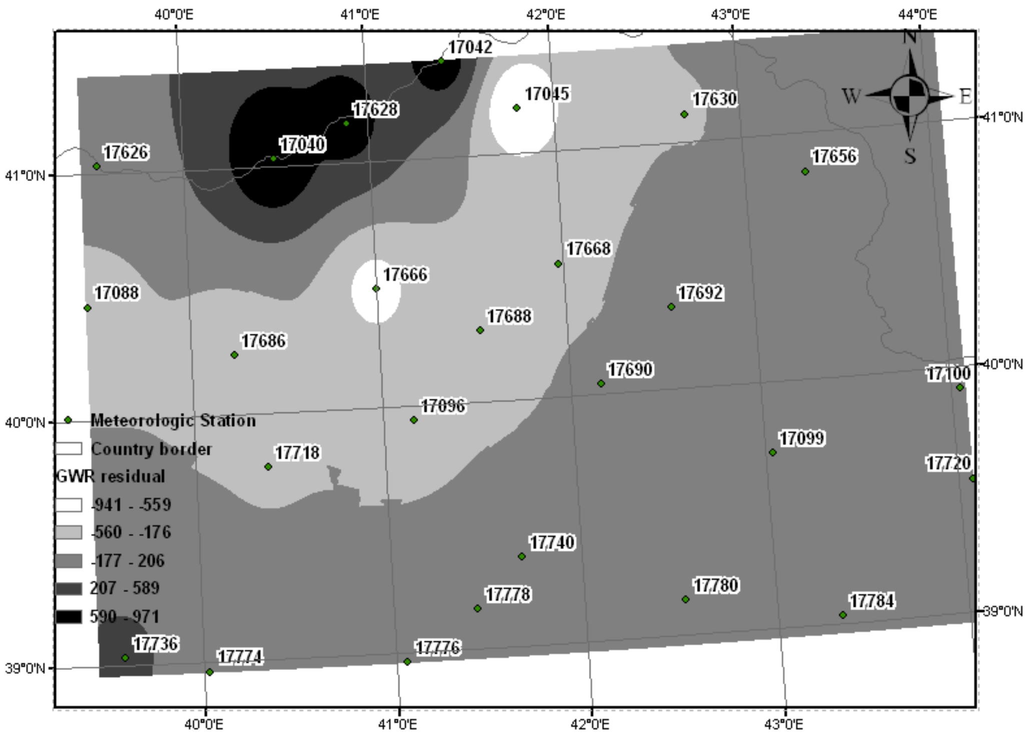

Figure 4.17 Representation of residual distribution

Figure 4.15 shows that, local R^2 has a tendency to distribute in north-south direction in the study area. Moreover, locations, where high precipitation amount are obtained (Figure 4.4 and 4.5) show high R^2 distribution. This shows that there is relationship between precipitation amount and local R^2 distribution in the studied area.

Ideally, for each location regression line intercepts and residuals are expected to be close to 0. However, results do not show the ideal situation.

4.2 Comparison of TRMM 3B42 (V6) and Raingauge Data

The same study which is done for TRMM 3B43 (V6) is applied also for TRMM 3B42 (V6) data. Comparisons are done in daily basis for 39 stations and for the period from July 2005 to September 2005. The selected stations can be seen in Figure 4.18 and properties of the new 13 stations are summarized in Table 3.1 in underlined form of station name. Other selected results can be seen in Appendix B.

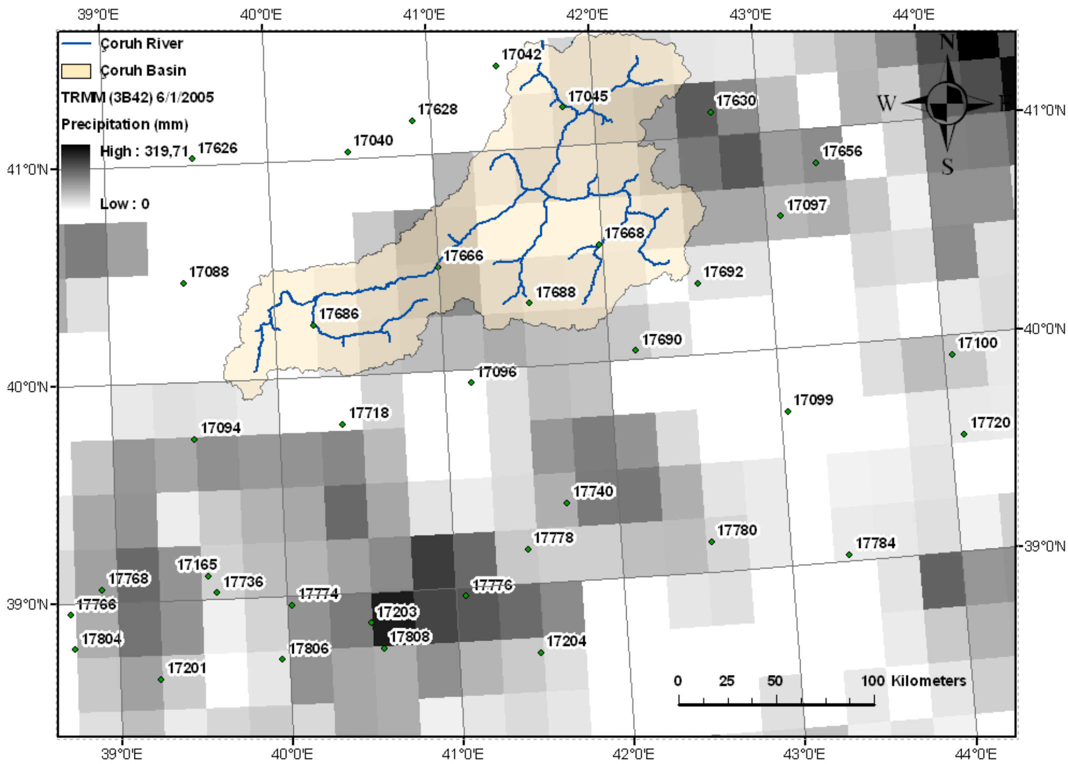

Figure 4.18 Meteorological stations over the TRMM 3B42 (V6) precipitation data (June 1, 2005 precipitation data (mm))

The comparison results can be seen Appendix B. Although, TRMM 3B43 (V6) seems to be more appropriate than the TRMM 3B42 (V6), HEC-HMS enables one day time interval for input data thus, studies are based on TRMM 3B42 (V6) product.

CHAPTER 5

MODEL SIMULATIONS

5.1 Basin Characterization

In this study, mainly two software packages are used, ArcGIS 9.2 with Geospatial Hydrologic Modeling Extension (HEC-GeoHMS 4.2) and HEC-HMS 3.3. In this part of the study basic features of the basin are formed by using HEC-GeoHMS as input files for hydrologic modeling in HEC-HMS.

HEC-GeoHMS is not a standalone computer software so it is used with ArcGIS 9.2. This extension was developed by U.S. Army Corps of Engineers to visualize spatial information, form basin characteristics, define subbasins and streams and create hydrologic model inputs (USACE, 2009a). Easy usability and comprehensibility allow users to create hydrologic models, which can be used in hydrologic modeling with HEC-HMS.

In Chapter 3, six grid layers (filled DEM, flow direction, flow accumulation, stream network, stream link and catchment grid layers) and three vector datasets (catchment, drainage line, adjoint catchment datasets) were presented. Using these layers with the original DEM and basin slope layer, basin process is initiated.

Using data management tool in HEC-GeoHMS corresponding map layers, which are defined above are confirmed. Then a new project is initiated. By adding a point at the end of basin outlet, project generation is completed. After this step, physical basin characteristics of streams and subbasins are extracted.

These characteristics are river length, river slope, longest flow path, basin centroid, basin centroid elevation, and centroidal flow path (Figure 5.1).

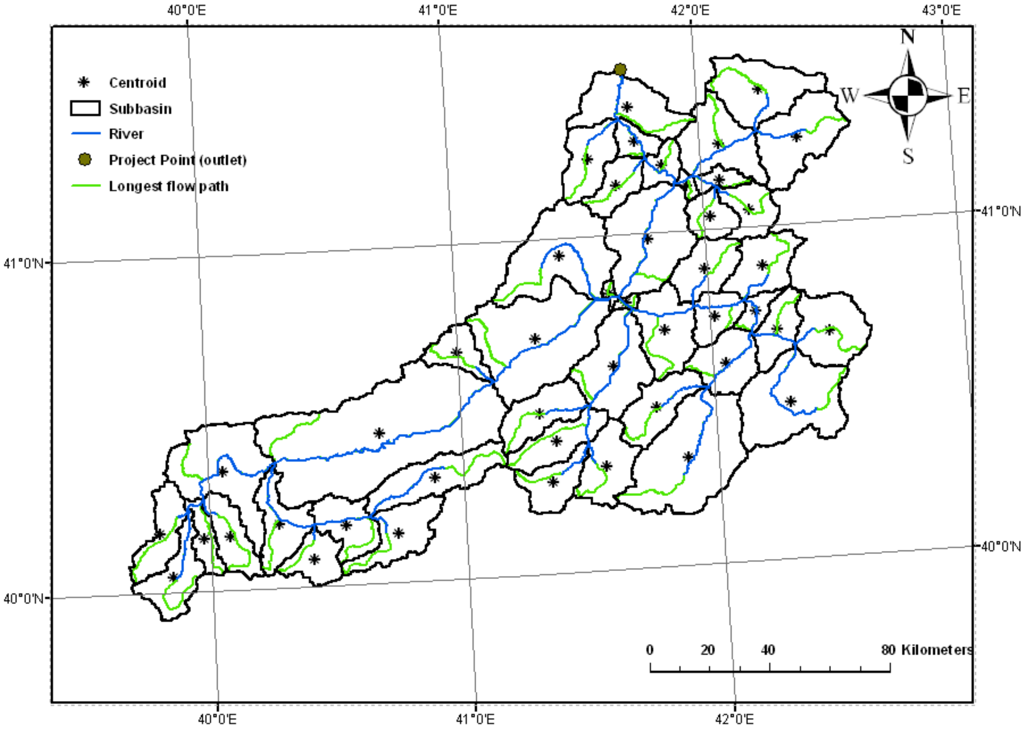

Figure 5.1 Representation of some basin characteristics

5.2 Parameter Estimation

Using hydrologic parameter menu in HEC-GeoHMS, basin, and stream parameters can be estimated or assigned. To prepare input data for the HEC-HMS, first, methods are assigned for subbasin and river. In this step, in order to use curve number data in the model, SCS curve number and SCS unit hydrograph are assigned for loss and transform methods respectively. Then, river and basin auto names are given to the subbasin and river feature classes in sequence from upstream to downstream to define elements in the model.

Using hydrologic parameters tool, curve number grid layer which is presented in Chapter 3 (Figure 3.6) is selected to have an average curve number value for each subbasin.

Using CN lag method function, time of concentration (time required for water dropping on remote point in the basin and travelling to the collection point) is calculated by using basin slope and curve number layers.

After this step input files for HEC-HMS are created by using HMS menu. Unit conversion, data check, HMS schematic, adding coordinates, data preparation, generating background map and basin file procedures are completed by using HMS menu through the extension of HEC-GeoHMS in ArcGIS. Schematic with HMS legend can be seen in Figure 5.2. These maps are formed to use as a background layer in HEC-HMS and show the basin boundaries and river branches. The continuation of the input creation process is completed at this stage.

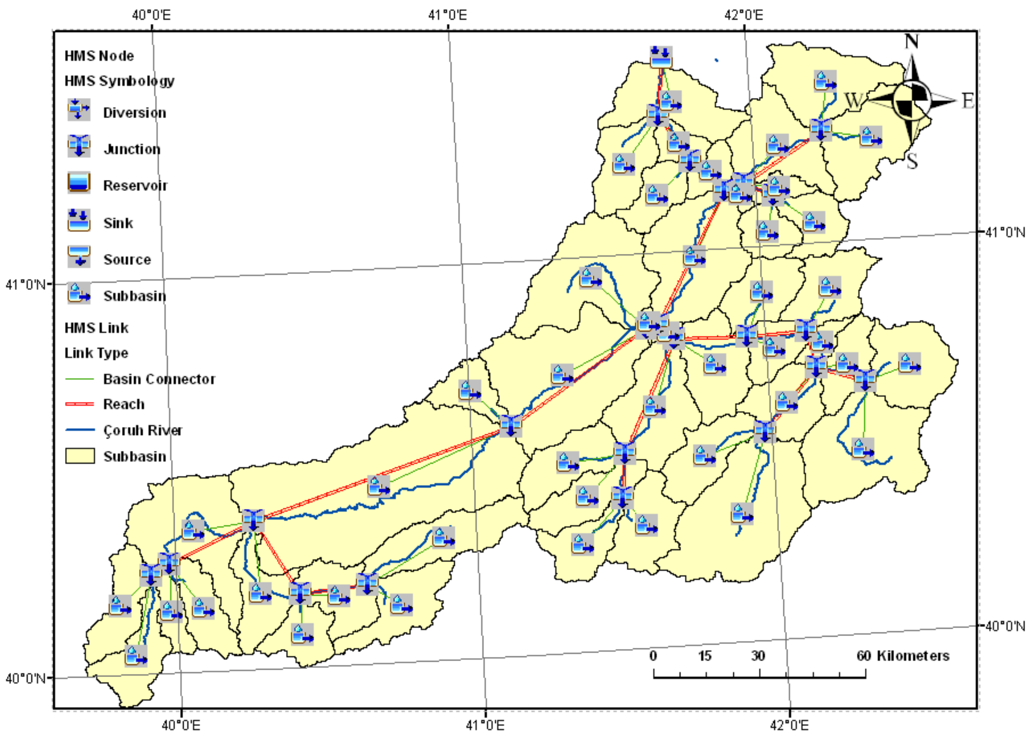

Figure 5.2 Schematic with HMS legend

With the completion of this stage, 45 subbasins are created in the study area. Although the entire basin is processed, designated area of the subbasins (16 subbasins) which is shown in Figure 5.3 is used due to the single available flow monitoring station at downstream and there is no reservoir or manmade structures at the upstream.

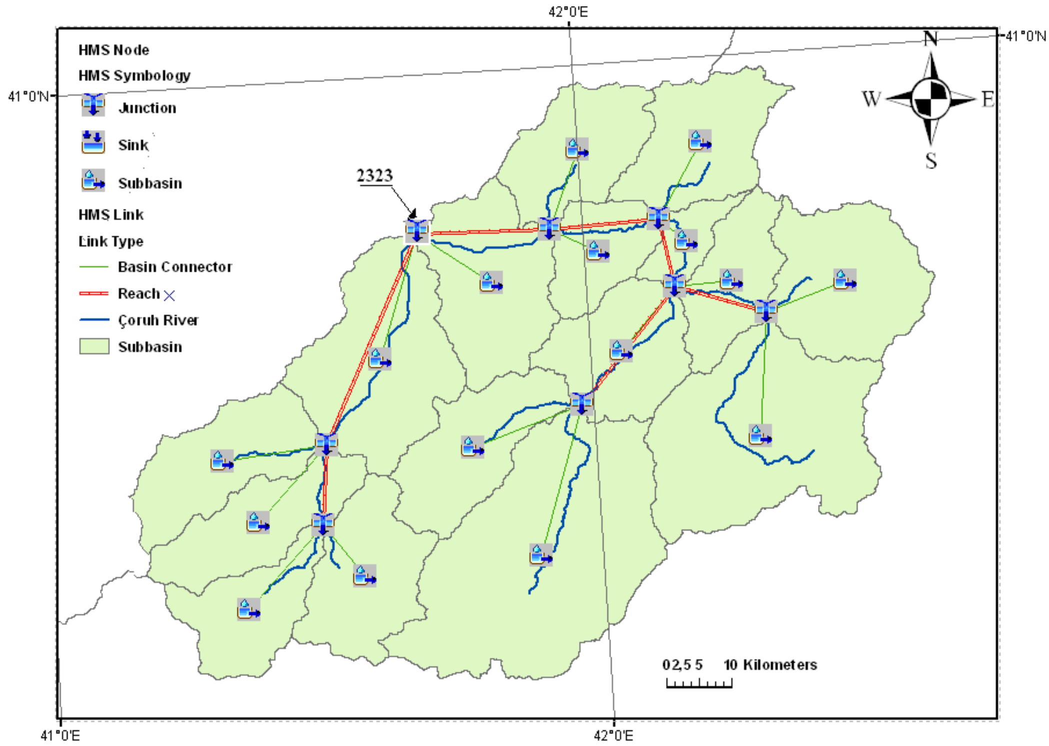

Figure 5.3 Study area with the location of flow monitoring station (2323)

In modeling, three hydrologic elements are used; subbasin, reach and junction. Subbasin represents the physical basin, reach defines the stream conveying process from upstream to downstream and junction calculates the entire stream flow coming from upstream.

5.3 Modeling

To simulate hydrologic response in a basin, HMS model components are used. Hydrologic Modeling System (HEC-HMS) is developed by U.S. Army Corps of Engineer to simulate precipitation runoff procedure in many geographic areas with the aim of solving problems like flood damage reduction, future urbanization effect and, wetlands hydrology (USACE, 2009b). The model components are basin model, meteorologic model, input data and control specifications. Precipitation runoff simulation in the model basin is constituted by using the input data from meteorologic model and defined time period from control specifications (USACE, 2009b).

Components; basin model, meteorologic model, input data and control specification, and their method types are represented in Figure 5.4

Modeling studies are done for two different daily based rainfall data; TRMM 3B42 (V6) data and meteorological station data separately. In these separate studies, identical methods are selected in basin model and meteorologic model components and also the same time adjustments are done in control specification component.

5.3.1 Basin Model Component

Representation of the physical basin is controlled by basin model. Physical process in the basin is defined by hydrologic elements like subbasin, reach, and junction (USACE, 2009b). All hydrologic elements have their own calculation types and methods. For instance, in each subbasin, loss, transform and baseflow calculations (Figure 5.4) are done with the selected methods taken in the program. List of the methods for subbasin and reach elements can be seen in Table 5.1. In this table, bold ones show the selected methods in the study.

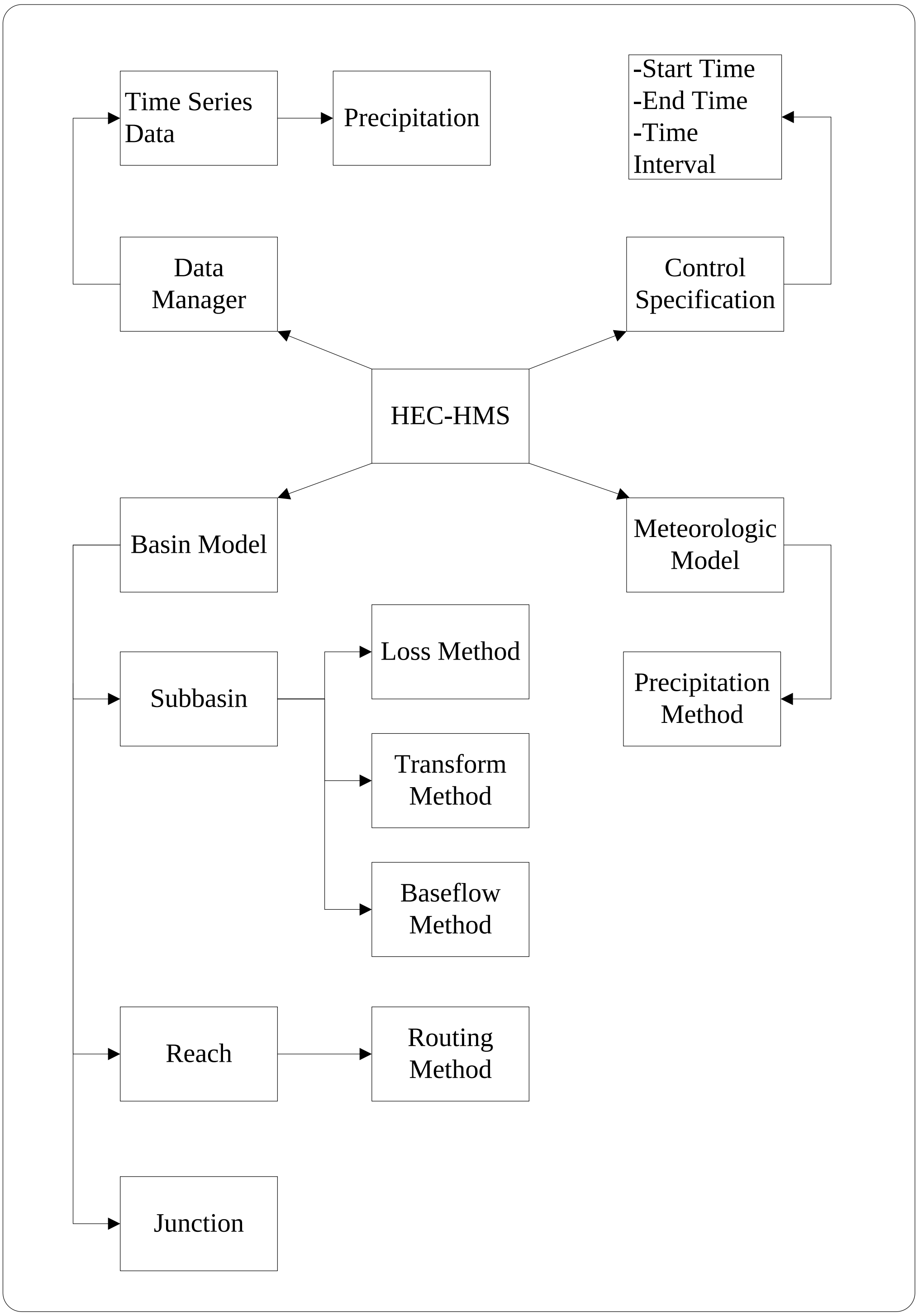

Figure 5.4 Model components and method types used in the study

Table 5.1 Subbasin and Reach Calculation Methods (USACE, 2009c)

Hydrologic Element	Calculation Type	Method
Subbasin (represents physical basin)	Loss Rate	Deficit and Constant Rate (also gridded)
		Exponential
		Green and Ampt
		Initial and constant rate
		SCS curve number (also gridded)
		Smith Parlange
		Soil moisture accounting
	Transform	Clark's unit hydrograph
		Kinematic wave
		ModClark
		SCS unit hydrograph
		Snyder's unit hydrograph
		User specified s-graph
		User specified unit hydrograph
	Baseflow	Bounded recession
		Constant monthly
		Linear reservoir
		Nonlinear Boussinesq
		Recession
Reach (convey stream flow from upstream basin to downstream)	Routing	Kinematic wave
		Lag
		Modified Puls
		Muskingum
		Muskingum Cunge
		Straddle stagger
	Gain/Loss	Constant
		Percolation

In the study three hydrologic elements are used to represent a basin; these are subbasin, reach and junction. For subbasin and reach elements in the basin model component, suitable methods depending on the availability of the needed data for the model are selected from available ones which are defined in Table 5.1. Junction element is responsible for combining stream flow coming from upstream thus method selection for this element is not defined in the model.

In the subbasin element of basin model component, subbasin properties like description, name and area can be displayed (Figure 5.5). Moreover, methods which calculate infiltration, surface runoff and subsurface process are assigned in this element. Methods in the subbasin element are defined in the following way,

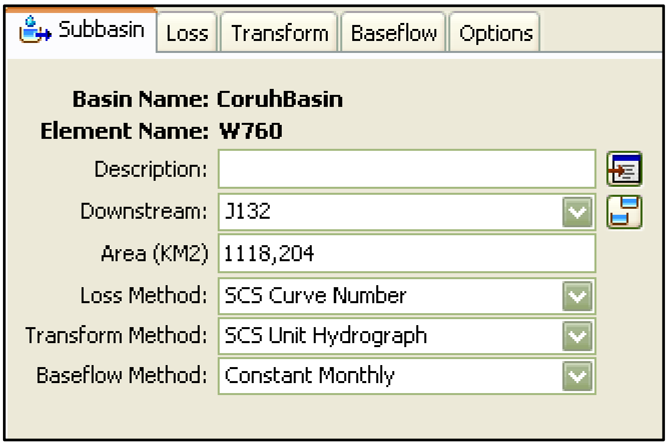

Figure 5.5 Subbasin component editor

- Loss method: In the subbasin element, infiltration calculations are performed by selecting the method type. In this study, SCS curve number loss method is selected in parameter estimation part (section 5.2). The required parameters for that method are initial abstraction, curve number and percentage of imperviousness. Except curve number parameter which is derived from curve number layer for each subbasin element, there is no information about initial abstraction and percentage of imperviousness. Initial abstraction defines the precipitation amount falling before the simulation start time and percentage of imperviousness denotes the percentage of area in which no loss calculations are performed. These two values are left as blank due to the lack of data. These values are calibrated in next sections. However, for initial abstraction parameter, program assigns an automatic value which is calculated from curve number.

- Transform method: In the subbasin element, surface runoff calculations are performed by selecting the method type. In this study, SCS unit hydrograph transform method is selected in parameter estimation part (section 5.2). For this method, the required parameters are type of graph and lag time. Graph type is related with unit hydrograph shape, one option is chosen from two, standard or Delmarva, namely. Standard graph type is selected because Delmarva shape is defined only for specific areas in the United States. Lag time describes the time between precipitation mass to resulting hydrograph. In this method for each subbasin element lag time is calculated by using results of the CN lag time method (According to Natural Resources Conservation Service, by getting 60% of time of concentration value, lag time can be obtained.).

- Baseflow method: In the subbasin element, subsurface calculations are performed by selecting the method type. In this study, constant baseflow method is selected because this method has the least parameters in all method types. However, required parameter value for baseflow computation remains as blank to handle it in calibration procedure.

To model rivers reach element is used. In the reach element of basin model component, river properties like description and downstream connection can be seen (Figure 5.6). Also, methods which calculate routing and loss/gain process are assigned in this element. Methods are defined in the following way,

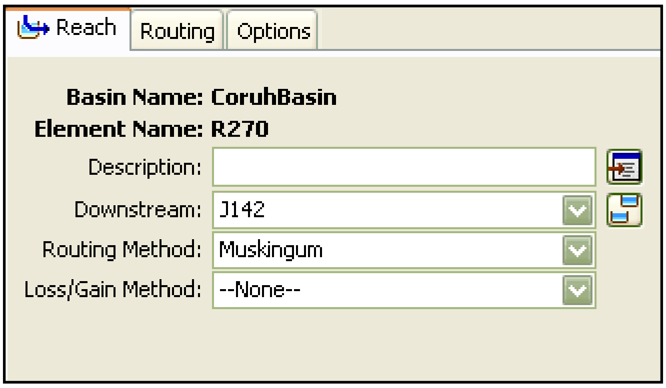

Figure 5.6 Reach component editor

- Routing method: In the reach element routing process calculations are performed by selecting the method type. In this study, Muskingum routing method is selected and its parameters, Muskingum K and Muskingum X are defined by making calibration according to results of flow monitoring station.

- Loss/gain method: In the reach element, losses from channel or gain from groundwater is represented by this method. However, this method is not used in the study due to the lack of data.

5.3.2 Control Specification Component

Control specification component manages the time functions like simulation time span, simulation start and end date, and computation time step (USACE, 2009b).

This component does not contain any parameter; it controls the simulation time process. In this study, 2005 and 2003 water years are simulated with the TRMM 3B42 (V6) data (Figure 5.7) and 2005 water year is simulated with meteorological station data.

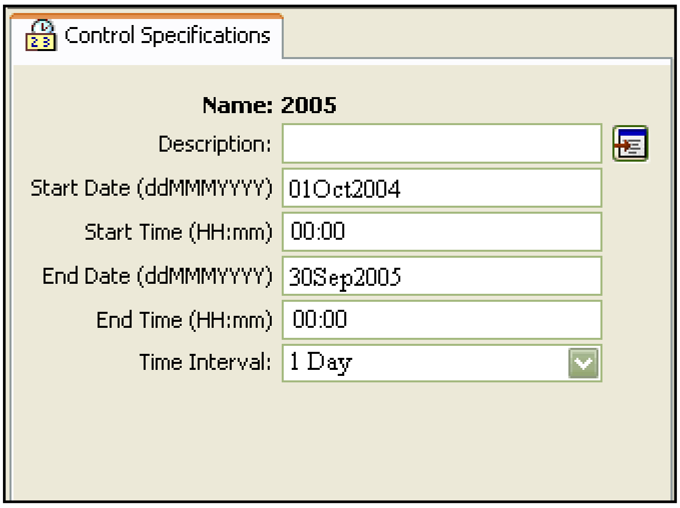

Figure 5.7 Control specification component editor

5.3.3 Meteorologic Model Component

Using the input data, which can be point or gridded, model calculates the precipitation for each subbasin element. Moreover model has options to define evapotranspiration and snowmelt processes (USACE, 2009c). The following table summarizes the available meteorologic model methods (Table 5.2). In this table, bold one shows the selected method in the study (Inverse Distance).

Table 5.2 Meteorologic Models and Corresponding Methods

Meteorologic Model	Methods
Precipitation	Frequency Storm, Gage Weights, Gridded Precipitation, **Inverse Distance**, SCS Storm, Specified Hyetograph, Standard Project Storm
Evapotranspiration	Gridded Priestley Taylor, Monthly Average, Priestley Taylor
Snowmelt	Gridded Temperature Index, Temperature Index

This component prepares the boundary condition and calculates the precipitation input for each subbasin. In this component, three hydrologic processes are defined; precipitation, evapotranspiration and snowmelt. Snowmelt and evapotranspiration processes are not used in this study due to the lack of necessary data. (Figure 5.8)

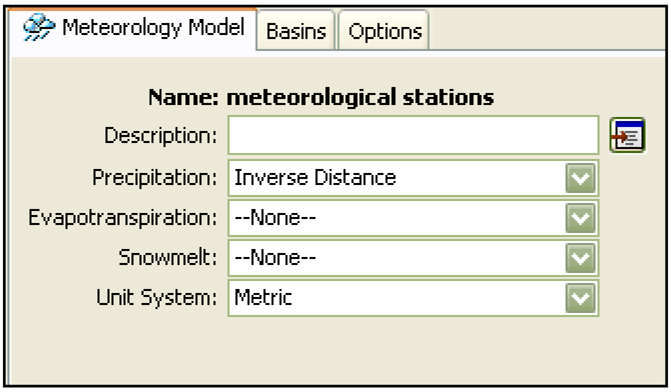

Figure 5.8 Meteorologic model component

For both precipitation data, inverse distance precipitation method is assigned. The advantage of using this method is that it can compensate for missing values of precipitation gages through interpolation of neighboring gages' values.

Latitude and longitude values are specified for each subbasin element under the meteorologic model component. For TRMM 3B42 (V6) data, basin centroid locations are used, whereas, for meteorologic data, original gage locations are used.

5.3.4 Data Manager Component

For basin and meteorologic model component, input data are required as a parameter or boundary condition; these can be time series data, paired data or gridded data (USACE, 2009c). Type of the data can be seen in Table 5.3.

Table 5.3 Input Data Components for HEC-HMS (USACE, 2009b)

Time Series Data	Paired Data	Gridded Data
-Precipitation gages, -Discharge gages, -Stage gages, -Temperature gages, -Solar radiation gages, -Crop coefficient gages, -Snow water equivalent gages.	-Storage-discharge functions, -Elevation-storage functions, -Elevation-area functions, -Elevation-discharge functions, -Inflow-diversion functions, -Cross sections, -Unit hydrograph curves, -Percentage curves, -ATI meltrate functions, -ATI coldrate functions, -Groundmelt patterns, -Meltrate patterns.	-Precipitation gridsets, -Temperature gridsets, -Solar radiation gridsets, -Crop coefficient gridsets, -Storage capacity grids, -Percolation rate grids, -Storage coefficients grids, -Moisture deficit grids, -Impervious area grids, -SCS curve number grids, -Elevation grids, -Cold content grids, -Cold content ATI grids, -Meltrate ATI grids, -Liquid water content grids, -Snow water equivalent grids.

This component controls all data which are used in the simulation. In this study, precipitation gages data type under the time series data component is used for both TRMM 3B42 (V6) and meteorological stations.

5.3.4.1 Preparation of TRMM 3B42 (V6) Input Data

In order to extract precipitation data from TRMM 3B42 (V6) raster dataset, zonal statistics tool in ArcGIS is used. This tool calculates the mean precipitation value which is held by TRMM 3B42 (V6) precipitation layer, for each subbasin zone in basin dataset layer (Figure 5.9).

These extraction procedures are done for 2005 and 2003 water years, for every 730 TRMM 3B42 (V6) precipitation layer. After this extraction process, all generated data are entered manually in HEC-HMS for each subbasin (Figure 5.10).

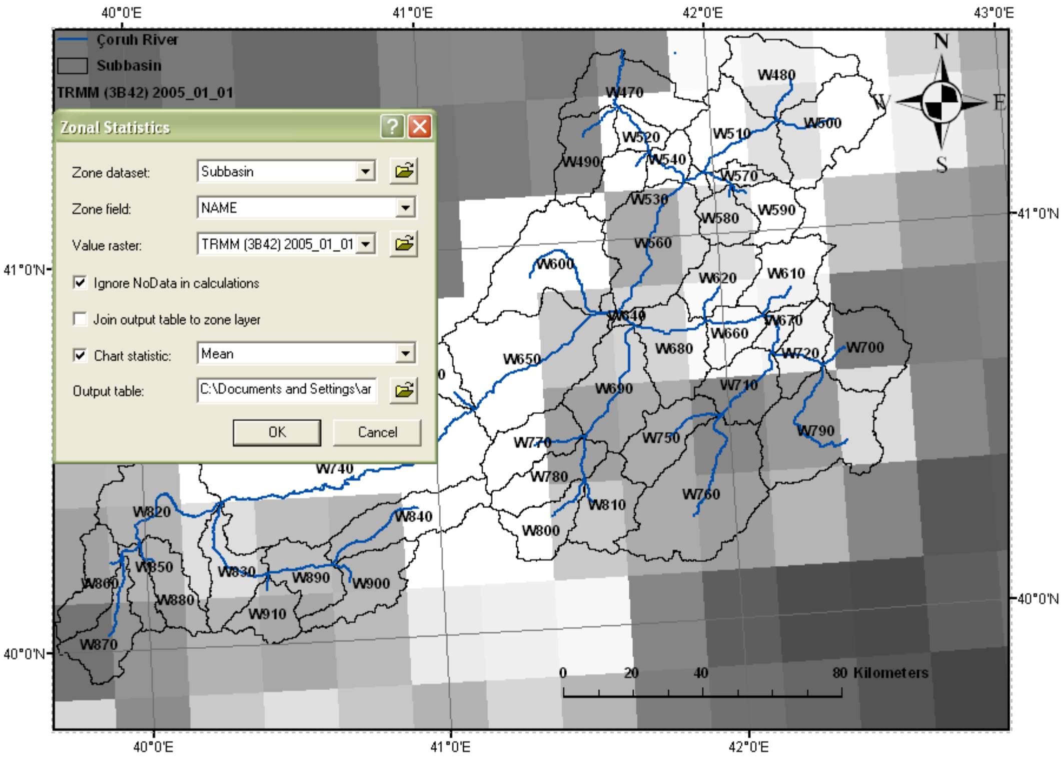

Figure 5.9 Extracting data by using zonal statistic tool in ArcGIS

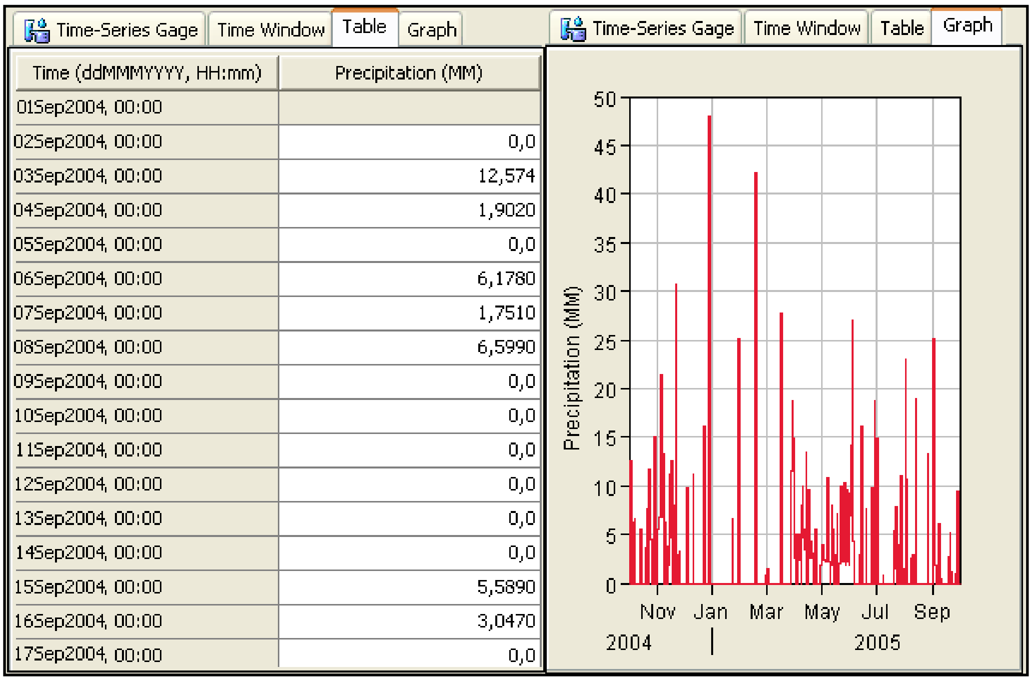

Time (ddMMMYYYY, HH:mm)	Precipitation (MM)
01Sep2004, 00:00	
02Sep2004, 00:00	0,0
03Sep2004, 00:00	12,574
04Sep2004, 00:00	1,9020
05Sep2004, 00:00	0,0
06Sep2004, 00:00	6,1780
07Sep2004, 00:00	1,7510
08Sep2004, 00:00	6,5990
09Sep2004, 00:00	0,0
10Sep2004, 00:00	0,0
11Sep2004, 00:00	0,0
12Sep2004, 00:00	0,0
13Sep2004, 00:00	0,0
14Sep2004, 00:00	0,0
15Sep2004, 00:00	5,5890
16Sep2004, 00:00	3,0470
17Sep2004, 00:00	0,0

Figure 5.10 Precipitation data entering for subbasin 760

5.3.4.2 Input Data from Meteorological Station

For the meteorological stations, 17668 and 17688, which are located in the studied area, daily precipitation values are used for the modeling study, because these stations represent the basin characteristics better than the other stations. Thus, such a long extraction process is not made with meteorological data. The scatter plot and time series diagrams are represented in Figures 5.11 - 5.14.

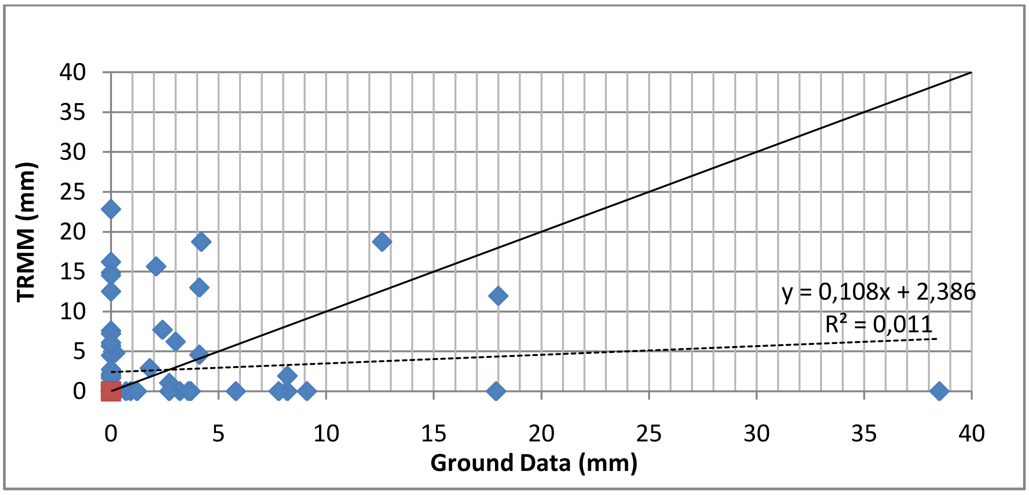

Figure 5.11 TRMM 3B42 (V6) vs. Ground Obser. data (daily) 17668 Oltu

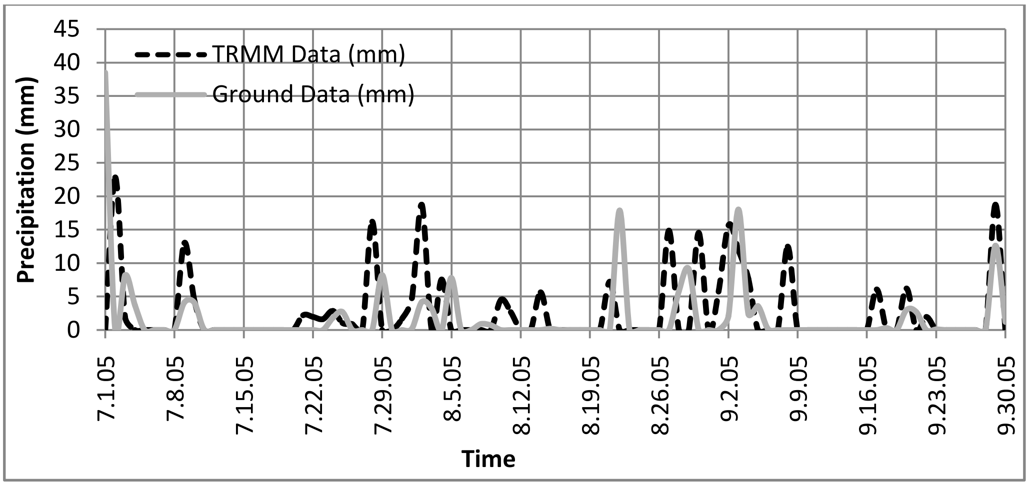

Figure 5.12 Daily Rainfall Diagrams for 17668 Oltu

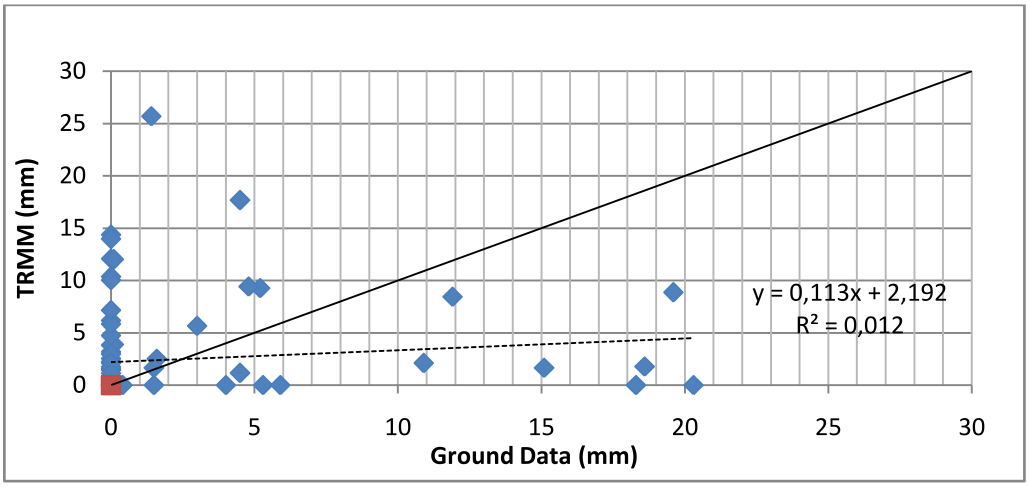

Figure 5.13 TRMM 3B42 (V6) vs. Ground Obser. data (daily) 17688 Tortum

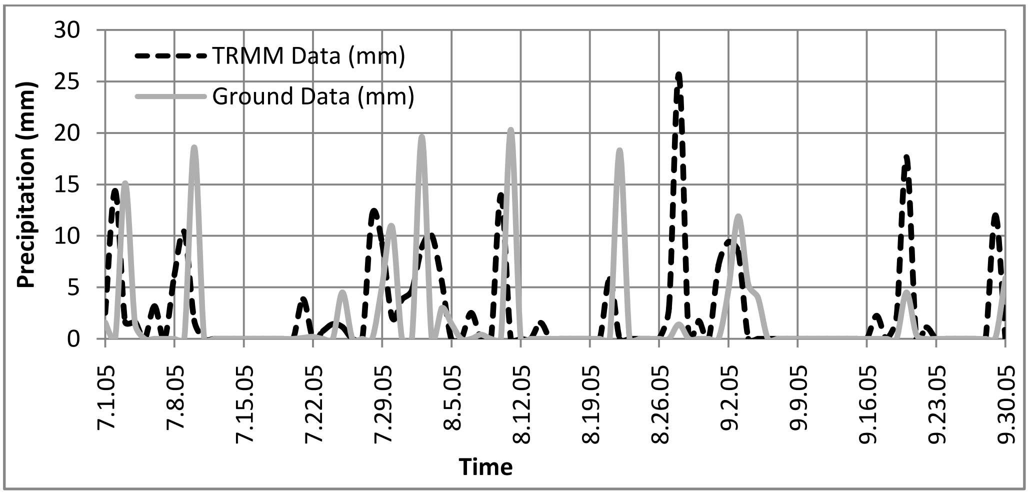

Figure 5.14 Daily Rainfall Diagrams for 17688 Tortum

5.4 Simulation

Simulations were done with the defined method types and prepared data for the spacified areai which is shown in Figure 5.3. The simulated hydrographs which are derived from TRMM 3B42 (V6) and meteorologic stations separately, are compared with the flow monitoring station (EIE 2323) located at the outlet of this area (Figure 5.15).

From this graph (Figure 5.15), snow melting effect can be seen between April and July. In the model, due to the absence of snow data, outputs of July, August and September (92 day simulation) are taken into consideration. In Figure 5.16 flow results can be seen in detail for the selected months. Up to this point, the baseflow parameter in subbasin element and Muskingum parameters in reach element are not assigned. Values which define the parameters in selected methods are summarized in Appendix D.

5.5 Calibration

Calibration is a procedure in which model outputs are adjusted to the observed flow. Some of the parameters which are not estimated or exactly known in the modeling operation can be defined in the calibration process.

Although calibration can be done manually, it is time consuming and success is subject to user interpretation (Şorman, 2005). On the other hand, calibration process can be done programmatically in a systematic manner, namely optimization that shows best fit between observed and simulated runoff (Yener, 2006).

Before starting the optimization process, parameters which are not defined in simulation process, are calibrated manually to make initial iteration. For this process, baseflow and routing parameters are studied separately for the simulation which is performed with meteorological station data.

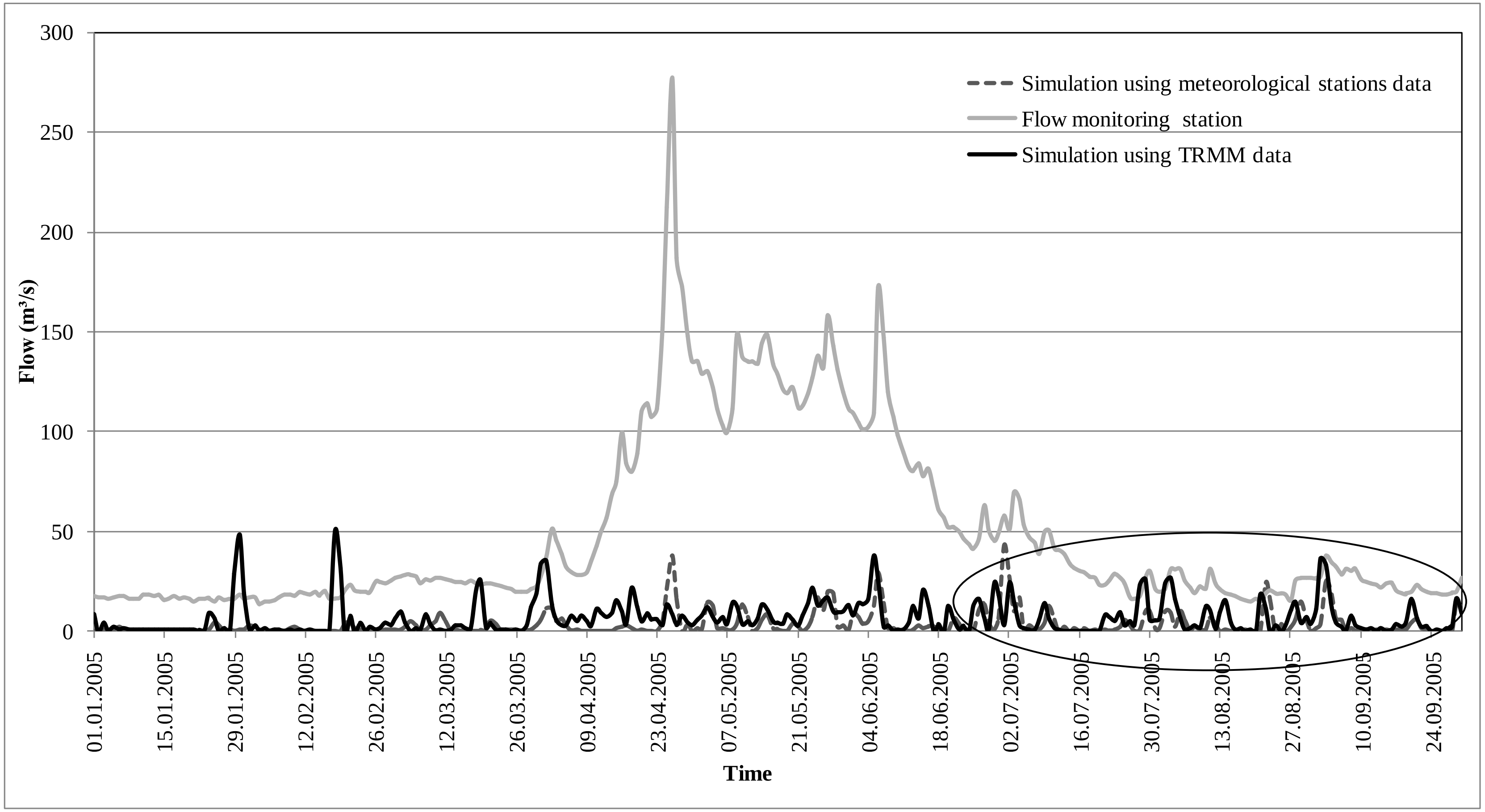

Figure 5.15 Simulated and observed flows

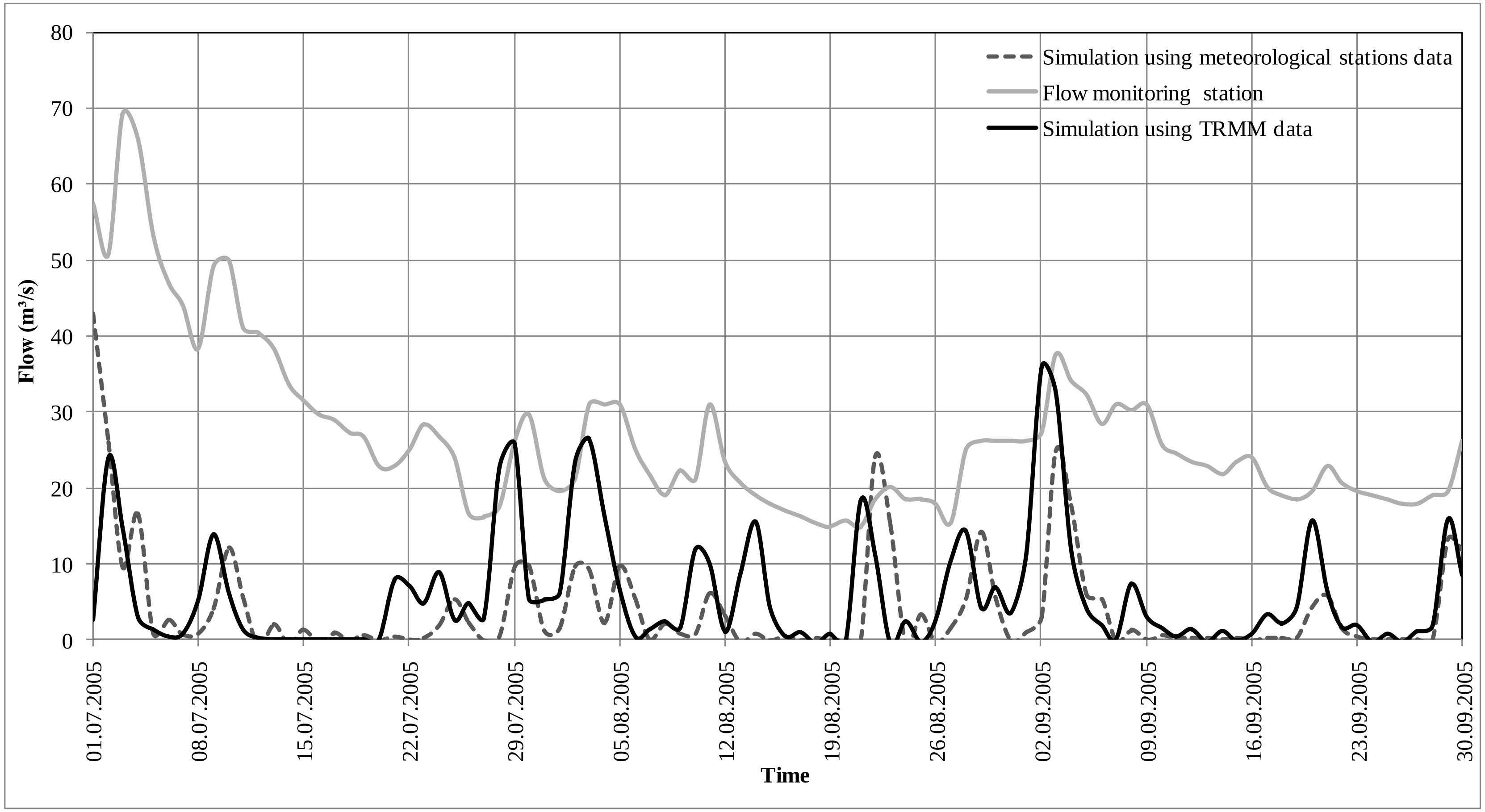

Figure 5.16 Simulation and observed results in detail

- For baseflow parameter estimation, all subbasins which are located in upstream of monitoring station are thought to be identical due to the lack of flow monitoring station and excessive number of basin. For this process four different baseflow values are given for each of 16 subbasin elements. The calibration result can be seen Figure 5.17.

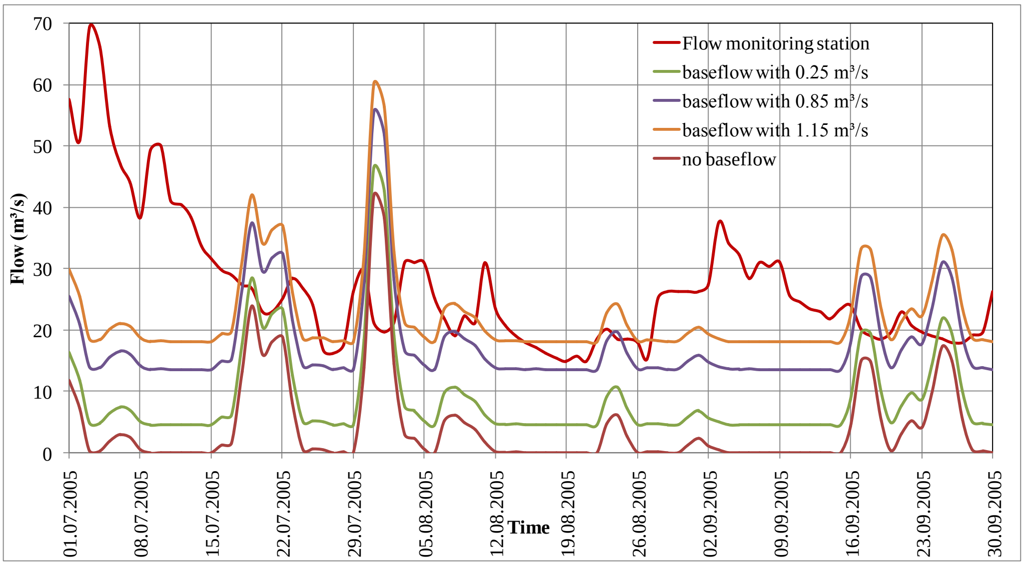

Figure 5.17 Baseflow calibration

From Figure 5.17 it is seen that, the forth alternative (shown in orange), where baseflow value, $1.15m^3/s$ is assigned for each subbasin element and is obtained as suitable for the modeling.

- Same assumption is made for reach elements like subbasin element. All reach elements are thought to be identical. Calibration procedure is applied for Muskingum K and Muskingum X parameters which are defined in reach element. Routing process is performed by taking one parameter as variable and the other one as constant. Firstly, K parameter is taken as constant and variable values are given to the X parameter (Figure 5.18). X is the relative weight coefficient of inflow and outflow which defines storage volume in the reach. (Das and

Salkia, 2009). This parameter ranges from 0.0 to 0.5. Following this, x parameter is taken as constant and different variables are given to the K parameter (Figure 5.19). K is the flood wave travel time from upstream to downstream in the reach element (Usul, 2005).

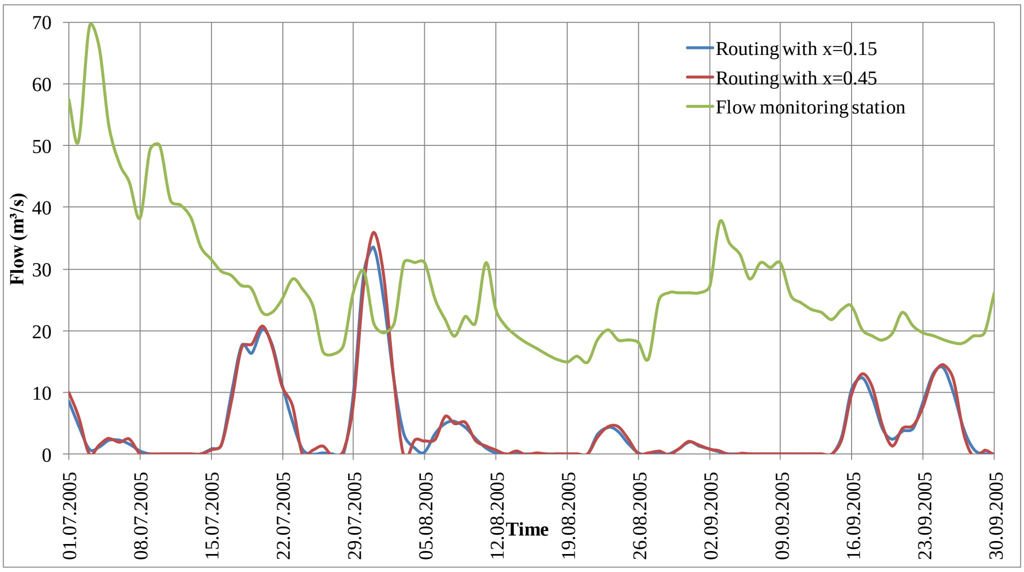

Figure 5.18 Routing procedure with Muskingum X parameter

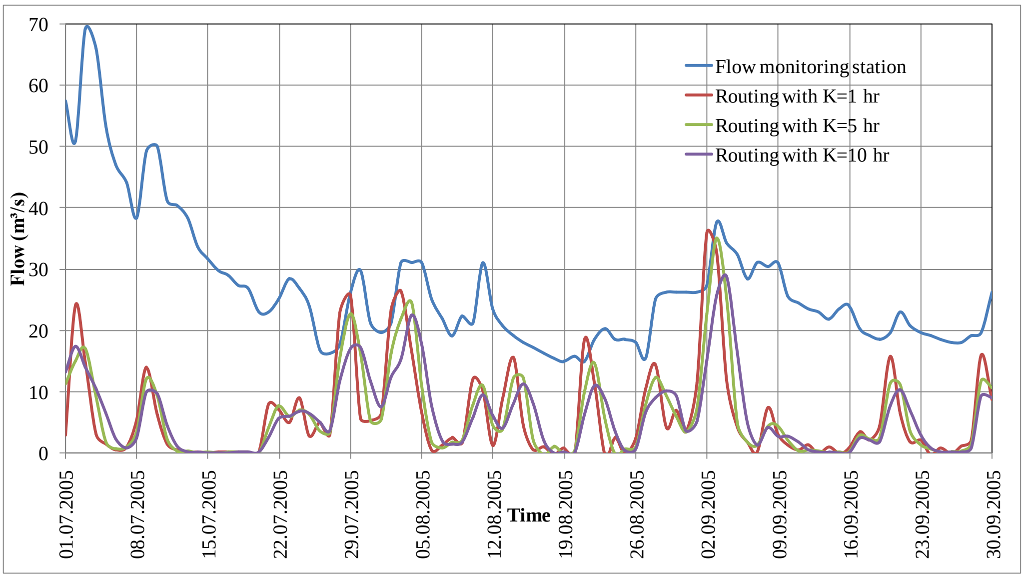

Figure 5.19 Routing procedure with Muskingum K parameter

From Figure 5.18 it is seen that increase of Muskingum X parameter widens the gap between minimum and maximum flow rates and stretches the hydrograph in Y-axis. In other words, decrease of Muskingum X parameter causes attenuation increase. Figure 5.19 shows that decrease of Muskingum K parameter ensures the rapid entering of flow from reach to the junction point.

In the light of these results, K and X are chosen as 5 hr. and 0.15 respectively to use as input for optimization process.

5.6 Optimization

In order to estimate unknown parameters automatically and remove the subjectivity, optimization trials are performed in HEC-HMS. This process adjusts the parameters which are roughly estimated in manual calibration. Due to the limitations of the program, not all parameters defined in the components can be optimized. Thus, in this study, routing parameters; Muskingum K and Muskingum X are optimized and baseflow parameter kept constant at a value of 1.15 m^3/s. The results of optimized values are shown in Appendix D. Up to this point all trials and calibration process are done for the sole purpose of modeling with meteorological station data. Same optimized results are used for modeling with TRMM 3B42 (V6) data. After extensive optimization iterations, hydrograph output shown in Figure 5.20 is obtained. In this figure, the precipitation values are derived from the averaged of the meteorological stations, 17668 and 17688.

From Figure 5.20 it is seen that hydrograph is sensitive to seasonal variations, for instance up to July 22, snow melting effect on flow monitoring station is apparent. Thus, high flow rate differences are observed between hydrographs derived from simulations and flow monitoring station.

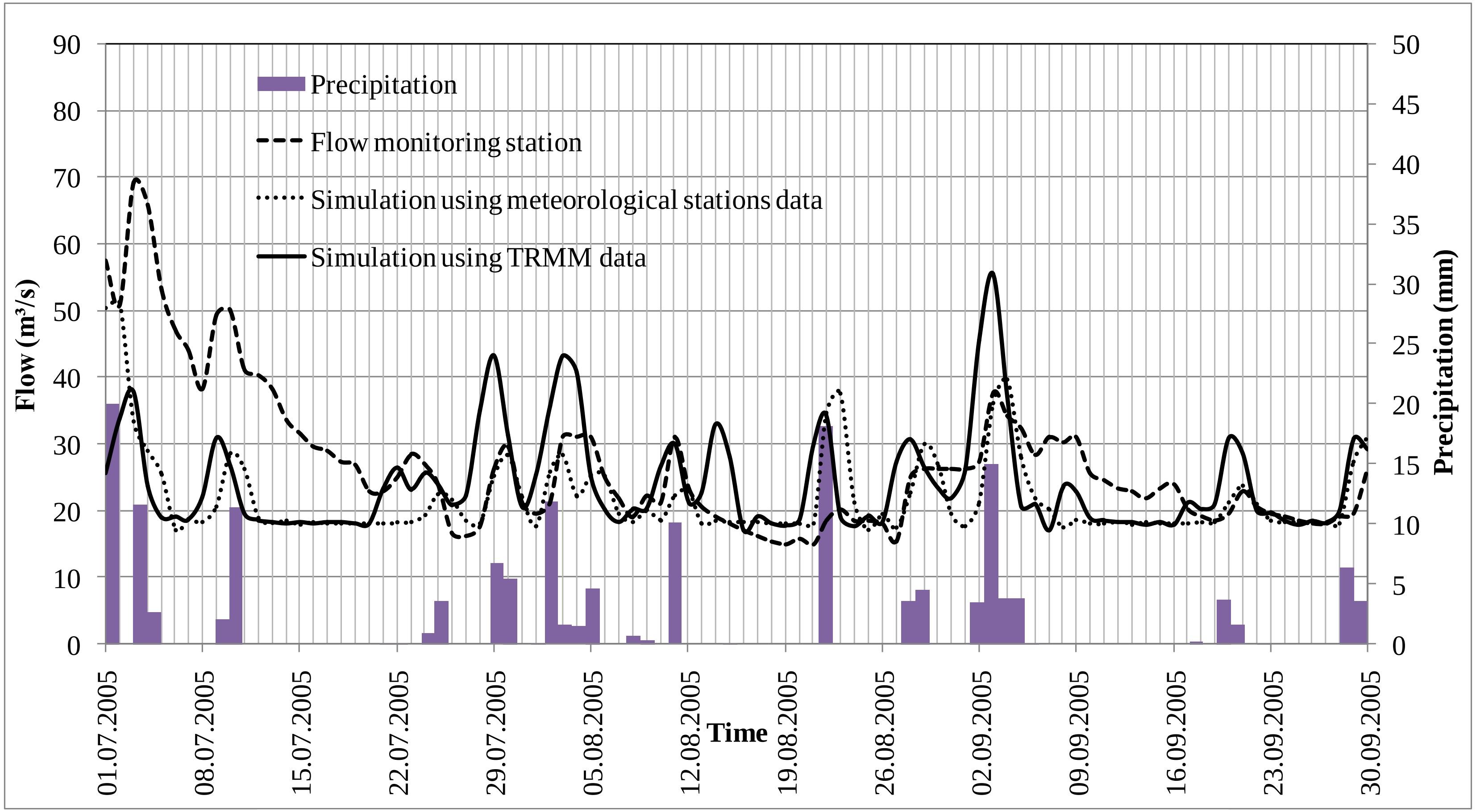

Figure 5.20 Optimization result

5.7 Model Performance

In order to assess performance of hydrologic model two statistical criteria are used; Root Mean Square Error (RMSE) and Nash and Sutcliffe Efficiency (NSE).

- RMSE, indicates the closeness of observed data to the predicted data and has same units of the assessed data. For perfect fit result should be near zero. The equation is:

$$\text{RMSE} = \sqrt{\frac{\sum_{i=1}^{n} (x_{obs,\, i} - x_{sim,\, i})^2}{n}} \qquad \text{(Eq. 5.1)}$$

where, x_{obs}: observed data, x_{sim}: simulated data and n: number of observations.

- NSE is developed by Nash and Sutcliff (1970) to indicate performance of the hydrologic model. It is dimensionless and ranging from -∞ to 0. An efficiency of greater than 0.7 indicates that modeled data are generally acceptable as accurate. The equation is:

$$\text{NSE} = 1 - \frac{\sum_{i=1}^{n} (x_{obs,\, i} - x_{sim,\, i})^2}{\sum_{i=1}^{n} (x_{obs,\, i} - \overline{x_{obs}})^2} \qquad \text{(Eq. 5.2)}$$

where, x_{obs}: observed data, x_{sim}: simulated data, overbar of x_{obs}: mean for all time period and n: number of observations.

Table 5.4 shows the performance results using these statistical criteria for discharge values in m^3/s. Table 5.5 shows the results for discharge values in hm^3 needed for the water potential determination.

Table 5.4 Statistical performance result (2005)

	TRMM 3B42 (V6)		Meteorological stations	
Months	RMSE	NSE	RMSE	NSE
July (first 20 days)	22.37	0.13	20.77	0.12
July (last 10 days)	8.02	-1.31	2.93	0.58
August	7.20	-1.10	5.47	-0.21
September	7.45	-1.00	5.67	-0.16
All months	12.32	-0.17	12.24	0.20
All months (last 72 days)	7.41	-0.80	5.48	-0.04

Table 5.5 Water budget with respect to simulation results and flow monitoring station (2005)

YEAR 2005	hm^3				
Months	Flow Mon. Station.	TRMM 3B42 (V6)	Bias %	Meteor. Station	Bias%
July (first 20 days)	69.62	38.18	-82.3	40.18	-73.3
July (last 10 days)	22.09	23.39	5.6	18.82	-17.4
August	57.03	68.08	16.2	58.33	2.2
September	62.47	60.84	-2.7	54.68	-14.2
All months	211.21	190.48	-10.9	172.01	-22.8
All months (last 72 days)	141.59	152.3	7.0	131.83	-7.4

Table 5.4 shows that for all selected time intervals, meteorological station statistical results are better than the TRMM 3B42 (V6) results. Modeling with meteorological stations gives higher Nash and Sutcliff coefficients and lower RMSE values (Table 5.4). TRMM 3B42 (V6) results are close to the results obtained by meteorological stations. When the predictions are compared with respect to water potential, underestimation is obtained from meteorological

stations’ predictions (-7.4 %), whereas overestimation is obtained from TRMM 3B42 (V6) predictions (7 %) for 72 days.

5.8 Validation

In previous sections, for July, August and September of year 2005, parameters are recalibrated by optimizing simulation of meteorological station data using flow monitoring station data. In order to ensure these parameters, simulations are performed for year 2003. Like 2005, snow melting effect is substantial between April and July. In order to see simulation result, time span is narrowed to three months (Figure 5.21). In this figure, the precipitation values are derived from the averaged of the meteorological stations, 17668 and 17688 for year 2003.

Although there is a matching flow trend between flow monitoring station and TRMM 3B42 (V6) simulated flow, the flow rate differences are higher than the previous study (Figure 5.21). Because, 2003 period is comparatively dry period with respect to 2005 period (Figure 5.22) and parameters in the model are not changed. The average rainfall and temperature values observed in 2005 and 2003 years are summarized in Table 5.6 for stations used in the modeling.

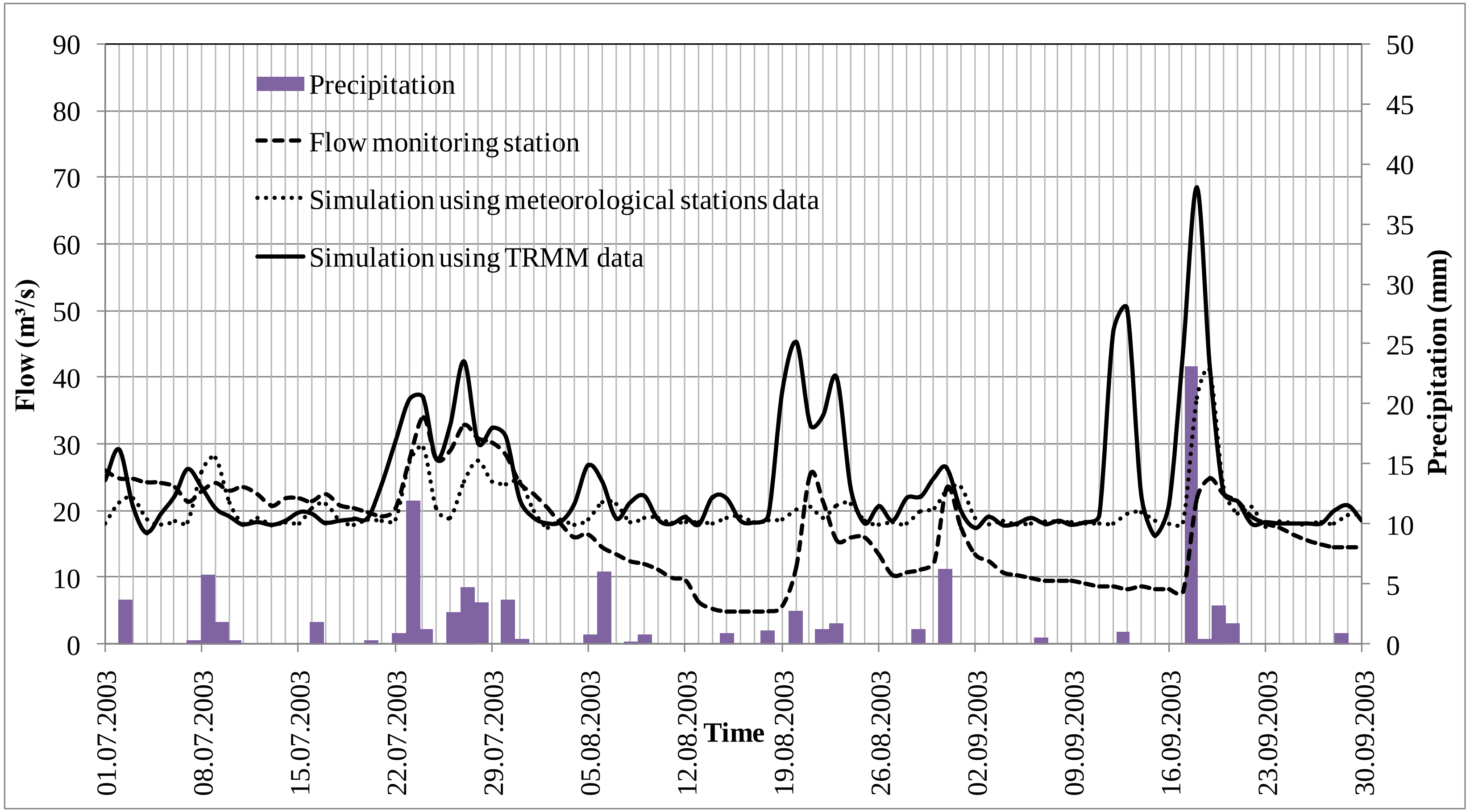

Figure 5.21 Simulation result (2003)

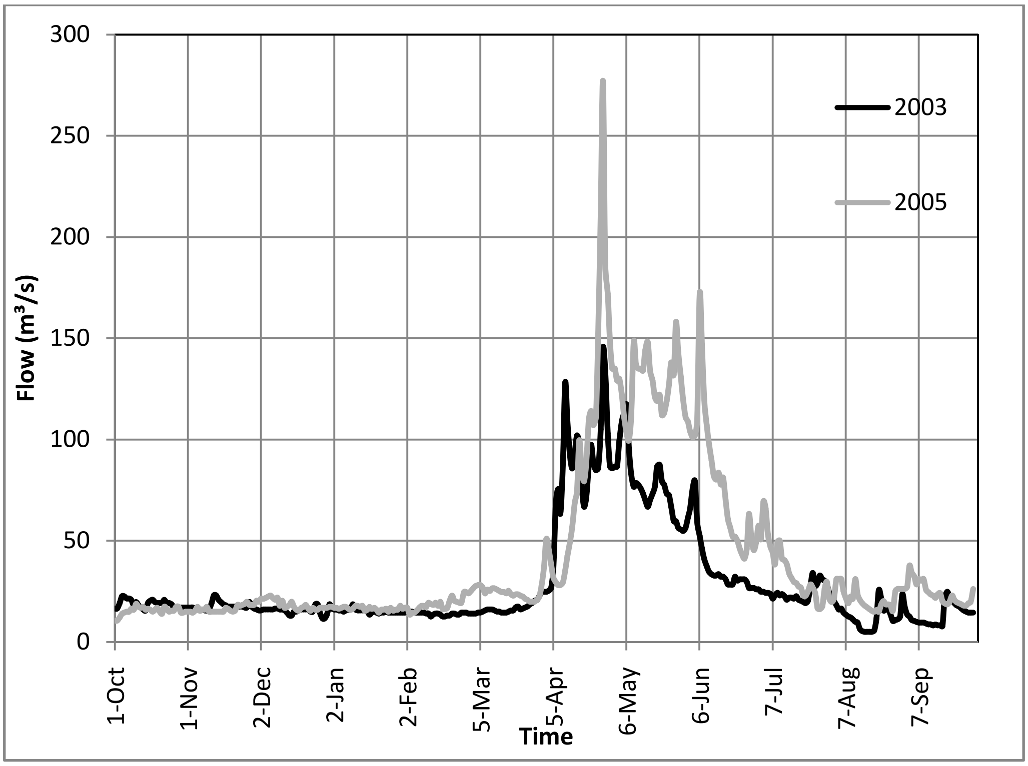

Figure 5.22 Flow monitoring station data for 2003 and 2005 years

It is seen that 2003 period is arid period with respect of 2005 period, especially after May (Figure 5.22). Moreover, Table 5.6 clarifies the condition. There is not a serious temperature change between two years but precipitation amount is noticeable.

Table 5.6 Average temperature and precipitation values

	Station	Year	July	August	September.	All month
Average Temp. (C°)	17668	2003	22.30	23.19	16.09	10.12
		2005	22.94	23.13	17.50	9.66
	17688	2003	19.99	19.82	14.78	8.46
		2005	21.29	20.85	14.37	9.38
Precipitation. (mm/month)	17668	2003	49.70	15.10	24.80	33.51
		2005	71.30	50.00	46.20	51.36
	17688	2003	36.60	31.30	37.30	41.67
		2005	57.70	64.50	36.90	54.74

In order to obtain statistical performance, aforementioned criteria are used for the selected months (Table 5.7).

Table 5.7 Statistical performance result (2003)

	TRMM 3B42 (V6)		Meteorological stations	
Months	RMSE	NSE	RMSE	NSE
July (first 20 day)	3.71	-0.73	3.95	-0.42
July (last 10 day)	5.54	0.39	3.19	0.57
August	13.36	-4.45	8.20	-1.05
September	16.51	-10.18	7.98	-1.61
All months	12.48	-0.54	8.01	0.19
All months (last 72 day)	13.97	-0.33	7.74	0.23

Using simulation results, water budget is obtained for 2003 year (Table 5.8).

Table 5.8 Water budget with respect to simulation results and flow monitoring station (2003)

YEAR 2003	hm^3				
Months	Flow Mon. Station	TRMM 3B42 (V6)	Bias %	Meteor. Station	Bias %
July (first 20 day)	37.3	33.45	-11.5	32.73	-14.0
July (last 10 day)	26.13	29.8	12.3	22.05	-18.5
August	34.72	62.89	44.8	51.5	32.6
September	35.5	63.1	43.7	52.59	32.5
All months	133.65	189.25	29.4	158.88	15.9
All months (last 72 day)	96.35	155.8	38.2	126.15	23.6

Form Table 5.8 it is seen that bias in the data of TRMM 3B42 (V6) and meteorological stations increases.

CHAPTER 6

DISCUSSION OF RESULTS AND CONCLUSIONS

This study mainly describes the methodology of evaluating the satellite based precipitation data as input for rainfall-runoff modeling applied to a mountainous basin, Çoruh in Turkey. Basin model is developed by using HEC-HMS modeling software due to its usability, automatic parameter optimization and integration with GIS.

6.1 Discussion of the Results

Two different TRMM (V6) products namely TRMM 3B43 (V6) (monthly) and TRMM 3B42 (V6) (daily) are compared with ground observations at meteorological stations. Through simple statistical techniques, 730 layers of TRMM 3B42 (V6) daily product, 132 layers of TRMM 3B43 (V6) monthly product and ground observations from 26 meteorological stations are used in the analysis. Spatial distribution of ground rainfall values in Çoruh basin is mainly influenced by elevation and the latitude is the secondary factor affecting the distribution of rainfall.

Monthly based comparisons (TRMM 3B43 (V6) data) with ground observations are performed for the period of 11 years, from January 1998 to December 2008. Results show that during 11 year period accumulated mean monthly rainfall of TRMM 3B43 (V6) data overestimate the precipitation approximately by 20%. The patterns of monthly rainfall determined by both

TRMM 3B43 (V6) and meteorological stations show good agreement in the amounts, as well as in the variation of average rainfall. The correlation coefficient of averaged monthly rainfall is 0.921. The distribution of both the accumulated precipitation values shows that, there is a strong direction dependency in north-south direction. It is observed that TRMM 3B43 (V6) products cannot capture the orographic precipitation in the exact location, a shift in the south-east direction is observed. The coarse spatial resolution of the TRMM 3B43 (V6) products leads to an overestimation for the meteorological stations 17718, 17096 and 17690 (Figure 4.4).

Direct point pixel and point neighbourhood pixel comparisons show that, both precipitation values have matching trend and acceptable correlation coefficients. In direct pixel comparison, 18 stations among 26 have ***R*** values greater than 0.7 in monthly based rainfall comparison. In neighborhood pixel comparison, it is seen that some of the neighborhood pixels have slightly better results than the results of original pixel comparison. Only for one station, Tortum, 10% difference is observed, but other ones remain virtually unchanged. Moreover, it is observed that correlation of the TRMM 3B43 (V6) and ground data are not related to the altitude, rainfall amount and aspect values. In view of all comparisons it can be said that, TRMM 3B43 (V6) data appears to define good results but ground data are indispensable for validation and improvement of the satellite data.

Using geographically weighted regression tool in ArcGIS, presence of nonstationarity between ground and satellite data is tested. At the end of the analysis, geographic region where satellite data perform better are obtained. The geographically weighted regression gives local regression parameters indicating better fits.

For TRMM 3B42 (V6) data (daily based), comparisons are performed for 39 meteorological stations, using 92 precipitation layers (01 June 2005 to 30 September 2005). In the comparison of daily satellite products with ground observations, the results are not promising like the monthly comparisons. Rather than TRMM 3B42 (V6) grids vs. point gauge comparison, the performance of the daily rainfall products is tested with hydrological modeling performance. This helps to integrate the rainfall effects over the basin in terms of river discharge.

The rainfall-runoff modeling is performed by using HEC-HMS. The input files for HEC-HMS are produced by using HEC-GeoHMS. Due to insufficient data in the studied area, model parameters in loss and transform methods are derived from curve number. The curve number generation is completed by using land use and soil cover datasets. DEM data is processed by using the extension of ArcHydro in GIS environment, basin boundaries are delineated and stream network configuration is formed.

The modeling is performed to simulate the hydrograph at EIE 2323 resulting from precipitation data of ground observations and satellite products. As two year of daily meteorological data are available, period of 2005 is taken as calibration period and period of 2003 is taken for validation.

Due to the snow effect, only months July, August and September (2005) are studied. By making calibration, unknown parameters, such as baseflow, Muskingum K and X values are determined. Parameters are redefined by making optimization in the modeling. For both precipitation values, model is run with the same methods and parameters. The output discharge values are compared with the flow monitoring station by using RMSE and NSE as statistical criteria. At the end of the comparison it is seen that, simulation using ground data shows better results than the TRMM 3B42 (V6) data in all months studied because calibration is performed with gauge data. For the last 72 days, it is seen that the bias of water budget results for both simulations does not exceed 10%.

To validate model parameters, different time interval is used. The same study with the same model parameters obtained from the modeling for 2005 is performed for 2003 year. The validation period performance is not satisfactory. There may be several reasons for poor results. Both studied periods do not reflect the same rainfall pattern. The period of 2003 is drier compared to 2005 period. Constant baseflow method may not be suitable for the study. Studies performed by Hughes et al. (2006) in Okavango River and Shrestha et al. (2008) in Bagmati basin, show similar findings. In these studies, it is pointed out that the result of validation period were poorer than the calibration period.

6.2 Conclusions and Recommendations

The spatial distribution of rainfall determined by TRMM 3B42 and raingauges all displayed strong variation with latitude in Çoruh Basin. The patterns of monthly rainfall determined by both TRMM 3B43 (V6) and raingauges showed good agreement in the amounts. TRMM 3B43 (V6) overestimation in the wet season was observed. TRMM 3B43 (V6) monthly data better correlated with the ground observations compared to the TRMM 3B42 (V6) daily data for a short comparison period. The need of accounting the topographic controls on rainfall is seen in the adjustment of the satellite data.

As time scale of the satellite products decreases, the comparison of satellite product (areal) with ground observations (point) may not give good results. The rainfall effects must be integrated over the basin and the comparison in terms of river discharge is more meaningful. In that sense TRMM 3B42 (V6) data appear to describe well the hydrological regimes in the subbasins of Çoruh River. TRMM 3B42 (V6) data has a potential to be used in data sparse regions to predict the runoff in order to predict the hydrograph and/or water potential in ungauged basins.

Neither the satellite data nor the raingauge data are sufficient to understand the climatology of a basin; they should be used in combination. Similar studies must be performed with more meteorological data covering the whole country.

In the rainfall-runoff modeling the evapotranspiration and snowmelt data can be included to observe the performance of the model for all seasons and to estimate the annual water potential of a basin.

REFERENCES

Adler, R. F., Huffman, G. J., Bolvin, D. T., Curtis, S., and Nelkin, E. J. (2000). Tropical Rainfall Distributions Determined Using TRMM Combined with Other Satellite and Rain Gauge Information. *Journal of Applied Meteorology and Climatology* , 2007-2023.

Al-Abed, N., Abdulla, F., and Khyarah, A. A. (2005). GIS-hydrological models for managing water resources in the Zaqra River Basin. *Environmental Geology* (47), 405-411.

Casimiro, W. S., Labat, D., Guyot, J. L., Ronchail, J., and Ordonez, J. J. (2009). TRMM rainfall data estimation over the Peruvian Amazon- Andes basin and its assimilation into a monthly water balance model. *New Approaches to Hydrological Prediction in Data Sparce Regions* (pp. 245-252). Hyderabad, India: IAHS Publ.

Charlton, M., and Fotheringham, A. S. (2009, 01 01). *Geographically Weighted Regression A Tutorial on using GWR in ArcGIS.* Retrieved 08 01, 2010, from National Center for Geocomputation: http://ncg.nuim.ie/

Chiu, L. S., Lim, C., and Teng, W. (August 2004). Development of Agricultural Information System (AIS): Comparison of TRMM and Climate Division Rain Rates over Oklahoma. *Presented at Second TRMM Int'l. Science Conf.* Nara, Japan.

Chokngamwong, R., and Chiu, L. (2008). Thailand Daily Rainfall and Comparison with TRMM Products. *Journal of Hydrometeorology* , 256-266.

Collischonn, B., Collischonn, W., and Tucci, C. E. (2008). Daily hydrological modeling in the Amazon basin using TRMM rainfall estimates. *Journal of Hydrology* , 207-216.

Colorado State University. (n.d.). *Climate Rainfall Data Center (CRDC).* Retrieved 07 05, 2010, from http://rain.atmos.colostate.edu/CRDC/frame_prod.html

Crawford, N. H., and Linsley, R. (1966). *Digital Simulation in Hydrology Stanford Watershed Model IV.* Stanford, California: Department of Civil Engineering, Stanford University.

Csiszár, I., Major, G., Kerényi, J., and Diószeghy, M. (1997). Precipitation estimation with satellites and radar. *Advances in Space Research* , 461-467.

Cunderlik, J. M., and Simonovic, S. P. (2007). Hydrologic Models for Inverse Climate Change Impact Modeling. *18th Canadian Hydrotechnical Conference.* Manitopa.

Das, M. M., and Salkia, M. D. (2009). *Hydrology*. New Delhi: PHI Learning Private Limited.

Dingman, S. L. (2002). *Physical Hydrology.* Boca Raton: Prentice Hall.

Dinku, T., Connor, S. J., and Ceccato, P. (2010). Comparison of CMORPH and TRMM-3B42 over mountainous regions of Africa and South America. In M. Gebremichael, and F. Hossain, *Satellite Rainfall Applications for Surface Hydrology* (pp. 193-204). Springer Netherlands.

Donigian, A. S., and Imhoff, J. (2006). History and Evolution of Watershed Modeling Derived from the Stanford Watershed Model. In V. P. Singh, and D. K. Frevert, *Watershed Models* (pp. 21-45). Florida: CRC press Taylor and Francis Group.

Feidas, H., and Chrysoulakis, N. (4 - 8 February 2008). Comparison of TRMM climate rainfall products and gauge observations over Greece. *Proc. of the Third NASA/JAXA International Science Conference.* Las Vegas, USA.

Gu, S., Gao, H., Zhu, Y., Zhao, B., Lu, N., and Zhang, W. (2002). Remote sensing land surface wetness by use of TRMM/TMI microwave data. *Meteorology and Atmospheric Physics* , 59-63.

Harris, A., Rahman, S., Hossain, F., Yarborough, L., C.Bagtzoglou, A., and Easson, G. (2007). Satellite-based Flood Modeling Using TRMM-based Rainfall Products. *Sensors* , pp. 3416-3427.

Hoblit, B. C., and Curtis, D. C. (2001). Integrating Radar Rainfall Estimates with Digital Elevation Models and Land Use Data to Create an Accurate Hydrologic Model. *Floodplain Management Association Spring 2001 Conference* . San Diego, Califronia, USA.

Hong, Y., Adler, R. F., Huffman, G. J., and Pierce, H. (2010). Applications of TRMM Based Multi Satellite Precipitation Estimation for Global Runoff Prediction: Prototyping a Global Flood Modeling System. In M. Gebremichael, and F. Hossaim, *Satellite Rainfall Applications for Surface Hydrology* (pp. 245-265). Srpinger Netherlands.

Hossain, F., and Anagnostou, E. N. (2004). Assessment of current passive-microwave- and infrared-based satellite rainfall remote sensing for flood prediction. *J. Geophys. Res* , pp. 109, D07102.

Huffman, G. J., Adler, R. F., Bolvin, D. T., Gu, G., Nelkin, E. J., Bowman, K. P., et al. (2007). The TRMM Multisatellite Precipitation Analysis (TMPA): Quasi-global, multiyear, combined-sensor precipitation estimates at fine scales. *Journal of Hydrometeorology* , 38-55.

Hughes, D. A. (2006). Comparison of satellite rainfall data with observations from gauging station networks. *Journal of Hydrology* (327), pp. 399-410.

Hughes, D. A., Andersson, L., Wilk, J., and Savenije, H. H. (2006). Regional calibration of the Pitman model for the Okavango River. *Journal of Hydrology*, 30-42.

Kadıoğlu, M. (2010). *Devlet Meteoroloji İşleri yeni bir yapılanmaya gitmeli.* Retrieved 07 01, 2010, from Hürriyet: http://www.hurriyet.com.tr/yazarlar/14175626_p.asp

Kafle, T. P., Hazarika, M. K., Karki, S., Shrestha, R. M., Sharma, S., and Samarakoon, L. (2007). Basin scale rainfall-runoff modelling for flood forecasts. *Proceedings of the 5th Annual Mekong Flood Forum.* Ho Chi Minh City, Vietnam.

Kamarianakis, Y., Feidas, H., Kokolatos, G., Chrysoulakis, N., and Karatzias, V. (2008). Evaluating remotely sensed rainfall estimates using nonlinear mixed models and geographically weighted regression. *Environmental Modelling and Software* , 1438-1447.

Kızılkaya, T. (1983). *Sulama ve Drenaj.* Ankara: General Directorate of State Hydraulic Works.

Knebl, M., Yang, Z.-L., Hutchison, K., and Maidment, D. (2005). Regional scale flood modeling using NEXRAD rainfall, GIS, and HEC-HMS/RAS: a case study for the San Antonio River Basin Summer 2002 storm event. *Journal of Environmental Management* , 325-336.

Kummerow, C., Simpson, J., Thiele, O., Barnes, W., Chang, A. T., Stocker, E., et al. (2000). The Status of the Tropical Rainfall Measuring Mission (TRMM) after Two Years in Orbit. *Journal of Applied Meteorology* , 1965-1982.

Kutoğlu, Y. (2010). Personal Contact.

Liu, Z., Chiu, L., Teng, W., Rui, H., and Serafino, G. (2002). TRMM Rainfall Products and Tools for Tropical Infectious Disease Studıes. *15th Conference on Biometerology/Aerobiology*. Kansas City, MO.

Liu, Z., Rui, H., Teng, W. L., Chiu, L. S., Leptoukh, G., and Vicente, G. A. (2007). Online Visualization and Analysis: A New Avenue to use Satellite Data for Weather, Climate, and Interdisciplinary Research and Applications. In V. Levizzani, P. Bauer, and F. J. Turk, *Measuring Precipitation From Space* (pp. 549-558). Springer Netherlands.

Minghu, C., Huizhong, H., Dongyan, M., Yanjun, Q., Zhehu, C., and Fengxian, Z. (2008). Study of 1998 heavy rainfall over the Yangtze River Basin using TRMM data. *Advances in Atmospheric Sciences* , 387-396.

Ministry of Environment and Forestry. (2010). *GMES Arazi İzleme Sistemi*. Retrieved August 01, 2010, from http://corine.cevreorman.gov.tr/? q=node/1

NASA. (2010, 07 30). *TRMM Online Visualization and Analysis System (TOVAS)*. Retrieved 04 01, 2010, from National Aeronautics and Space Administration: http://gdata1.sci.gsfc.nasa.gov/daac-bin/G3/gui.cgi?instance_id=TRMM_Monthly

Nash, J., and Sutcliffe, J. (1970). River flow forecasting through conceptual models. *Journal of Hydrology* , 282-290.

National Weather Service Oregon. (2001). *Oregon's Top Weather Events of the 20th Century*. Retrieved from National Weather Service Western Region Headquarters: nimbo.wrh.noaa.gov/Portland/OR_top10.html

Negri, A. J., Burkardt, N., Golden, J. H., Halverson, J. B., Huffman, G. J., Larsen, M. C., et al. (2005, September). The Hurricane-Flood-Landslide Continuum -Forecasting Hurricane Effects At Landfall. *Bulletin of American Meteorological Society* , pp. 1241-1247.

Nicholson, S. E., Some, B., McColumn, J., Nelkin, E., Klotter, D., Berte, Y., et al. (2003). Validation of TRMM and Other Rainfall Estimates with a High-Density Gauge Dataset for West Africa. Part I: Validation of GPCC Rainfall Product and Pre-TRMM Satellite and Blended Products. *Journal of Applied Meteorology* , 1355-1368.

Nijssen, B., and Lettenmaier, D. P. (2004). Effect of precipitation sampling error on simulated hydrological fluxes and states: Anticipating the Global Precipitation Measurement satellites. *Journal of Geophysical Research* .

Pistocchi, A., and Mazzoli, P. (2002). Use of HEC-RAS and HEC-HMS models with ArcView for hydrologic risk management. In I. E. Society (Ed.), *Integrated Assessment and Decision Support, I*, pp. 305-310. Lugano, Switzerland.

Pretty, G. W. (1995). The status of satellite-based rainfall estimation over land. *Remote Sensing of Environment* , 125-137.

Shrestha, M., Artan, G., Bajracharya, S., and Sharma, R. (2008). Using satellite-based rainfall estimates for streamflow modelling: Bagmati Basin. *Journal of Flood Risk Management* , 89-99.

Sivapalan, M., Takeuchi, K., Franks, S., Gupta, V., Karambiri, H., Lakshmı, V., et al. (2003). IAHS Decade on Predictions in Ungauged Basins (PUB), 2003-2012:Shaping an exciting future for the hydrological sciences. *Hydrological Sciences Journal* , 857-880.

Şensoy, A., Tekeli, A. E., Şorman, A. A., and Şorman, A. Ü. (2003). Simulation of event based snowmelt runoff hydrographs based on snow depletion curves and the degree-day method. *Canadian Journal of Remote Sensing* , 693-700.

Şorman, A. A. (2005). *Use of Satellite Observed Seasonal Snow Cover in Hydrological Modeling and Snowmelt Runoff Prediction in Upper Euphrates Basin, Turkey*. PhD Thesis, Civil Engineering Department, METU, Ankara, Turkey.

Su, F., Hong, Y., and Lettenmaier, D. P. (2008). Evaluation of TRMM Multisatellite Precipitation Analysis (TMPA) and Its Utility in Hydrologic Prediction in the La Plata Basin. *Journal of Hydrometeorology* , 622-640.

Temelsu Mühendislik Limited Şirketi. (1982). *Çoruh Nehri Havzası Master Plan Raporu.* Ankara.

United States Department of Agriculture. (1986). *Urban hydrology for small watersheds.* USA: Technical Release 55 (TR-55) (Second Edition). Natural Resources Conservation Service, Conservation Engineering Division.

USACE. (1998). Flood Hydrograph Package HEC-1 Version 4.1 User's Manual. Davis, CA, USA.

USACE. (2009a). Geospatial Hydrologic Modeling Extension HEC-GeoHMS Version 4.2 User's Manual. Davis, CA, USA.

USACE. (2009b). Hydrologic Modeling System HEC-HMS Quick Start Guide Version 3.4. Davis, CA, USA.

USACE. (2009c). Hydrologic modeling System HEC-HMS Version 3.4 User's Manual. Davis, CA, USA.

Usul, N. (2005). *Engineering Hydrology*. Ankara: METU Press.

Wang, H., Ren, L., and Yang, X. (2009). Prospect for TRMM in rainfall estimates: a case study in the Laohahe basin, China. *New Approaches to Hydrological Prediction in Data Sparce Regions* (pp. 253-258). Hyderabad, India: IAHS Publ.

Wilheit, T. T. (1986). Some of comments on passsive microwave measurement of rain. *Bulletin of the American Meteorological Society* , 1226-1232.

Yener, M. K. (2006). *Semi Distributed Hydrologic Modeling Studies in Yuvacık Basin.* M.S. Thesis, Civil Engineering Department, METU, Ankara, Turkey.

Yuter, S., Miller, M., Stout, J., Wood, R., Kwiatkowski, J., Horn, D., et al. (2006). Remaining Challenges in Satellite Precipitation Estimation Using the Tropical Rainfall Measuring Mission. *Fourth European Conference on Radar in Meteorology and Hydrology*, (pp. 603-607). Barcelona.

APPENDIX A

COMPARISON RESULTS (TRMM 3B43 (V6))

In this part, some of the monthly based rainfall comparisons are represented. These comparisons are performed with the data obtained from TRMM 3B43 (V6) and four different meteorological stations during time period from January 1998 to December 2008.

The selected stations are Akçaabat (17626), Ardahan (17630), Arpaçay (17656), and Solhan (17776). Stations are selected according to their correlation coefficient results.

- Solhan (17776) has the best (after Karakocan, which is shown in the text part),
- Ardahan (17630) has the worst (after Bayburt, which is shown in the text part),
- Arpaçay (17656) and Akçaabat (17626) have the average

correlation coefficient results (monthly base) among 26 meteorological stations.

The correlation coefficient (r) and slope (m) of the fitted line for different time scale for each station are depicted in Table 4.2.

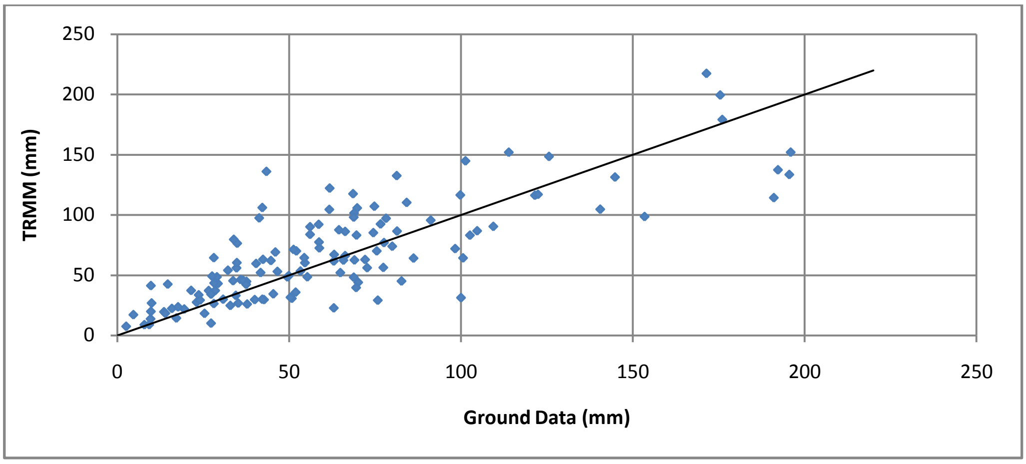

Figure A 1 TRMM vs. Ground Obser. (monthly) 17626 Akçaabat

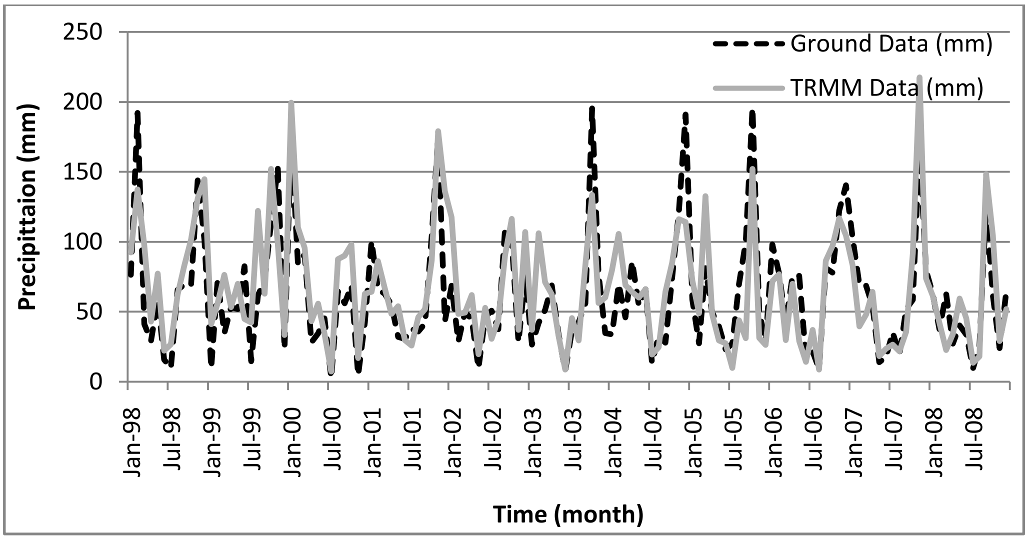

Figure A 2 Monthly Rainfall Diagrams for 17626 Akçaabat

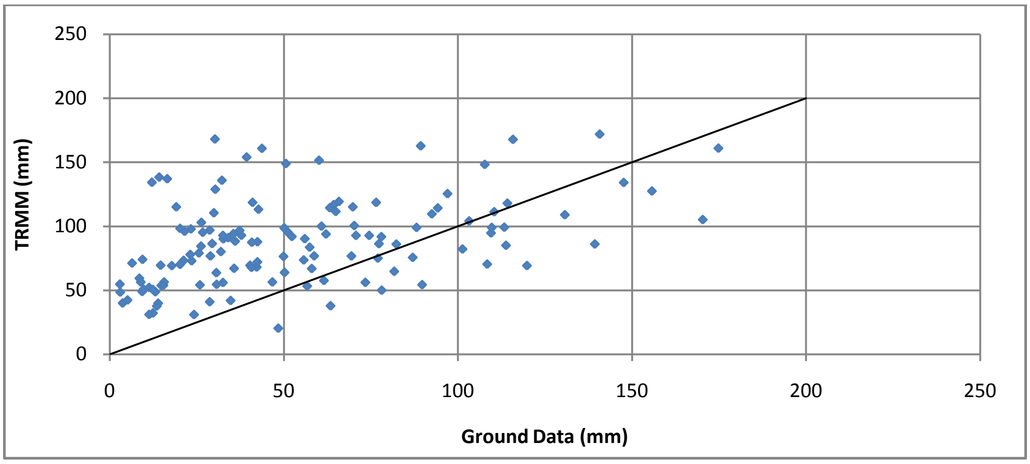

Figure A 3 TRMM vs. Ground Obser. (monthly) 17630 Ardahan

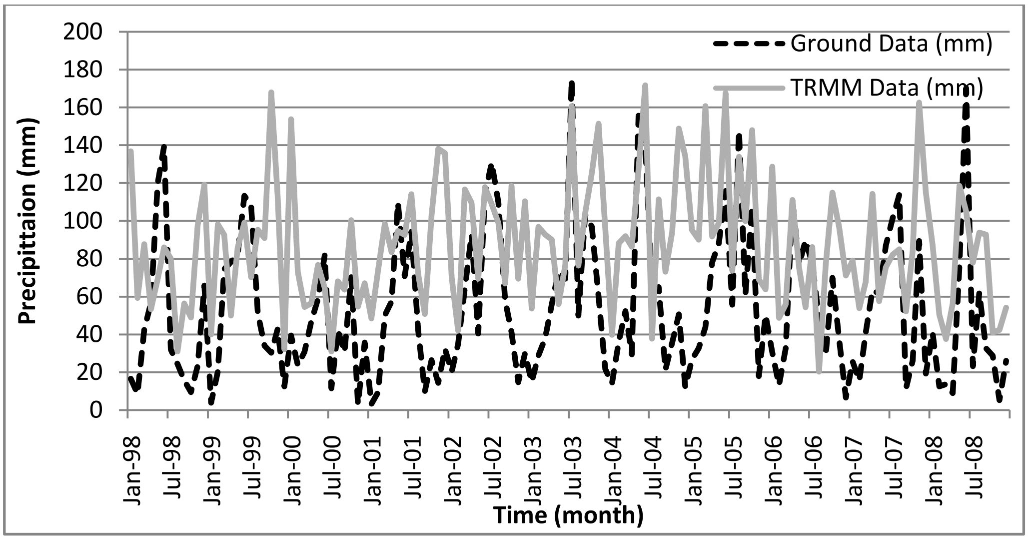

Figure A 4 Monthly Rainfall Diagrams for 17630 Ardahan

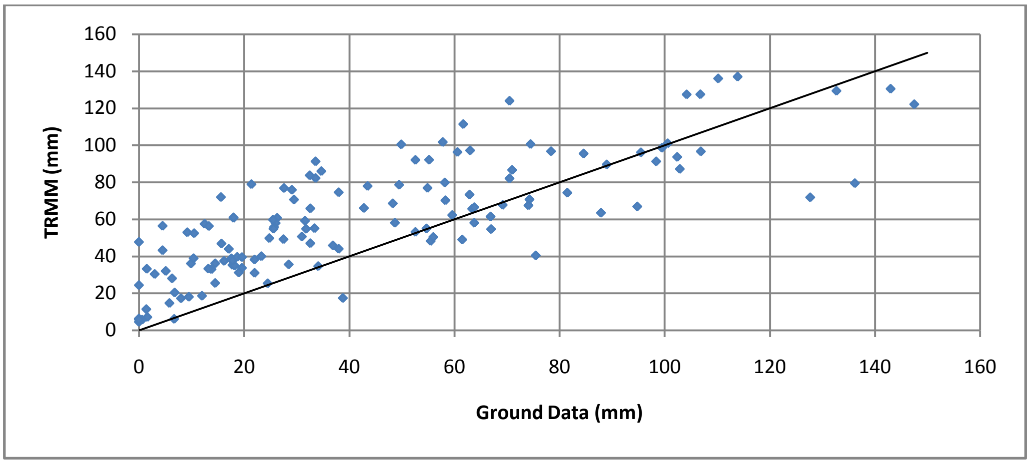

Figure A 5 TRMM vs. Ground Obser. (monthly) 17656 Arpaçay

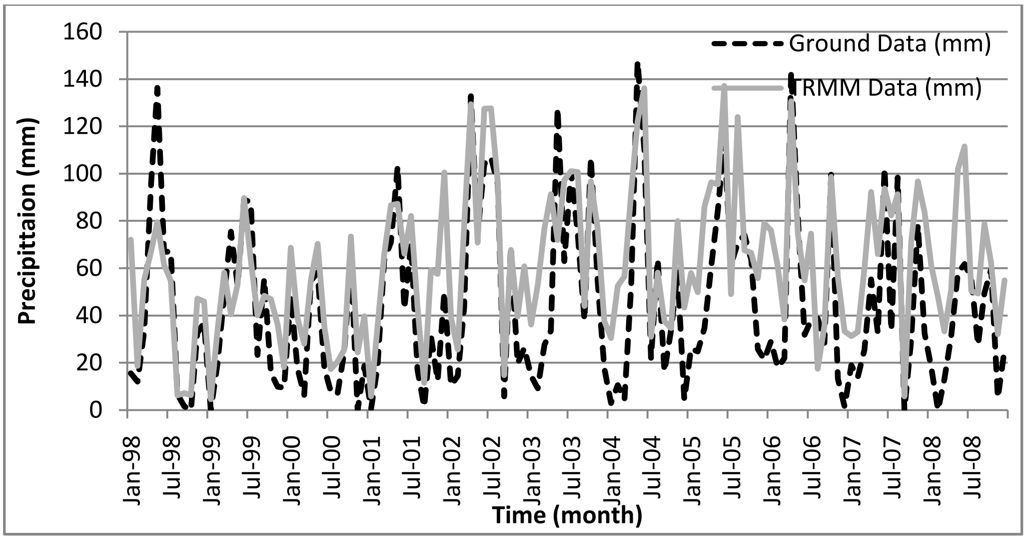

Figure A 6 Monthly Rainfall Diagrams for 17656 Arpaçay

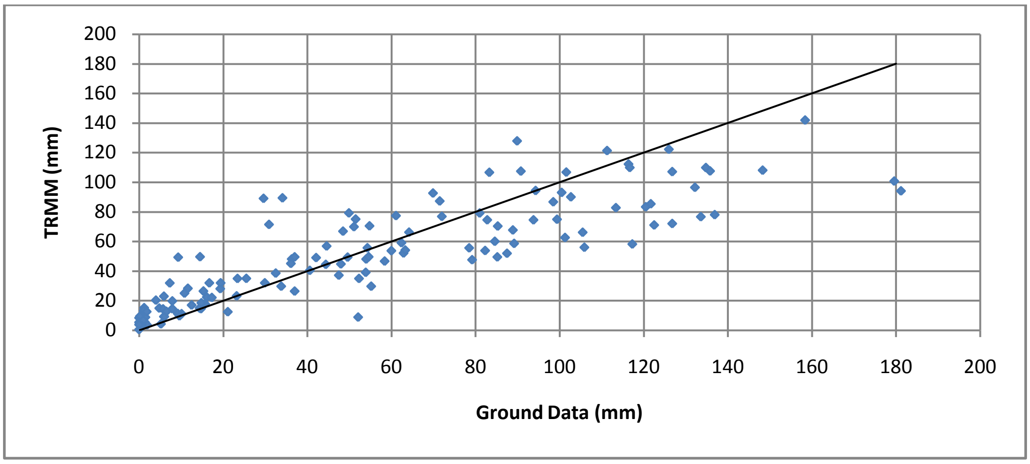

Figure A 7 TRMM vs. Ground Obser. (monthly) 17776 Solhan

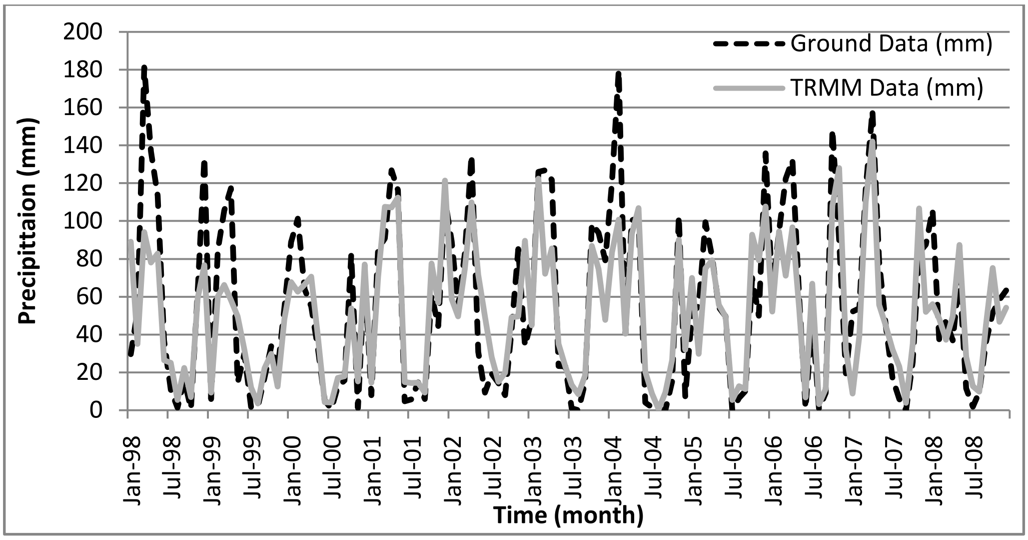

Figure A 8 Monthly Rainfall Diagrams for 17776 Solhan

APPENDIX B

COMPARISON RESULTS (TRMM 3B42 (V6))

In this part, some of the daily based rainfall comparisons are represented. These comparisons are performed with the data obtained from TRMM 3B42 (V6) and six different meteorological stations during time period from July 2005 to September 2005.

The selected stations are Hopa (17042), Ağrı (17099), Akçaabat (17626), Solhan (17776), Malazgirt (17780), and Erciş (17784). Stations are selected according to their correlation coefficient results.

- Erciş (17784) and Hopa (17042) have the best,
- Solhan (17776) and Malazgirt (17780) have the worst,
- Ağrı (17099) and Akçaabat (17626) have the average

results of correlation coefficient (daily base) among 39 meteorological stations.

The correlation coefficient (r) and slope (m) of the fitted line for each station are depicted in Table B 1.

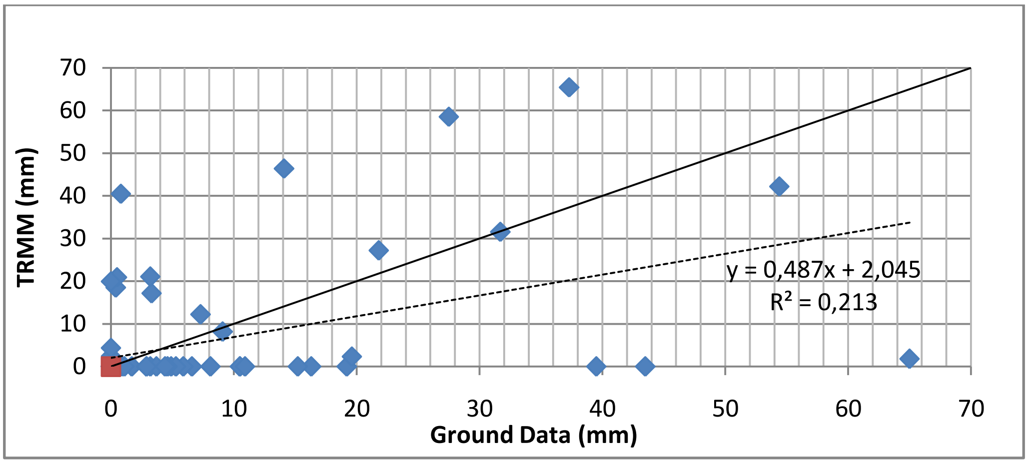

Figure B 1 TRMM vs. Ground Obser. (daily) 17042 Hopa

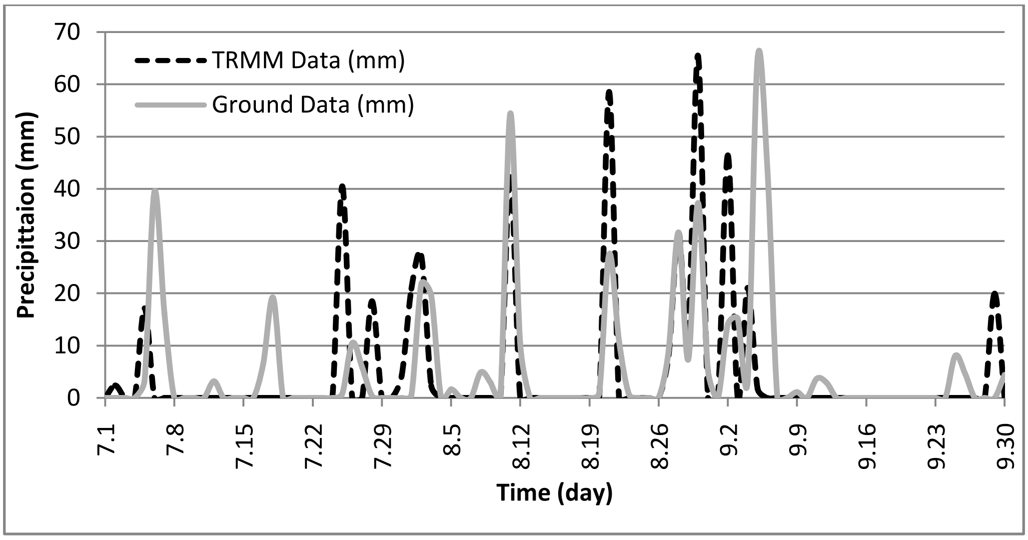

Figure B 2 Daily Rainfall Diagrams for 17042 Hopa

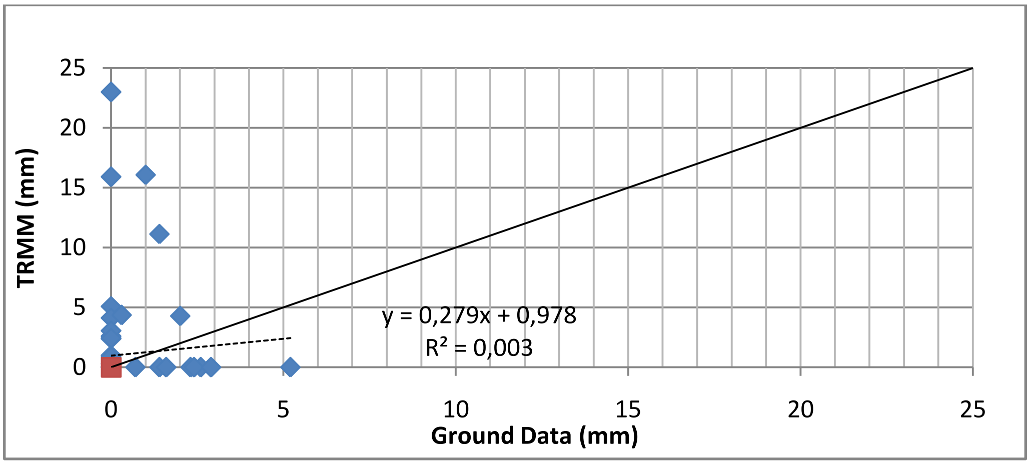

Figure B 3 TRMM vs. Ground Obser. (daily) 17099 Ağrı

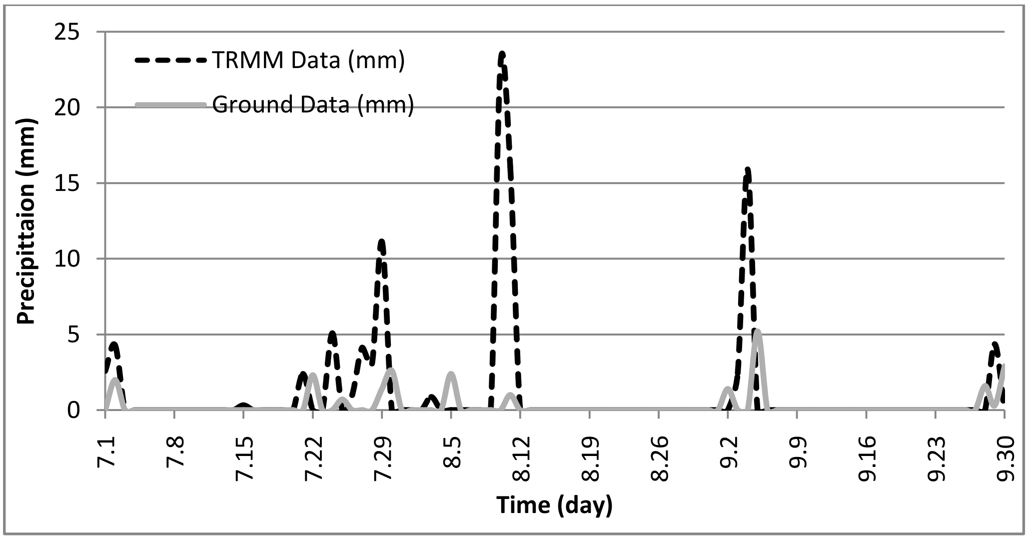

Figure B 4 Daily Rainfall Diagrams for 17099 Ağrı

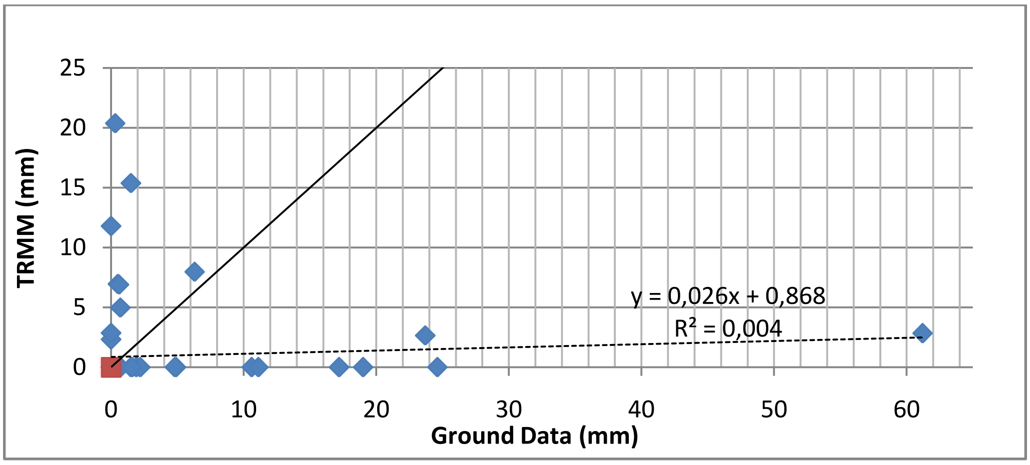

Figure B 5 TRMM vs.Ground Obser. (daily) 17626 Akçaabat

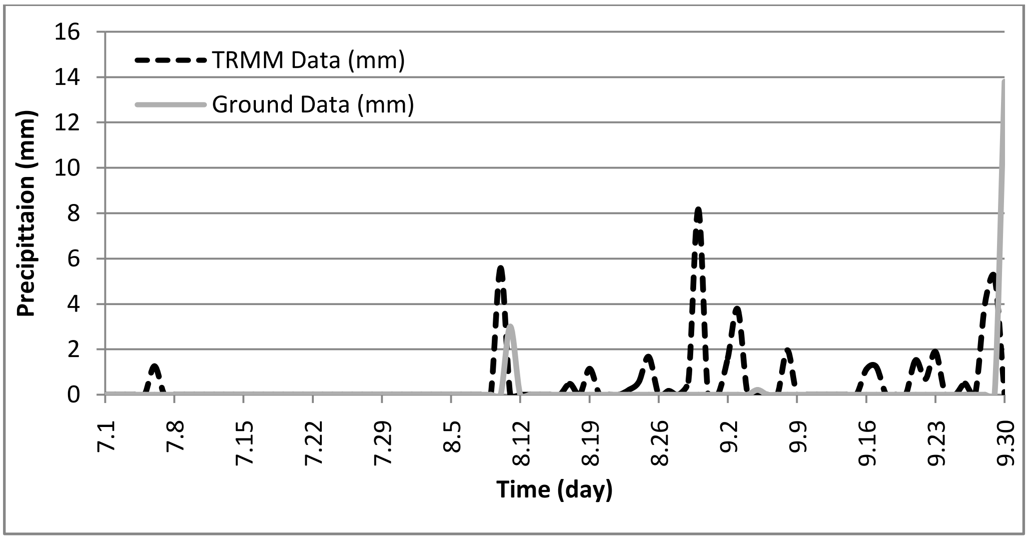

Figure B 6 Daily Rainfall Diagrams for 17626 Akçaabat

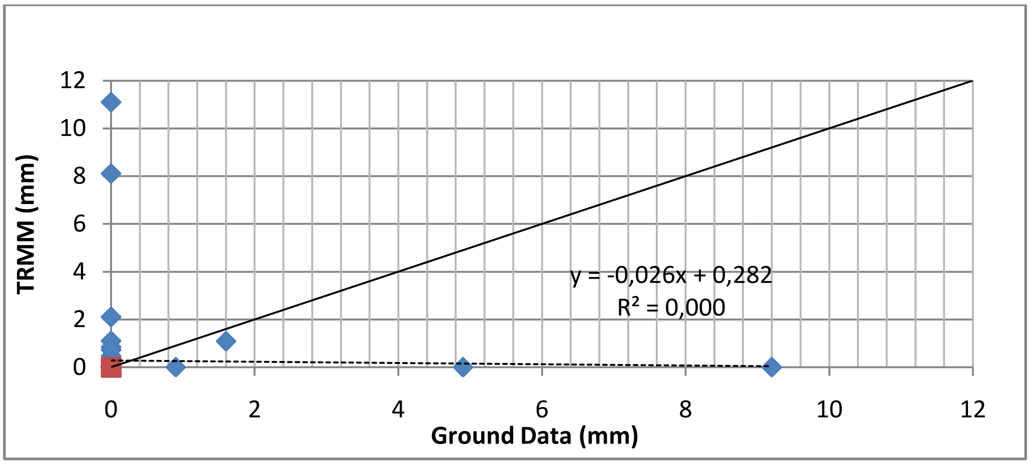

Figure B 7 TRMM vs. Ground Obser. (daily) 17776 Solhan

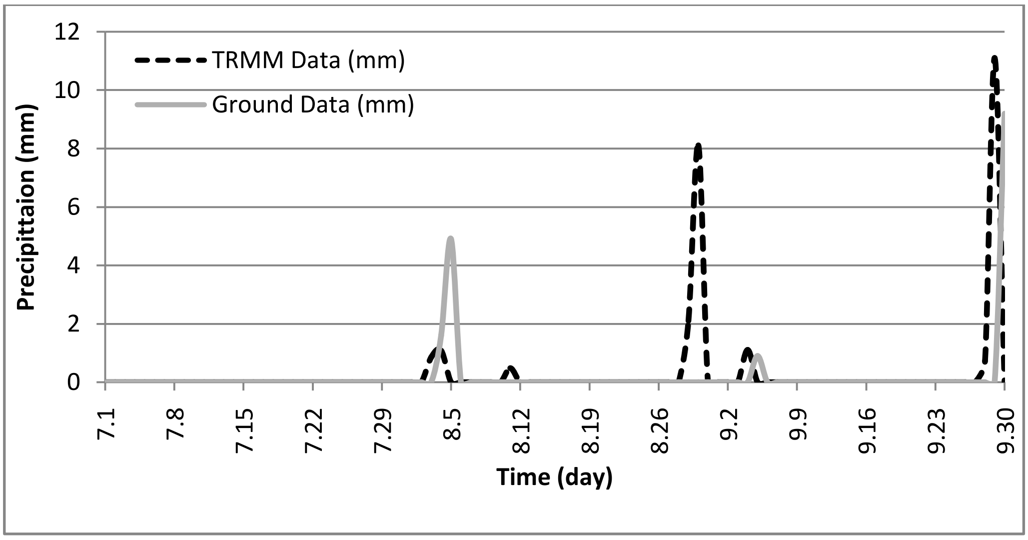

Figure B 8 Daily Rainfall Diagrams for 17776 Solhan

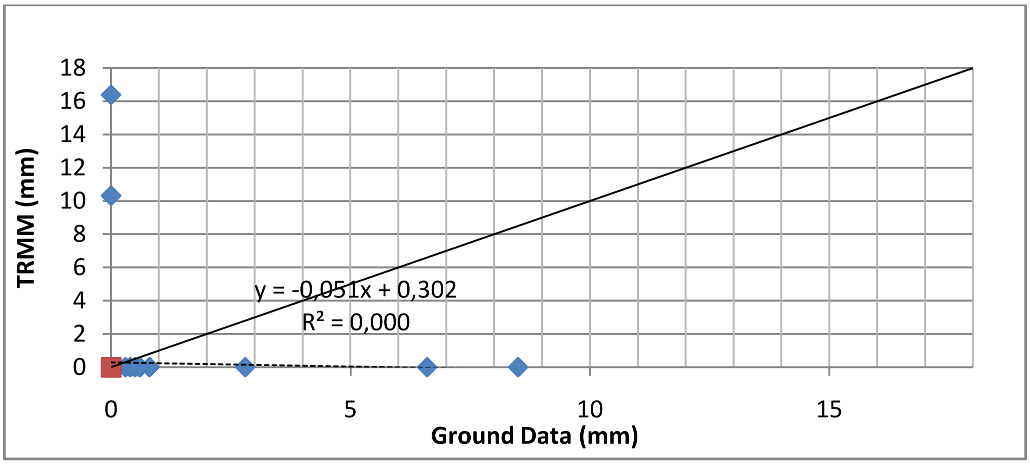

Figure B 9 TRMM vs.Ground Obser. (daily) 17780 Malazgirt

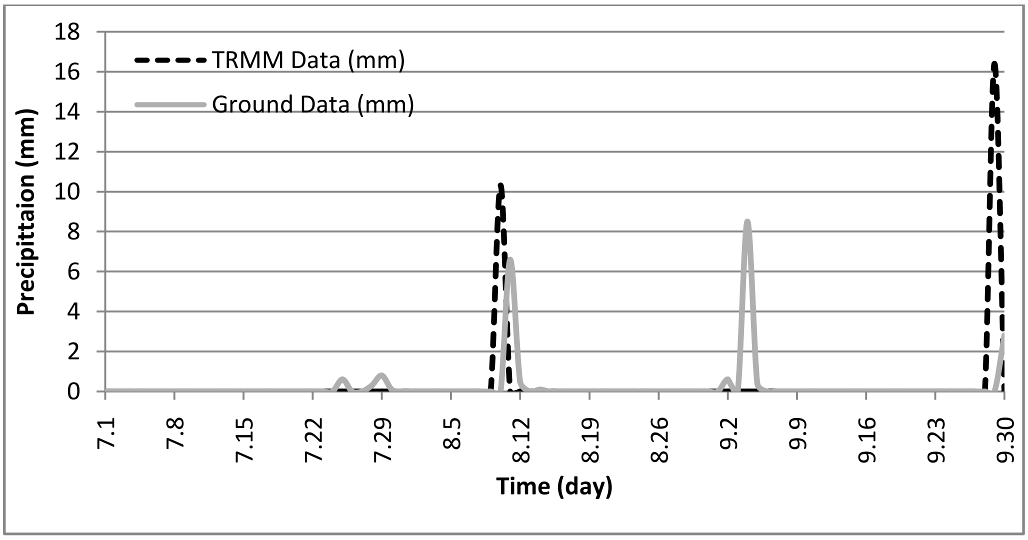

Figure B 10 Daily Rainfall Diagrams for 17780 Malazgirt

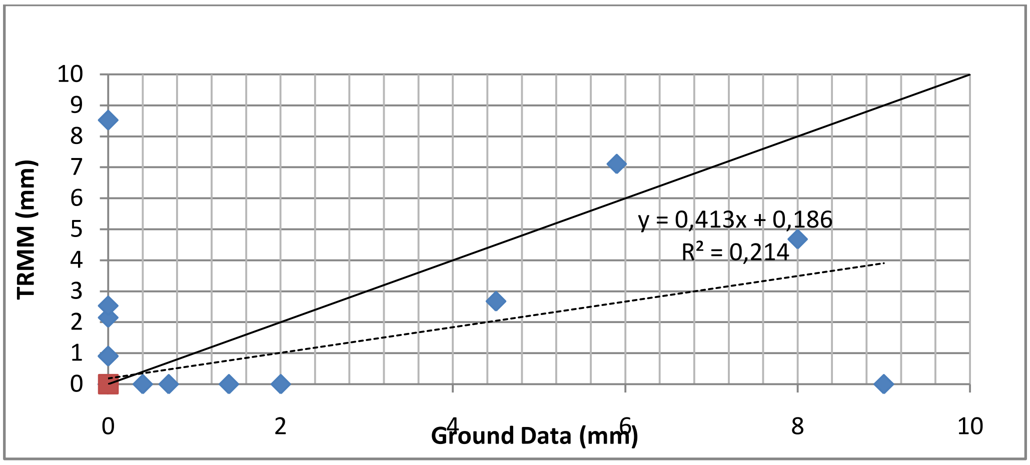

Figure B 11 TRMM vs.Ground Obser. (daily) 17784 Erciş

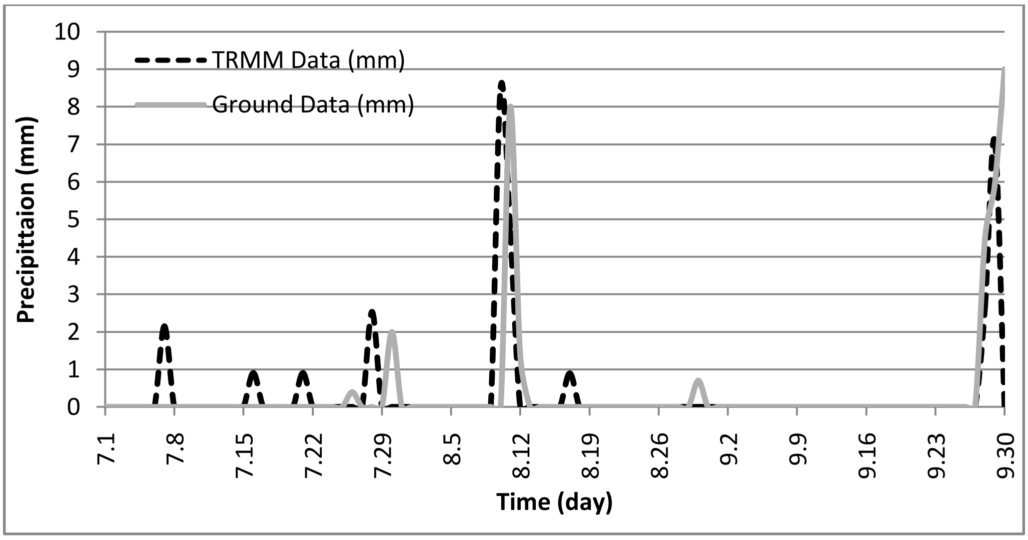

Figure B 12 Daily Rainfall Diagrams for 17784 Erciş

Table B 1 Comparison of TRMM 3B42 with the meteorological stations

ID	Name	r	slope (m)	ID	Name	r	slope (m)
17040	Rize	0.071	0.03	17688	Tortum	0.110	0.113
17042	Hopa	0.462	0.487	17690	Horasan	0.170	0.17
17045	Artvin	0.295	1.202	17692	Sarıkamış	0.417	0.451
17088	Gümüşhane	0.327	0.618	17718	Tercan	0.000	0.006
17094	Erzincan	0.100	0.257	17720	Doğubeyazıt	0.118	0.208
17096	Erzurum	0.077	-0.1	17734	Divriği	0.055	0.204
17097	Kars	0.000	-0.033	17736	Mazgirt	0.000	-0.033
17099	Ağrı	0.055	0.279	17740	Hınıs	0.045	-0.032
17100	Iğdır	0.032	-0.069	17764	Arapkir	0.084	0.131
17165	Tunceli	0.000	-0.049	17766	Ağın	0.145	0.597
17201	Elazığ	0.000	-0.019	17768	Çemişgezek	0.045	0.064
17203	Bingöl	0.032	0.066	17774	Karakoçan	0.000	0.023
17204	Muş	0.045	-0.04	17776	Solhan	0.000	-0.026
17626	Akçaabat	0.063	0.026	17778	Varto	0.084	0.106
17628	Pazar-Rize	0.226	0.101	17780	Malazgirt	0.000	-0.151
17630	Ardahan	0.000	0.016	17784	Erciş	0.463	0.413
17656	Arpaçay	0.032	0.036	17804	Keban	0.179	0.597
17666	İspir	0.176	0.253	17806	Palu	0.045	-0.055
17668	Oltu	0.105	0.108	17808	Genç	0.089	0.192
17686	Bayburt	0.105	0.131				

APPENDIX C

RUNOFF CURVE NUMBERS

In this part, runoff curve numbers are represented. Using hydrologic soil group data with land use description curve numbers are determined for the studied area.

Table C 1 Runoff Curve Numbers (Kızılkaya, 1983)

Land use	Treatment of Practice	Hydrologic Condition	Curve Numbers for Hydrologic Soil Group			
			A	B	C	D
Fallow	SR		77	86	91	94
Row Crops	SR	Poor	72	81	88	91
	SR	Good	67	78	85	89
	C	Poor	70	79	84	88
	C	Good	65	75	82	86
	C and T	Poor	66	74	80	82
	C and T	Good	62	71	78	81
Small Grain	SR	Poor	65	76	84	88
	SR	Good	63	75	83	87
	C	Poor	63	74	82	85
	C	Good	61	73	81	84
	C and T	Poor	61	72	79	82
	C and T	Good	59	70	78	81
Close Seeded Legume or Rotation Meadow	SR	Poor	66	77	85	89
	SR	Good	58	72	81	85
	C	Poor	64	75	83	85
	C	Good	55	69	78	83
	C and T	Poor	63	73	80	83
	C and T	Good	51	67	76	80

Table C 1 Runoff Curve Numbers (Kızılkaya, 1983) (cont.)

Noncultivated Agricultural Land	-	Poor	68	79	86	89
	-	Fair	49	69	79	84
	-	Good	39	61	74	80
	C	Poor	47	67	81	88
	C	Fair	25	59	75	73
	C	Good	6	35	70	79
Meadow	-	-	30	58	71	78
Forestland	-	Poor	45	66	77	83
	-	Fair	36	60	73	79
	-	Good	25	55	70	77
Building	-	-	59	74	82	86
Road (dirt)	-	-	72	82	87	89
Road (paved)	-	-	74	84	90	92

Table C 2 Hydrologic soil group definition (Kızılkaya, 1983)

A	High infiltration (low runoff). Sand, loamy sand, or sandy loam.
B	Moderate infiltration (moderate runoff). Silt loam or loam.
C	Low infiltration (moderate to high runoff). Sandy clay loam.
D	Very low infiltration (high runoff). Clay loam, silty clay loam, sandy clay, silty clay, or clay

Table C 3 Description of abbreviations

SR	Straight Row
C	Contoured
T	Terraces
C and T	Contoured and Terraces

APPENDIX D

REPRESENTATION OF THE BASIN, PARAMETERS, AND OPTIMIZATION

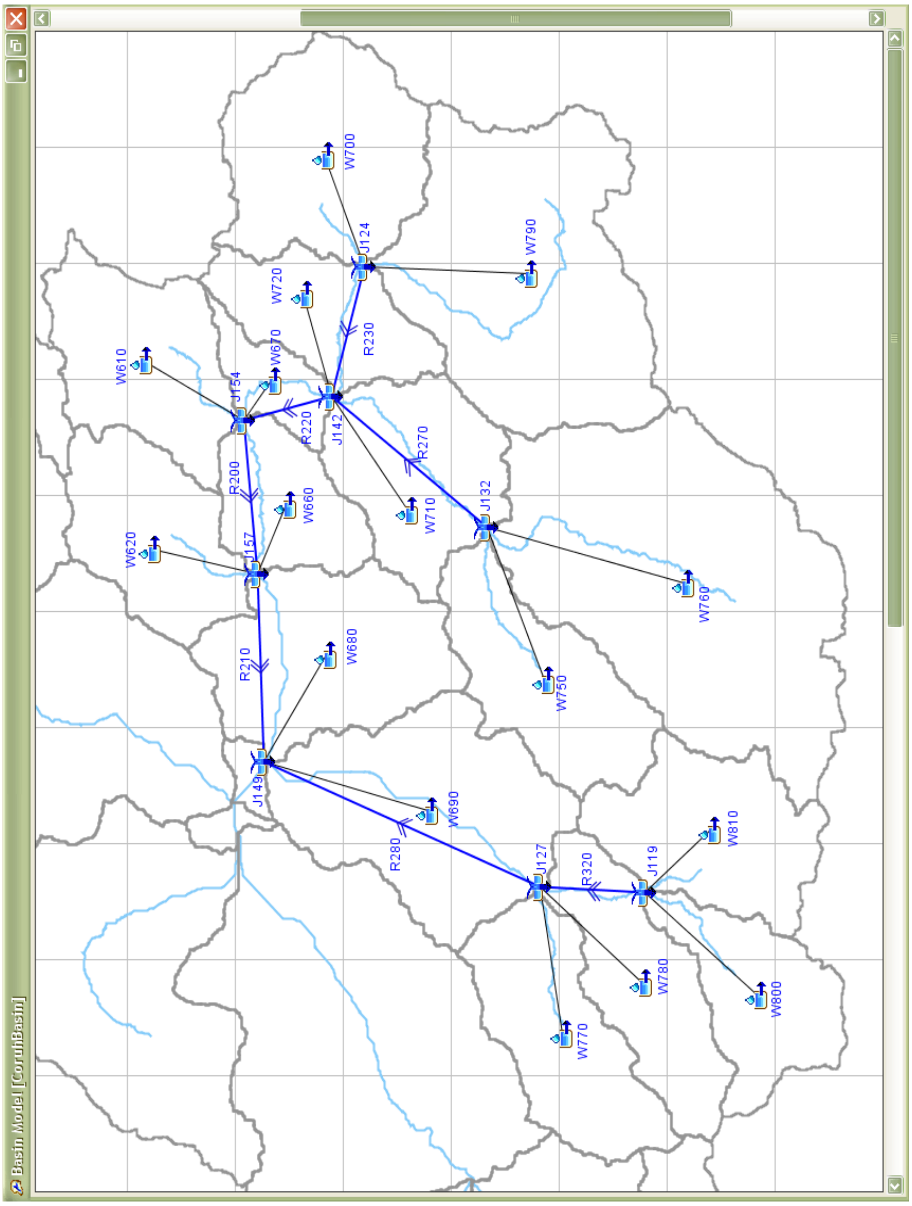

Figure D 1 Representation of basin stream and junction names on HEC-HMS

Table D 1 Values found in hydrologic parameter estimation for each subbasin

Subbasin Area		Loss Method		Transform Method
Basin	Area (km^2)	Initial abstraction (mm)	Curve Number	Lag Time (min)
W610	374.74	0	68.43	353.59
W620	339.04	0	54.89	380.26
W660	224.45	0	55.79	288.24
W670	111.22	0	62.67	219.60
W680	463.98	0	55.91	416.21
W690	612.30	0	61.73	408.44
W700	476.99	0	79.17	242.28
W710	364.65	0	67.81	339.05
W720	269.37	0	76.64	236.91
W750	371.73	0	57.65	467.99
W760	1118.21	0	79.98	438.86
W770	375.42	0	78.63	239.40
W780	339.61	0	74.16	286.07
W790	841.35	0	84.09	332.06
W800	291.05	0	81.07	221.19
W810	384.65	0	64.80	313.74

Table D 2 Optimization results

Routing Method		
Reach	Muskingum K (hr.)	Muskingum X
R200	3.21	0.147
R210	3.52	0.362
R220	2.46	0.151
R230	2.62	0.151
R270	4.48	0.151
R280	6.01	0.402
R320	2.15	0.402